ACANTHAMOEBA spp. SECRETE A MANNOSE-INDUCED PROTEIN THAT CORRELATES WITH ABILITY TO CAUSE *ACANTHAMOEBA* KERATITIS

APPROVED BY SUPERVISORY COMMITTEE

Jerry Niederkorn, Ph.D._____

Nancy Street, Ph.D._____

Kevin McIver, Ph.D._____

Michael Bennett, MD._____

DEDICATION

I would like to thank the members of my Graduate Committee and everyone that has helped support me through this long journey.

ACANTHAMOEBA spp. SECRETE A MANNOSE-INDUCED PROTEIN THAT CORRELATES WITH ABILITY TO CAUSE *ACANTHAMOEBA* KERATITIS

by

MICHAEL ALLEN HURT

DISSERTATION

Presented to the Faculty of the Graduate School of Biomedical Sciences

The University of Texas Southwestern Medical Center at Dallas

In Partial Fulfillment of the Requirements

For the Degree of

DOCTOR OF PHILOSOPHY

The University of Texas Southwestern Medical Center at Dallas

Dallas, Texas

October, 2003

ACKNOWLEDGEMENTS

I would like to first thank my mentor, Dr. Jerry Niederkorn, for giving me not only a place in which to conduct my research but also countless hours of invaluable advice and discussion that will shape my future career. I could not have asked for a better mentor.

I would also like to thank my coworkers, past and present, in the Niederkorn lab. I am particularly grateful to Dr. Henry Leher and Robert Ritter (Dr. Edwards Lab), who were there to help during my early days in the lab. I thank Dr. Hassan Alizadeh, Dr. Sylvia Hargrave, Dr. Kathy McClellan, Dr. Hao-Chuan Li, Dr. Shixuan Wang, Dr. Molly Skelsey, Dr. Clay Beauregard, Dr. Alper Alkozek, Dr. Yu-guang He, Jessemee Mellon, Elizabeth Mayhew, Sherine Apte, Christina Hay, Sudha Neelam, Daniel Clarke, Dru Dace, Hossam Ashour, Wanda Harlan, Barbara Linzy, Kevin Howard, and Mindy Westbrook for their advice, assistance, and friendship. Thanks to Vincent Proy, Sabrina Carrillo, and Kalisa Myers for technical assistance and to Karen Kazemzadeh for administrative support.

I thank the Division of Cell and Molecular Biology and the Molecular Microbiology program, and especially the members of my committee, Dr. Nancy Street, Dr. Kevin McIver, and Dr. Henry Leher.

Finally, I would like to thank my father, Clyde Wilson, who stood beside me and believed that I would eventually graduate.

ACANTHAMOEBA spp. SECRETE A MANNOSE-INDUCED PROTEIN THAT CORRELATES WITH ABILITY TO CAUSE *ACANTHAMOEBA* KERATITIS

Publication No._____

Michael Allen Hurt, Ph.D.

The University of Texas Southwestern Medical Center at Dallas, 2003

SUPERVISING PROFESSOR: JERRY NIEDERKORN, PH.D.

ABSTRACT

Acanthamoeba spp. are ubiquitously distributed in the environment. The trophozoite form can infect the cornea and cause sight-threatening corneal inflammation known as *Acanthamoeba* keratitis. The pathogenic cascade of *Acanthamoeba* keratitis begins when *Acanthamoebae* bind to mannose expressed on traumatized corneas. Published reports indicate that mannose is upregulated on the corneal surface during wound healing. Experiments in laboratory animals have shown that corneal abrasion prior to infection is essential for generating *Acanthamoeba* keratitis. Furthermore, supernatants from *Acanthamoeba*

trophozoites grown in medium supplemented with mannose were found to be more toxic to corneal cells than from those without mannose. After binding to mannose ligands, the amoebae desquamate the corneal epithelial cells, perforate the Bowman's membrane, and invade the corneal stroma. Once inside the stroma, the amoebae secrete collagenolytic factors that dissolve the stromal matrix. Collectively, these data suggest that binding to mannose induces *Acanthamoeba* trophozoites to secrete cytotoxic factors necessary for causing keratitis.

The data showed that mannose induced *A. castellanii* to secrete a novel 133 kDa protein that is cytolytic to corneal epithelial cells. Cytolytic activity of the mannose-induced protein (MIP-133) was abrogated with the addition of serine protease inhibitors, indicating that MIP-133 is a serine protease. Examination of the cytolytic mechanism revealed that cell death was due to the activation of the caspases-3 and -10-dependent apoptotic cascade. Incubations of MIP-133 with artificial Bowman's membrane and stromal matrix demonstrated that MIP-133 degraded the collagen comprising the bulk of these layers.

Analysis of *Acanthamoeba* spp. revealed that production of MIP-133 correlated with ability to cause keratitis. Soil isolates neither made MIP-133 nor produced significant keratitis. All clinical isolates examined produced MIP-133 and keratitis in laboratory animals.

Anti-MIP-133 antibodies neutralized the cytolytic and collagenolytic activity of MIP-133 *in vitro*. Additionally, incubations of anti-MIP-133 with whole trophozoites inhibited their migration through an extracellular matrix.

Oral immunization with MIP-133 resulted in reduced severity and duration of *Acanthamoeba* keratitis. Mucosal antibodies isolated from orally immunized animals inhibited cytolytic activity *in vitro*. Furthermore, oral immunization in animals with existing chronic *Acanthamoeba* keratitis (mimicking human disease) displayed immediate reduction in disease severity and mitigation of corneal disease.

TABLE OF CONTENTS

PRIOR PUBLICATIONS

Hurt, M., S. Neelam, J. Y. Niederkorn, and H. Alizadeh. Association between endogenous bacteria and contact lens corneal trauma on *Acanthamoeba* keratitis. **In Preparation.**

Hurt, M., S. Neelam, J. Y. Niederkorn, and H. Alizadeh. 2003. Pathogenic *Acanthamoeba* spp. Secrete a mannose-induced cytolytic protein that correlates with ability to cause disease. Infect. Immun. **71**:6243-6255.

Hurt, M., J. Niederkorn, and H. Alizadeh. 2003. Effects of mannose on *Acanthamoeba castellanii* proliferation and cytolytic ability to corneal epithelial cells. Invest. Ophthalmol. Vis. Sci. **44:**3424-3431.

Hurt, M., V. Proy, J. Y. Niederkorn, and H. Alizadeh. 2003. The interaction of *Acanthamoeba castellanii* cysts with macrophages and neutrophils. J. Parasitol. **89:**565-572.

Alizadeh, H., S. Apte, M. S. El-Agha, L. Li, **M. Hurt**, K. Howard, H. D. Cavanagh, J. P. McCulley, and J. Y. Niederkorn. 2001. Tear IgA and serum IgG antibodies against *Acanthamoeba* in patients with *Acanthamoeba* keratitis. Cornea. 20:622-627.

Hurt, M., S. Apte, H. Leher, K. Howard, J. Niederkorn, and H. Alizadeh. 2001. Exacerbation of *Acanthamoeba* keratitis in animals treated with anti-macrophage inflammatory protein 2 or antineutrophil antibodies. Infect. Immun. 69:2988-2995.

Niederkorn, J. Y., H. Alizadeh, H. Leher, S. Apte, S. E. Agha, L. Ling, **M. Hurt**, K. Howard, H. D. Cavanagh, and J. P. McCulley. 2002. Role of tear anti-*Acanthamoeba* IgA in *Acanthamoeba* keratitis. Adv. Exp. Med. Biol. 506:845-850.

LIST OF FIGURES

LIST OF TABLES

LIST OF ABBREVIATIONS

ABTS	2,2'-azinobis (3-ethylbenzthiazoline-6-sulfonic acid)
AIDS	Acquired immune deficiency syndrome
APC	Antigen presenting cell
BALT	Bronchi associated lymphoid tissue
BP	Bisphosphonate
BSA	Bovine serum albumin
CALT	Conjunctival associated lymphoid tissue
CF	Carboxyfluorecein
CNS	Central nervous system
CPE	Cytopathic effect
cpm	Count per minute
CT	Cholera toxin
DMEM	Dulbecco's modified Eagle's medium
ELISA	Enzyme linked immunosorbant assay
EMEM	Minimum essential medium Eagle
FADD	Fas-Associated Death Domain protein
FBS	Fetal bovine serum
FHs	Human small intestinal epithelial cells
GAE	Granulomatous amebic encephalitis
GALT	Gastrointestinal tract associated lymphoid tissue
H2O2	Hydrogen peroxide
HBSS	Hank's balanced salt solution
HCE	Human corneal epithelial cells
HCN	Chinese hamster corneal endothelial cells
HCORN	Chinese hamster corneal epithelial cells
HRP	Horseradish peroxidase

HSV	Herpes-Simplex Virus
ICB	Iris ciliary body cells
Ig	Immunoglobulin
IL-8	Interleukin-8
IM	Intramuscularly
IP	Intraperitoneally
KC	Keratinocyte-derived factor
kDa	Kilodalton
KGM	Keratinocyte growth medium
LC	Langerhan's cells
MAb	Monoclonal antibody
MALT	Mucosal associated lymphoid tissue
MCAF	Monocyte chemotactic and activating factor
MIP-1 alpha	Macrophage inflammatory protein 1 alpha
MIP-133	Mannose-induced protein 133
MIP-2	Macrophage inflammatory protein 2
NHK	Human stromal cells
OD	Optical density
PBS	Phosphate buffered saline
PI	Propidium iodide
PMSF	Phenylymethylsulfonyl fluoride
PS	Phosphatidylserine
PYG	Peptone-yeast-glucose medium
rDNA	Ribosomal deoxyribonucleic acid
RNA	Ribonucleic acid
RPE	Retinal pigmented epithelial cells
rpm	Rotations per minute
RPMI	Roswell Park Memorial Institute medium

rRNA	Ribosomal ribonucleic acid
SDS	Lauryl sulfate, sodium salt
SDS/PAGE	SDS polyacrylamide gel electrophoresis
STS	Staurosporine
T/G HA-VSMC	Human smooth muscle cells
TNF	Tumor necrosis factor
TRAIL	Tumor necrosis factor-related apoptosis-inducing ligand
TRK	Rabbit stromal cell Line
° C	Degrees Celsius
^{51}Cr	^{51}Chromium

CHAPTER ONE
Introduction and Literature Review

THE EYE

The eye collects light, processes this light into visual stimuli, and then sends this information to the brain to be decoded into an actual image. Light first comes in contact with, and penetrates, the cornea. Once beyond the cornea, the light travels through the fluid filled space of the anterior chamber, called aqueous humor, and is focused through the narrow pupil, which is regulated by the iris (Figure 1). This narrow beam of light is then conveyed onto the lens. The lens acts both as a barrier between the posterior and anterior portions of the eye, and as the focus-point of the incoming light. Through a process called "accommodation," the focused light is projected through the semi-viscous fluid of the posterior compartment, called vitreous humor, back onto the millions of tiny photoreceptors that line the posterior portion of the eye, called the retina. The retina then transmits the information to the brain via the optic nerve, where the visual image is decoded.

The cornea is the outermost portion of the eye. Although it is clear and devoid of blood vessels, it is a highly organized structure arranged in 5 layers (Figure 2). The most outer layer of the corneal is comprised of the epithelium. The epithelium functions as the primary barrier to foreign material and organisms. Additionally, these cells form a smooth surface through which oxygen and nutrients are absorbed.

Figure 1. Cross-section of the eye. The anterior segment of the eye is comprised of the cornea, iris ciliary body, and aqueous humor. The posterior compartment is filled with vitreous humor and lined by the retina. Both chambers are separated by the lens.

Figure 1

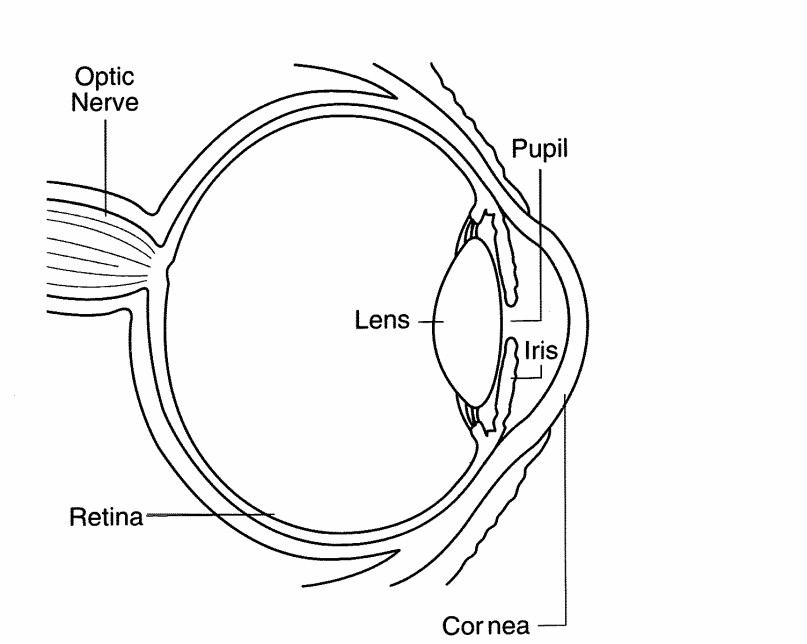

Figure 2. Cross-section of the cornea. The cornea is comprised of 5 primary components: the epithelium, Bowman's membrane, stroma, Descemet's membrane and the endothelium.

Figure 2

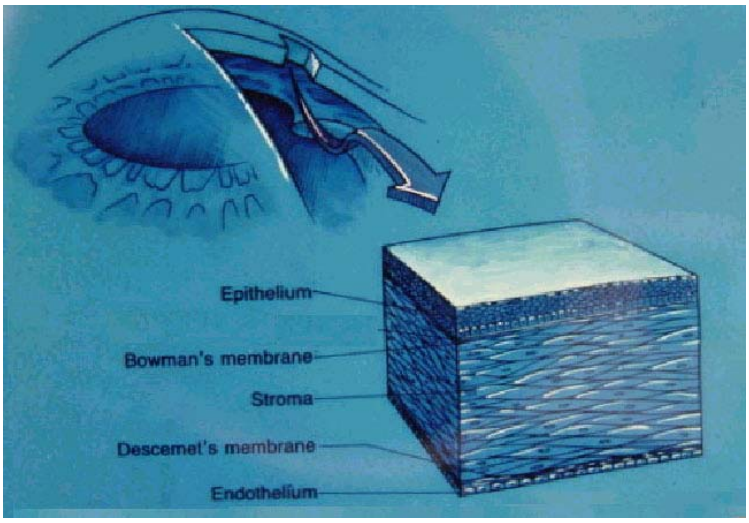
Epithelium
Bowman's membrane
Stroma
Descemet's membrane
Endothelium

Damaged epithelial cells are quickly replaced, and new cells are continuously regenerated. Underlying the epithelium is Bowman's Membrane. Bowman's Membrane is a transparent sheet comprised primarily of type IV collagen. Although capable of regeneration, scars can form as this layer heals, thereby reducing visual acuity. The middle portion of the cornea is the stroma. The stroma is the thickest layer of the five layers, representing approximately 90 percent of the cornea. This layer consists of water, type I collagen and keratocytes that maintain the collagen matrix. Under the stroma is another sheet of collagen called Descemet's Membrane. This thin layer is very resilient and serves as an additional barrier against infection. The final portion of the cornea is comprised of a single layer of cells called the endothelium. The endothelium is essential for pumping the excessive fluid out of the stroma and into the anterior chamber, and is responsible for maintaining corneal transparency. The endothelium also maintains Descemet's Membrane. However, endothelial cells do not regenerate, and damage to this cell layer can cause blindness.

The two main functions of the cornea are to serve as the refractive surface of the eye and to shield the eye from foreign material. The cornea is the main refractive surface of the eye, and has most of the power to focus light. Secondly, the cornea provides an effective barrier to foreign materials. As the ocular surface is constantly exposed to materials such as dust, pollen and pathogenic organisms, it is essential for it to be protected. Although the cornea is an effective barrier, it also relies on both specific and non-specific immune effectors, such as the tear film. The tear film bathes the surface of the cornea, and provides the main immune protection against corneal pathogens. This protection is imparted from the mixture of proteins, lipids,

salts, and metabolites that not only function as a rich source of antimicrobial products, but also aid in preventing pathogens from adhering to the corneal surface (1, 194). Additionally, the cornea can enlist specific elements of the immune system, such as neutrophils and macrophages. Macrophages have been shown to be recruited by monocyte chemotactic and activating factor (MCAF) produced by a variety of cells, including monocytes and macrophages, fibroblasts, endothelial cells, keratinocytes, smooth muscle cells, astrocytes, and various tumor cells lines (16, 218, 219). Corneal lesions from pathogens, including *Acanthamoeba* spp., have been shown to be heavily infiltrated by neutrophils (86, 98). Neutrophils have been shown to be recruited by several chemokines, including interleukin-8 (IL-8)(15), keratinocyte-derived factor (KC)(136), and macrophage inflammatory protein 2 (MIP-2)(74, 84, 216). The cornea provides an essential barrier to foreign particles, and any inability to protect the eye from pathogens can lead to severe visual impairment or blindness.

One might expect that pathogens on the ocular surface would encounter effective corneal defenses and be rapidly eliminated. However, the three most common forms of infectious blindness in the world, *Chlamydia trachomatis*, *Herpes-Simplex Virus* (HSV) and *Onchocerca volvulus*, are actually immune-mediated diseases (150, 158, 186). In all three cases, an overzealous immune response actually contributes to overall disease symptoms and can lead to corneal opacity and blindness. In fact, reduction in neutrophilic infiltration, via neutralizing antibodies against MIP-2, significantly reduced corneal opacity in HSV infected BALB/c mice (189, 216). Moreover, studies with HSV infected T-cell deficient nude mice have

shown that fewer neutrophils were recruited to the site of infection, and the corneas were resistant to HSV keratitis (42, 67). Along with HSV, *Pseudomonas aeruginosa* is one of the leading causes of infectious blindness in North America (153, 158, 186). Recent studies have shown that *Pseudomonas* keratitis is also immune-mediated (98). Recruitment of neutrophils to *Pseudomonas aeruginosa* infected corneas, via recombinant MIP-1 alpha and MIP-2, significantly exacerbated disease in mice (84, 85). Furthermore, elevated levels of interleukin-1 expression were shown to be responsible for increased MIP-2 expression, prolonged neutrophil influx, and increased corneal destruction in *Pseudomonas*-infected corneas (170). These are but a few examples of how immune-mediated diseases of the cornea can arise from a variety of pathogen categories, including helminths, viruses, and extracellular bacteria.

With this information in mind, one would expect that corneal disease associated with extracellular protozoal pathogens might also be immune-mediated. One such protozoal pathogen, *Acanthamoeba* spp., can cause a severe form of inflammation called *Acanthamoeba* keratitis. Histological examination of *Acanthamoeba* keratitis lesions in both humans and experimental animals reveals large numbers of neutrophils and macrophages (14, 57, 63, 102, 124). However, elimination of either cell type drastically exacerbates the disease in experimental animals (74, 199). Unlike the infectious corneal diseases mentioned above, *Acanthamoeba* keratitis is not an immune-mediated disease, and clearance of the organisms relies on the participation of host innate immune cells. However, this susceptibility of *Acanthamoebae* to the innate immnune system in experimental

animals does not tell the full story. In fact, *Acanthamoeba* keratitis in humans is often chronic, even in the face of a robust immune response. Furthermore, the amoebae are very efficient at overcoming the initial corneal defenses, and invading the stroma. Further elucidation of the immune responses and pathogenic mechanism are necessary for understanding *Acanthamoeba* keratitis.

***ACANTHAMOEBA* CLASSIFICATION AND BIOLOGY**

Acanthamoeba was first discovered in 1930 by Castellani while examining cultures of the yeast *Cryptococcus pararoseus* (26). The following year, Volkonsky classified the new amoeba species as *Hartmanella castellanii* (205). This early classification was ill-defined, and was based on both the presence of the double-wall cyst and the position of the spindle fibers at mitosis. By the 1960s and 1970s, it was clear that a new system of classification was needed as more strains of *Acanthamoeba* were described. This new scheme divided *Acanthamoeba* spp. into three morphological groups based on cyst size and shape (156, 163). However, classification based on the cyst size and shape was unreliable, as cysts morphology can change due to culture conditions. Moreover, this classification system does not incorporate biochemical or immunological criteria (41, 185). In 1991, Visvesvara created a new species classification scheme dividing *Acanthamoeba* spp. into three different subgroups based on morphology, isoenzyme analysis and serology (202). This scheme is widely used today and places *Acanthamoeba* into the suborder Acanthopodina and the genus *Acanthamoeba* (Figure 3A). However, many species

Figure 3. Phylogenetic tree of *Acanthamoeba* spp. A) Scheme of classification used in the early 1990s. Based on morphology, isoenzyme analysis and serology. B) Present day schematic based on morphology, rRNA and rDNA.

Figure 3

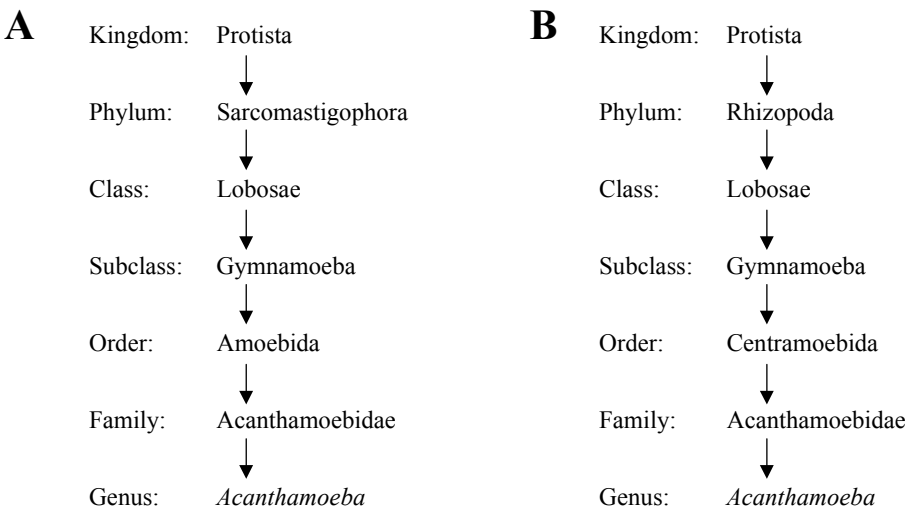
A
Kingdom: Protista
Phylum: Sarcomastigophora
Class: Lobosae
Subclass: Gymnamoeba
Order: Amoebida
Family: Acanthamoebidae
Genus: Acanthamoeba
B
Kingdom: Protista
Phylum: Rhizopoda
Class: Lobosae
Subclass: Gymnamoeba
Order: Centramoebida
Family: Acanthamoebidae
Genus: Acanthamoeba

share antigenic determinants, and isoenzyme patterns also change when strains are cultured under different conditions (77, 210).

During the late 1990s, attempts to rectify the problems in classification focused on nuclear rRNA. Under this system, *Acanthamoeba* species were divided into 12 sequence types, and in combination with morphologies established by Pussard and Pons (163), helped to create the most current phylogenetic tree (Figure 3B) (59, 184).

Acanthamoeba spp. are ubiquitous in nature and have been isolated from a wide variety of environments, including swimming pools, hot tubs, lakes, soil, dust, drinking fountains, eyewash stations and the nasopharyngeal mucosa of healthy individuals (11, 23, 27, 90, 114, 157, 167, 203, 208). In addition, several strains have also been isolated from vegetation and several species of animals, including mammals, reptiles, and fish (30, 48, 206). *Acanthamoebae* exist in 2 stages; the motile free-living trophozoite and the dormant cyst (Figure 4). The trophozoites of at least seven species of *Acanthamoeba* are the causative agents of disease and range from 25 – 40 μm in size. They are easily identified at the genus level due to the presence of spiny surface psuedopodia, called acanthapodia, from which their name is derived.

In unfavorable conditions, such as starvation, hyperosmolarity, dessiccation, freezing, and extreme temperatures or extreme pH, the trophozoite will encyst (29, 37, 60, 211). The cyst is 10-25 μm in diameter and is encapsulated within a double wall that is primarily comprised of cellulose and chitin. The cyst is highly resistant to environmental assault and has been shown to tolerate both repeated freeze-thawing

Figure 4. Photomicrographs of *Acanthamoeba castellanii* trophozoites and cysts. Photos were taken at 100x. Bar = 12 μm.

Figure 4

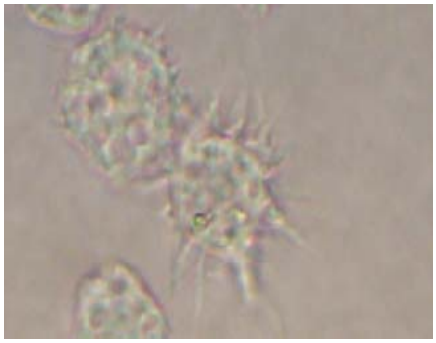

Trophozoites

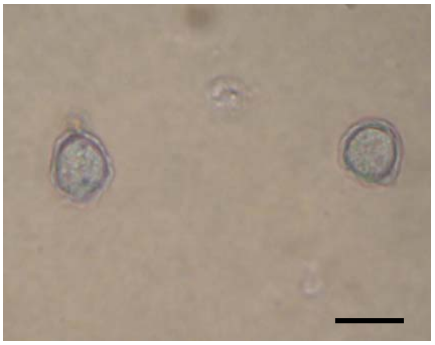

Cysts

and very high doses of UV and gamma radiation (3). Such resistance is beneficial for the organism as it enhances it's survival during periods of very harsh environmental conditions, which might include immunological attack.

ACANTHAMOEBA INFECTIONS AND PATHOGENESIS OF *ACANTHAMOEBA* KERATITIS

Acanthamoeba infections are found in both immunocompetent and immunosupressed individuals. Although the most common form of infection is *Acanthamoeba* keratitis, *Acanthamoeba* species can also cause granulomatous amebic encephalitis (GAE) and cutaneous acanthamebiasis. GAE is a very rare, and potentially fatal, infection of the central nervous system (CNS) (47, 82, 117, 120, 122). Incubation periods and routes of infection are still unclear, yet the initial infection is believed to arise from inhalation of infectious *Acanthamoebae* or via invasion of skin lesions (118). Immunocompetent patients generate well-developed granulomas around *Acanthamoeba* spp., while immunosuppressed patients form very weak granulomas. Once the organisms spread to the CNS, symptoms occur, including severe hemorrhagic necrosis. Proper diagnosis of GAE is very important, as most patients with disease spreading to the CNS will die. Cutaneous acanthamebiasis is a severe skin disease primarily found in individuals with AIDS, but has also been reported in patients undergoing treatment for organ transplants and in patients with underlying immunological disorders (25, 44, 68, 116, 178, 195).

Classical symptoms of cutaneous acanthamebiasis include the presence of firm erythematous nodules and ulcers (31, 68, 111, 193). *Acanthamoeba*-derived skin ulcers often progress into non-healing purulent ulcerations (127, 187). Approximately 73 percent of patients with cutaneous acanthamebiasis die; however, if the organisms disseminate to the CNS, 100 percent fatality ensues (193).

Acanthamoeba keratitis is a very painful, sight-threatening corneal infection caused by several species of free-living pathogenic *Acanthamoeba* (133, 204). *Acanthamoeba* keratitis was first reported by Dr. Daniel Jones as a presentation at the Ocular Microbiology and Immunology group meeting in Dallas, Texas, in 1973, and later published in 1975 (81, 82). In this presentation, a 59 year-old rancher had traumatized his right eye by straw fragments, and then washed the eye with water from a tap in his house that was fed from the ranch river tributary. The initial clinicians prescribed antibiotics and corticosteroids. One month later, the rancher's visual acuity was restricted to counting fingers at a length of one foot, and the patient was referred to Dr. Jones at Baylor College of Medicine, Houston, Texas. The initial impression was fungal keratitis with ring infiltrate, and atropine was administered. Corneal scrapings revealed unidentifiable thick-walled cysts, and over the next 10 days, confusion over the identity of the causative agent led to the administration of several different treatments, including prednisolone phosphate, bacitracin, gentamicin, and atropine. Then it was noticed that initial blood agar plates contained wave-like tracks, which subsequently contained cysts and free-living amoebae. Telephone conversation with Dr. Culbertson in Indianapolis suggested the probability of a strain of either *Hartmanella* or *Acanthamoeba*. Subcultures sent to the Center for Disease Control identified the organism as *Acanthamoeba polyphaga*. Over the next 11 months, the patient experienced 5 more relapses of keratitis, until finally ending with the perforation of the infected cornea. Keratoplasty and lens extraction were performed the following day.

The "first" published peer review article reporting *Acanthamoeba* keratitis was by Nagington et al. in Great Britain in 1974 (145). During the next 10 years, only 10 cases of *Acanthamoeba* keratitis were reported (213). However, between 1984 and 1985, the number of reported cases began to increase, with nearly 200 cases reported in 1990 alone (181, 213). This increase in *Acanthamoeba* keratitis has been directly linked to contact lens wear with preexisting corneal trauma (11, 36, 142, 181, 196, 204). Characteristic symptoms of *Acanthamoeba* keratitis include a ring-like corneal infiltrate, epithelial destruction, disproportionately severe ocular pain and resistance to antimicrobial agents (7, 125, 160). Typical treatment consists of around-the-clock, hourly, topical applications of chlorhexidine, brolene, or polyhexamethylene biguanide, alone or in combination. Even with such regimented therapies, patients often experience severe corneal destruction and require corneal transplants. *Acanthamoeba* cysts persist in the conjuctiva for several months, and can subsequently excyst and reinfect the corneal transplant (7). These dormant cysts are believed to be the source of recurrent infections in *Acanthamoeba* keratitis patients (7, 57, 124, 133, 198). It is not completely understood what conditions are necessary for excystment in the eye. However, our lab has shown that cellulase and treatments with the steroid dexamethasone greatly accelerated the rate of excystment (3, 131). Furthermore, cysts have been shown to remain viable even after 24 years when stored in water (129).

The pathogenesis of *Acanthamoeba* keratitis occurs in a sequential manner. Binding of the trophozoites to the corneal epithelial surface is an essential first step in the infectious cascade. A mannose-specific surface receptor is believed to mediate

the adhesion of the amoeba to the mannose on the corneal epithelium (217). Adhesion of the amoeba is highly specific for mannose and appears to be independent of the nature of the mannose linkage (78). Although a normal eye possesses a degree of mannose on the corneal surface, induction of *Acanthamoeba* keratitis in experimental animals requires corneal abrasion prior to exposure to infectious trophozoites (153, 196). This trauma is essential for generating disease. Furthermore, even subtle corneal surface injury has been associated with an upregulation of mannose-glycoproteins to which the amoeba can adhere with high affinity (78, 143, 217). Binding of the amoeba to the corneal epithelial cells is believed to induce the secretion of cytolytic molecules responsible for trophozoite-mediated killing (78, 108, 126). *In vitro* experiments have shown that *Acanthamoeba* trophozoites produce contact-dependent killing of a wide range of mammalian cells (12, 99, 101, 141, 175). Contact-dependent cell death using *Acanthamoebae* cell extracts is due to the induction of apoptosis, and not due to the "piecemeal" necrotic destruction of target cells as seen by *Naegleria* spp., further emphasizing the importance of secreted factors in *Acanthamoeba* pathogenesis (8, 22). However, contact-independent mechanisms of target cell death by secreted factors have also been reported. Mattana et al. reported that *A. castellanii* trophozoites constitutively secrete low molecular weight metabolites that are cytolytic to human corneal epithelial cells (126). These metabolites were isolated from mid-log phase trophozoites grown in PYG, and induced a transmembrane influx of extracellular calcium resulting in cytolysis from the elevation of cytosolic free-calcium levels. Leher et al. showed that soluble mannose could also induce *A. castellanii* to elaborate

a cytolytic factor that was found to be greater then 100 kDa (108). The cytolytic activity of this factor could be inhibited with the addition of the serine protease inhibitor PMSF. Further evidence of soluble pathogenic factors has been reported in the literature. *A. culbertsoni* constitutively produces the proteolytic enzyme elastase at comparable levels with the highly pathogenic *N. fowleri* (51). *A. castellanii* elaborates a novel 40 kDa plasminogen activator that does not cross-react with antibodies to either urokinase- or tissue-type plasminogen activators (139, 197). A number of studies have shown that tumor cell expression of urokinase plasminogen activator correlates with invasive potential in animal models (65, 97, 155). Elaboration of plasminogen activators may play an important role in the penetration of extracellular matrix. Furthermore, axenic cultures of *A. castellanii* constitutively produce collagenolytic factors that are capable of dissolving collagen shields *in vitro* (64). Intrastromal injections of the *Acanthamoeba*-conditioned medium in Lewis rats produced corneal lesions clinically similar to biopsies taken from *Acanthamoeba* keratitis patients (64). Further studies demonstrated that a variety of serine and cysteine proteases are secreted by *Acanthamoeba* spp., ranging from 33 – 230 kDa (4, 24, 34, 87, 94). In the final analysis, the pathogenesis of *Acanthamoeba* keratitis can be attributed to multiple virulence factors.

Following the destruction of the epithelial cells, trophozoites perforate Bowman's membrane. Perforation of this layer may be due to the production of plasminogin activators, collagenolytic factors, or yet to be described proteases. Penetration of Bowman's membrane is followed by the invasion of the stroma. Once in the stroma, the trophozoites produce soluble collagenase, which dissolves the

collagen matrix that forms the stromal layer. Van Klink et al. showed that *Acanthamoebae* are chemotactically attracted to corneal endothelial cell products, but do not respond to corneal epithelial or stromal extracts (197). This finding is puzzling, as there are only a few isolated reports of *Acanthamoeba* trophozoites penetrating the endothelial cell layer and entering the interior of the eye (80, 144, 197).

Once inside the stroma, trophozoites incite an inflammatory response that is comprised of macrophages and neutrophils. *In vitro* studies have shown that macrophages are capable of killing *Acanthamoeba* trophozoites in an antibody-dependent mechanism (182). Depletion of conjunctival macrophages with clodronate-encapsulated liposomes prior to infection with *A. castellanii* produces a severe infection that does not resolve (199). This finding suggests that macrophages are important for limiting the severity and duration of disease, however, they do not prevent the initial corneal infection (152). This is consistent with *in vitro* studies, which have demonstrated macrophage activation is key for successful elimination of the trophozoites (115). As a result, resting macrophages were unable to effectively kill trophozoites, and in fact, succumb to trophozoite-mediated killing.

Neutrophils have also been shown to be effective at killing *Acanthamoeba* trophozoites and are very abundant in corneas afflicted with *Acanthamoeba* keratitis (50, 133, 183). In humans, the influx of neutrophils have been blamed for mediating a portion of the stromal necrosis (133). However, studies in Chinese hamsters have shown that the migration of neutrophils into the cornea during *Acanthamoeba* keratitis is important for mitigating disease (74). Intracorneal injections of MIP-2

prior to infection with *Acanthamoeba* trophozoites greatly increased neutrophil migration into the cornea and resulted in milder disease and earlier resolution. By contrast, inhibition of neutrophil recruitment with a neutralizing antibody to MIP-2 significantly increased both disease severity and duration. Furthermore, injection of anti-Chinese hamster neutrophil antibodies prior to infection also exacerbated disease severity and duration (74).

The discussion of *Acanthamoeba* pathogenesis would not be complete without mentioning the role of *Acanthamoeba* cysts. Trophozoites have been shown to encyst in response to a number of unfavorable conditions, including starvation, hyperosmolarity, dessication, extreme temperatures, and extreme pH changes (29, 37, 60, 211). Furthermore, cysts are highly resistant to harsh environmental conditions, such as repeated freeze-thawing and high doses of both UV and gamma radiation (3). The conversion to cysts poses a unique set of problems for clinicians, as cysts can persist in the stroma for months, and are believed to be the source of recurrent infections of *Acanthamoeba* keratitis (7, 57, 124, 133). Presently, there are no known antimicrobials for eliminating cysts from the eye. Moreover, the use of dexamethosone, a topical steroid typically used to control pain and inflammation after eye surgery, has been shown to induce conversion of the dormant cysts to infectious trophozoites (131). Further compounding the problem is the fact that cysts appear to evade elimination by the immune system. McClellan et al. showed that cysts are both immunogenic and antigenic (130). Intraperitoneal immunizations of cysts in experimental animals generated serum IgG antibodies that bound to both cysts and trophozoites. It is unclear what role such antibodies might have in human patients

with *Acanthamoeba* keratitis. Once in the stroma, the cysts must then evade the macrophages and neutrophils that respond to the infection. Recent studies in our lab were aimed at understanding how the cysts were able to avoid being eliminated by the innate arm of the immune system. The results showed that neither macrophages nor neutrophils were chemotactically attracted to whole cysts *in vitro* (76). By contrast, both of these immune cells were highly attracted to cyst lysate. *In vitro* studies showed that both neutrophils and macrophages were efficient at killing *Acanthamoeba* cysts in a contact-dependent fashion. Macrophages were shown to kill the cysts through phagocytosis, while neutrophils were shown to kill cysts by way of a myeloperoxidase-dependent method (76). To understand the immunobiology of *Acanthamoeba* keratitis, it is necessary to review how the cornea defends itself against microbial attack.

CORNEAL IMMUNITY AND WOUND HEALING

The corneal epithelium, along with tears and the blinking reflex, provide the first line of defense for the eye. Corneal epithelium, conjunctiva, and eyelids provide important barrier functions, while the lacrimal glands found in the superolateral orbit provides both specific and non-specific protection. Foreign objects first become trapped in the tear film (described below) on the corneal surface, and are then cleared away by the sweeping action of the eyelids. This sweeping motion of the eyelids provides the cornea with the immediate removal of foreign materials, and simultaneously functions to distribute tear film evenly along the ocular surface.

Lining the inside of the eyelid is the tarsal conjunctiva and approximately 30 meibomian glands that secrete the lipid layer of the tears, which forms the outer layer of the tear film (104). The conjunctiva continues around the globe (bulbar conjunctiva) and ends at the corneal limbus. The conjunctiva is comprised of tightly packed stratified squamous epithelial cells that provide a formidable barrier against foreign invaders. Furthermore, the conjunctiva contains lymphocytes, T-cells, natural killer cells, mast cells, macrophages and indigenous aerobic and anaerobic flora (2, 18, 70, 180). This local accumulation of activated lymphocytes is a key function of mucosal immunity and is part of the "mucosal associated lymphoid tissue" (MALT; described in the mucosal immunity section) (46). The cornea is avascular and depends on immune elements found within the conjunctiva for protection against foreign invaders. Following injury or infection, blood vessels can extend into the corneal tissues, thus allowing recruitment of immune elements to the site of infection.

The tear film is an essential component of the cornea's defense and health. It serves several purposes: it keeps the eye moist, creates a smooth surface for light to pass through the eye, nourishes the front of the eye and provides protection from injury and infection. Tears are comprised of three layers: oil, water, and mucus. The top layer is the lipid layer, and it is secreted by the meibomian glands found along the underside of the eyelids. This layer is comprised of cholesterols and lipids, and functions to smooth the tear surface and reduce tear evaporation (91). The middle layer forms the bulk of the tears. This aqueous layer is secreted by the lacrimal glands and functions to hydrate, clean, and protect the eye against foreign materials (104). The lacrimal glands secrete a host of non-specific defensive molecules and are

the main site of secretory IgA synthesis (9). Key antigen non-specific molecules include lactoferrin, lysozyme, lactoperoxidase metabolites, beta-lysin, interferon, prostaglandins, and complement (2, 55, 79, 88, 100, 104, 128). The bottom layer of the tear film is the mucus (mucin) layer and is produced by the conjunctival goblet cells. This layer spreads evenly over the surface of the cornea to make an even base for the watery middle layer, thus aiding in keeping the cornea hydrated (2, 104). Additionally, the mucin layer also helps in the elimination of foreign materials by trapping them and facilitating their removal by the blinking reflex.

The corneal epithelium functions as an effective barrier against foreign invaders. The outermost layer is comprised of five to seven layers of stratified squamous epithelial cells. Even mild trauma to the surface of the cornea induces epithelial cells to move into the injured area before infection can occur. Additionally, studies have shown that trauma to corneal epithelial cells causes them to upregulate mannose-glycoproteins to the cell surface during the wound healing response (78, 143, 217). The reason for glycopotein upregulation is still unclear, however, these glycoproteins may facilitate infection by microorganisms as they are important ligands for pathogens such as *A. castellanii* (217). Although the cornea is normally avascular, infection of the ocular surface can induce extensive corneal neovascularization. This vascularization facilitates recruitment of both the innate and adaptive immune systems.

MUCOSAL IMMUNITY AND IgA

The mucosal surface represents the largest surface area of the human body and is over one hundred times larger than the total area of the skin (20). The average adult has approximately 400 m^2 of mucosal epithelium, while the skin only represents about 1.8 m^2 (20) This vast surface is dependent on a series of barriers that can provide a local immune response.

The common mucosal immune system refers to the distribution of activated lymphocytes in exocrine tissues throughout the body (20). These sites represent aggregates of lymphoepithelial tissue, and are referred to as "mucosal associated lymphoid tissue" (MALT). These specialized lymphoid tissues are directly associated with the mucosa, and though they are part of the immune system, they function independently from the central immune system (49). MALT sites are strategically distributed along the vast mucosal surface and serve as key antigen sampling sites (96). The MALT accumulates antigens and orchestrates the generation of mucosal immune elements. Following their uptake by antigen presenting cells, antigens are transported, processed, and presented to T-cells and B-cells, which can induce either tolerance or specific immunity in the form of IgA antibodies (20, 138). The specialized compartments are found in the bronchi (BALT) (19), the gastrointestinal tract (GALT) (137), and the conjunctiva of the eye (CALT) (54, 92).

Gut associated lymphoid tissue (GALT) has been well studied, and was first described by Johann Peyer in 1677 (161). Antigens are typically ingested, and are eventually delivered to the small intestine. Specialized lymphoepithelial structures, called Peyer's patches, line the intestinal epithelial surface and are designed to

capture antigen. Antigen uptake is facilitated by specialized epithelial cells in the Peyer's patch, called M-cells. M-cells have numerous invaginations along their apical surface (membrane microdomains) that aid in direct uptake of antigens from the gastrointestinal lumen via endocytosis (146). Captured antigen is then transported across the M-cell and delivered to large intracellular pockets in the basolateral membrane that can contain T-cells (the most common), plasma cells, natural killer cells, mast cells and professional antigen-presenting cells such as Langerhans cells and macrophages (70, 147). Antigen in the intracellular pockets are processed and and can directly activate helper T-cells and B-cells (147). Activated B-cells (mainly IgA producers) leave the MALT and migrate to mucosal sites where they differentiate into IgA secreting plasma cells (40, 134, 135).

The main mediators of the mucosal immune system are secretory IgA and IgM. In the tear film, IgA is the most abundant immunoglobulin and is found in higher concentrations than in serum (55, 62, 128, 212). Secretory IgA antibodies work in conjunction with several antigen non-specific effectors (such as lactoferrin, lactoperoxidase, and mucin) and are essential for maintaining mucosal integrity (21, 56, 188). Secretory IgA, the dimeric form, is the predominant isotype found on mucosal surfaces and is usually produced locally (9). Like other immunoglobulins, IgA has a basic monomeric structure composed of two heavy chains and two light chains, arranged into two identical Fab arms and one Fc region. The tips of the Fab arms are responsible for recognizing and binding to epitopes found on the surface of foreign material/organisms. The Fc portion is a critical region that is recognized by specific receptors on the surface of phagocytic immune cells and subsequently

triggers reactions such as phagocytosis. IgA fixes complement weakly and it is believed that its primary protective effect comes from attaching to pathogens and preventing them from binding directly to mucosal surfaces (123, 171). This inhibitory activity prevents infection with bacteria, viruses and amoebae, and it has also been shown to directly neutralize toxins (17, 52, 71, 192).

Exposure to antigens via mucosal surfaces, such as the eye, nose, or throat, induces the preferential generation of secretory IgA antibodies (61, 140, 166). IgA antibody responses can be further enhanced through the use of mucosal adjuvants such as neutralized cholera toxin, thus providing strong resistance to multiple pathogens that invade mucosal surfaces (17, 72, 112, 162). Importantly, oral immunization with *Acanthamoeba* antigens conjugated to neutralized cholera toxin protects both pigs and Chinese hamsters from corneal infection with *Acanthamoeba* (105, 106).

CHINESE HAMSTER MODEL

During the mid-1980s and early 1990s, several laboratories worked on developing a valid animal model to study *Acanthamoeba* keratitis. Establishing the infection in mice would have allowed a wide array of immunological and genetic analysis; however, *Acanthamoeba* spp. were incapable of producing keratitis in various normal and immunosuppressed mice (154). *Acanthamoeba* keratitis was putatively induced in a rabbit, but only if the animals were simultaneously treated with corticosteroids and if the trophozoites were injected directly into the corneal

stroma (38). Disease symptoms did not mimic the human counterpart and the use of steroids raised concern about the validity of the rabbit model. Badenoch et al. successfully established *Acanthamoeba* keratitis in rats (13, 14). However, these infections required the coinjection of *Corynebacterium xerosis* to produce disease. The function of *C. xerosis* in this model is controversial and it is unclear whether the bacteria serves as cofactor or as a food source for the *Acanthamoeba* trophozoites. Moreover, this model required the injection of amoebae into the stroma and did not represent the typical mode of infection or make use of the primary risk factor for *Acanthamoeba* keratitis—contact lens wear. In an effort to establish an animal model that more closely represented the normal mode of infection, Niederkorn et al. examined the ability of *A. castellanii* trophozoites to bind to a wide array of corneas, including dog, horse, cow, mouse, rat, cotton rat, chicken, rabbit, Guinea pig, pig, Chinese hamster and human (154). This study revealed that *A. castellanii* trophozoites preferentially bound to human, pig, and Chinese hamster corneas. Furthermore, unlike the rabbit, mouse, and rat, both the pig and the Chinese hamster developed *Acanthamoeba* keratitis following application of contact lenses laden with *Acanthamoeba* trophozoites (63, 196). Chinese hamsters have been used in numerous *in vivo* studies on *Acanthamoeba* keratitis as the disease closely resembles the clinical and histopathological symptoms seen in human infections (74-76, 105-108, 196, 198, 199). Disease symptoms typically include neutrophil migration, corneal opacity, epithelial destruction, edema and neovascularization. Although the corneal disease symptoms mimic those seen in human infections, the disease is acute in both pigs and Chinese hamsters and does not mimic the chronicity of the disease in humans. In

Chinese hamsters, *Acanthamoeba* keratitis is acute and normally resolves in approximately 21 days. In humans, *Acanthamoeba* produces a chronic keratitis that does not appear to resolve without medical intervention. However, chronic *Acanthamoeba* keratitis can be produced in Chinese hamster if the conjunctival macrophages are depleted prior to corneal infection (199). In conjunctival macrophage-depleted Chinese hamsters, the disease progresses as a severe chronic infection that mimics the human counterpart.

OBJECTIVES AND RATIONALE OF RESEARCH

Acanthamoeba spp. are ubiquitous organisms that can be isolated from a wide variety of environments. Frequent exposure to viable *Acanthamoeba* spp. would lead one to believe that there would be a high incidence of disease. However, the incidence of disease is very low-only one in every 10,000 contact lens wearers (172). The events necessary to generate *Acanthamoeba* keratitis are sequential and begin with the amoebae binding to the surface of the corneal. This binding is the crucial first step to causing disease, and it is known that *Acanthamoeba* trophozoites bind with high affinity to the upregulated mannosylated glycoproteins found on the surface of a traumatized cornea (78). After the amoebae bind to the corneal surface, they must penetrate the epithelial layer, Bowman's membrane, and gain entry into the stroma. After the amoebae bind to the mannosylated glycoproteins on the corneal

epithelium, it is unclear how they are able to penetrate the corneal defenses and gain entry to the stroma. Corneal disease might be attributed to a variety of factors. One possible explanation is that the *Acanthamoeba* trophozoites may use mannose as a food source. In this scenario, mannose stimulates trophozoites to proliferate, and disease is attributed to increased numbers of proliferating trophozoites. However, Leher et al. showed that soluble mannose inhibited binding of *Acanthamoeba* trophozoites to Chinese hamster corneal epithelial cells *in vitro*; yet, inhibition of trophozoite binding did not prevent the killing of corneal epithelial cells (108). In experimental animals, the upregulation of mannose, via corneal trauma, is essential for generating disease. Moreover, Leher et al. showed that supernatants from mannose-stimulated trophozoites were capable of killing Chinese hamster epithelial cells *in vitro*, and that this killing could be blocked with the addition of a serine protease inhibitor (108). Therefore, it was hypothesized that soluble mannose bound to a mannose-binding protein on the surface of *Acanthamoeba* trophozoites, and induced the amoebae to secrete cytolytic protein(s) that were responsible for killing the corneal epithelial cells.

Acanthamoebae are thought to be normal human commensals and it has been hypothesized that the majority of adults have been exposed to *Acanthamoeba* spp., resulting in the production of antibodies to *Acanthamoeba* antigens (167, 208). Two independent studies have shown that 52 – 100% of individuals examined possess circulating IgG antibodies to *Acanthamoeba* (27, 39). Our laboratory has shown that 100% of individuals examined possessed both serum IgG and tear IgA antibodies against *Acanthamoeba* antigens (5). Although robust anti-*Acanthamoeba* antibody

responses can be generated in laboratory animals, serum IgG does not provide protection against *Acanthamoeba* keratitis (6, 107, 151, 153). However, stimulation of mucosal anti-*Acanthamoeba* IgA antibodies through oral immunizations with *Acanthamoeba* antigens produces partial protection against *Acanthamoeba* keratitis (105-107).

This dissertation addressed four specific aims. The First Specific Aim was to characterize how *Acanthamoeba* trophozoites respond to binding of mannosylated glycoproteins on a traumatized cornea. Two hypotheses were proposed. The first hypothesis proposed that mannosylated glycoproteins affect proliferation, encystment, or excystment of the trophozoites. The second hypothesis proposed that binding to the mannosylated glycoproteins stimulates the amoebae to secrete one or more mannose-induced proteins that aid in the desquamation of the corneal epithelial cells.

The Second Specific Aim examined the mechanisms by which mannose-induced proteins kill corneal epithelial cells. This aim also examined the pathogenic activity of these proteins among different species and strains of *Acanthamoeba*. Two hypotheses were proposed. The first hypothesis proposed that the mannose-induced protein killed corneal epithelial cells by membrane disruption. Membrane disruption due to glycoprotein-induced secreted proteins has been reported in other pathogenic amoeba, such as *Entamoeba histolytica* (109, 132, 201). The second hypothesis proposed that secretion of a cytolytic mannose-induced protein correlated with the ability of pathogenic *Acanthamoeba* spp. to produce disease.

The Third Specific Aim proposed that the mannose-induced protein plays an important role in the subsequent steps of the pathogenic cascade of *Acanthamoeba* keratitis. Two hypotheses were considered. The first hypothesis proposed that the mannose-induced protein plays a direct role in aiding the amoeba in penetrating Bowman's membrane and the stroma. The second hypothesis proposed that the mannose-induced protein is cytolytic to a broad range of mammalian cells. As cell killing in crude supernatants from mannose-stimulated trophozoites was inhibited by serine protease inhibitors, we predict that the mannose-induced protein will display the same cytotoxicity seen with other serine proteases.

The Fourth Specific Aim examined the potential of the mannose-induced protein as an immunogen to either mitigate or prevent *Acanthamoeba* keratitis. Two hypotheses were proposed. The first hypothesis suggested that antibodies against the mannose-induced protein could block its cytolytic functions *in vitro*. Neutralizing antibodies have been generated against a host of known cytolytic proteins, including serine proteases. It is feasible that neutralizing antibodies could be generated against the mannose-induced protein. The second hypothesis suggested that the mannose-induced protein could be effectively used as an immunogen, offering protection against disease *in vivo*. Reports have shown that inducing mucosal immunity through oral immunization, and thus, the secretion of *Acanthamoeba* antigen-specific IgA, has been successful in protecting against *Acanthamoeba* keratitis in Chinese hamsters. Thus, oral immunizations with the mannose-induced protein may prevent or mitigate *Acanthamoeba* keratitis.

CHAPTER TWO
Materials And Methods

ANIMALS

Chinese hamsters (*Cricetulus griseus*) were purchased from Cytogen Research and Development (West Bury, MA). The Chinese hamsters were the 17A strain of inbred hamsters and were from 4-6 weeks of age. All animals were free of corneal defects and abnormalities prior to experiments and were handled in accordance with the Association of Research in Vision and Ophthalmology (ARVO) Statement on the Use of Animals in Ophthalmic and Vision Research.

AMOEBAE AND CELL LINES

All *Acanthamoeba* species were originally obtained from the American Type Culture Collection, Rockville, MD. *A. castellanii* (ATTC#30868), *A. culbertsoni* (ATTC#30171), *A. polyphaga* (ATTC#30461) and *A. rhysodes* (ATTC#50368) were isolated from human corneas. *A. hatchetti* (ATTC#30730), *A. astronyxis* (ATTC#30137), and *A. castellanii neff* (ATTC#30010) were isolated from soil. The chosen species represent all three of the different subgroups of *Acanthamoeba* based on morphology, isoenzyme analysis, and serology (202). Amoebae were grown as axenic cultures in peptone-yeast extract glucose (PYG) at 35° C with constant agitation (108, 203).

Mammalian cells lines were grown in their appropriate medium (see Table 1) containing 1% L-glutamine (BioWhittaker, Walkersville, MD), 1% penicillin, streptomycin, and amphotericin B (Fungizone; BioWhittaker), 1% sodium pyruvate (BioWhittaker), and 10% fetal calf serum (FCS; HyClone Laboratories, Logan, UT) (complete medium). All cells were incubated at 35°C with 5% carbon dioxide.

Chinese hamsters corneal epithelial cells (HCORN) and endothelial cells (HCN) were immortalized from a corneal explant using the E6/E7 papilloma virus oncogenes as previously described (214).

Spleens and mesenteric lymph nodes were harvested from C57BL/6 mice as previously described (176, 177). Spleens and mesenteric lymph nodes were ground between two glass slides and erythrocytes were lysed. Cells were resusupended in five ml complete RPMI and placed in Primaria petri dishes (Becton Dickinson Labware, Franklin lakes, NJ). Splenocytes and mesenteric lymph node cells were incubated for two hours at 37° C in 5% CO_2. The nonadherent cells were carefully drawn off and put into 96-well plates for cytopathic assays (mentioned below).

Table 1. Mammalian cell lines used as target cells for *in vitro* cytotoxicity assays.

Table 1

Corneal Cells	Description	Source	Medium
HCE	Human Epithelial Cells	Gift from Dr. Ward [2]	KGM
HCORN	Hamster Epithelial Cells	Produced in Lab [1]	EMEM
HCN	Human Endothelial Cells	Produced in Lab [1]	EMEM
TRK	Human Stromal Cells	Gift from Dr. Jester [1]	DMEM
NHK	Rabbit Stromal Cells	Gift from Dr. Jester [1]	RPMI
Human Melanoma			
OM 431	Ocular Melanoma	Gift from Dr. Albert [3]	Hams
MEL 202	Ocular Melanoma	Gift from Dr. Ksander [4]	RPMI
MEL 270	Ocular Melanoma	Gift from Dr. Ksander [4]	RPMI
OCM 1	Ocular Melanoma	Gift from Dr. Kan-Mitchel [5]	Hams
OCM 8	Ocular Melanoma	Gift from Dr. Kan-Mitchel [5]	Hams
OMM-1	Ocular Melanoma	Gift from Dr. Luyten [6]	DMEM
OMM-1.5	Ocular Melanoma	Gift from Dr. Ksander [4]	DMEM
92-1	Ocular Melanoma	Gift from Dr. Luyten[6]	RPMI
Mel-290	Ocular Melanoma	Gift from Dr. Ksander [4]	RPMI
Miscellaneous Cells			
Jurkat	Human T Cells	ATCC # TIB-152	RPMI
Chang	Human Liver Cells	ATCC # CCL-13	RPMI
FHS	Human intestinal epithelial Cells	ATCC # CCL-241	Hybricare (ATCC #46-x)
RPE	Human Retinal Pigmented Epithelial Cells	Gift from Dr. Edwards [1]	DMEM
ICB	Iris Ciliary Body Cells	Produced in Lab [1]	DMEM [7]
T/G HA-VSMC	Human Smooth Muscle Cells	ATCC # CRL-1999	HAMS
Mouse Cells			
B6 Splenocytes Cells		Produced in Lab [1]	RPMI
B6 Mesenteric Lymph node Cells		Produced in Lab [1]	RPMI

1; Department of Ophthalmology, UT Southwestern Medical Center at Dallas, Dallas, TX.

2; Gillette Medical Evaluation Laboratories, Gaithersburg, MD.

3; Department of Ophthalmology, University of Wisconsin, Madison, WI.

4; Schepens Eye Research Institute, Harvard Medical School, Boston, MA.

5; Department of Pathology, University of Southern California, Los Angeles, CA.

6; Department of Ophthalmology, University Hospital at Rotterdam, Rotterdam, Netherlands

7; ICB cells supplemented with 10% human serum

EFFECTS OF MANNOSE ON *ACANTHAMOEBAE* PROLIFERATION AND CYST ANALYSIS

Acanthamoeba trophozoites were grown in 200 ml of PYG either with or without 100 mM methyl-α-D-mannopyranoside (Sigma Chemical Co., St.Louis, MO) on a shaker incubator set at 125 rpm and at 35° C. Initial cultures were seeded with a total of 1 x 10^7 trophozoites in 5 ml PYG. Control experiments were performed using either 100 mM galactose or 100 mM lactose. One milliliter samples were removed approximately every twelve hours for 200 hours, with additional samples taken at 270, 290, and 320 hours. Samples were either immediately examined for trophozoites and cysts by direct counts using a compound microscope or examined spectrophotometrically using an optical density of 480 nm. All direct counts were performed using a hemocytometer viewed at 20x. Assays were performed in triplicate.

Excystment assays were performed in 100 ml of PYG either with or without 100 mM methyl-α-D-mannopyranoside on a shaker incubator set at 125 rpm and at 35° C. Initial cultures were seeded with a total of 1 x 10^7 cysts (10^7/ml) (0% trophozoites, verified by calcofluor white staining (35). One milliliter samples were removed every 24 hours for ten days and examined by direct microscopy. The experiment was ended on day 10 to prevent the excysted trophozoites from proliferating to stationary phase and encysting. Control experiments were duplicated using phosphate buffered saline (PBS). Assays were performed in triplicate.

INDUCTION OF MANNOSE-INDUCED PROTEINS

Acanthamoeba spp. were grown in peptone-yeast extract glucose (PYG) either with or without 100 mM methyl-α-D-mannopyranoside at 35° C with constant agitation. Amoebae cultures were grown to mid-log phase (approximately 48 hours), centrifuged at 700 x *g* for 10 minutes to pellet the trophozoites, and supernatants were carefully removed. Supernatants were then sterilized using low protein binding 0.22 μm filter units (Corning, Corning, NY) and then analyzed by 4-15% SDS/PAGE Ready Gels (Bio-Rad, Hercules, CA) under both reducing and non-reducing conditions. SDS/PAGE analysis revealed the production of a mannose-induced protein of approximately 133 kDa (MIP-133). Supernatants were stored at 4° C for future use and used within five days of initial storage.

CHROMIUM RELEASE ASSAY

A standard chromium (^{51}Cr) release assay was performed as mentioned before, with modification (66). 2 x 10^6 ^{51}Cr-labeled human corneal epithelial cells (per well) were dispensed in a 96-well flat-bottomed micotiter plate (Corning Inc., Corning, NY) with 200 μl complete KGM medium. Plates were centrifuged at 700 x g for five minutes and washed with complete KGM three times. After washing, the medium was removed and 200 μl of 0.22 μm filter-sterilized supernatant from *A.*

castellanii stimulated with 100 mM mannose for 48 hours were added to each well. Controls included 200 µl of complete KGM medium, PYG alone, PYG with 100 mM mannose, and supernatant from *A. castellanii* trophozoites grown in PYG for 48 hours. Plates were incubated at 35° C for 18 hours. After 18 hours, plates were centrifuged at 700 x g for five minutes and the supernatants were carefully removed from each well and counted on a gamma counter (Tracor Analytical, Atlanta, GA). Total release was determined by solubilizing the cells with detergent. All experiments were performed in triplicate. Cytoxicity was determined by the amount of ^{51}Cr released by the human corneal epithelial cells, and specific lysis was calculated as follows:

$$\frac{\text{(experimental cpm)-(spontaneous release cpm)}}{\text{(max. release cpm)-(spontaneous release cpm)}} \times 100\%$$

MOLECULAR WEIGHT SEPARATION OF SUPERNATANTS

Supernatants from mannose-stimulated cultures were removed during mid-log phase, sterilized using low protein binding 0.22 µm filter units, and fractionated using microcentrifugal concentrators with membranes having a molecular mass cut-off of approximately 50 or 100 kDa (Pall-Filtron, Northborough, MA). Three milliliters of culture supernatant were added to the centrifugal concentrator and centrifuged at 1,900 × g in a Sorvall RC5C floor centrifuge (Dupont, Newtown, CN) for one hour.

Supernatants were removed from the top chamber at 10x concentration, and 25 µl were used directly in the cytopathic effect assays (described below)

.

PROTEIN PURIFICATION

All purification procedures were performed at room temperature. Protein concentrations were determined by bicinchoninic acid protein assay (BCA) (Rockford, IL) using bovine serum albumin as a standard (179). Ten-fold concentrated PYG and ten-fold concentrated *Acanthamoeba* culture supernatants, either with or without 100 mM methyl-α-D-mannopyranoside, were analyzed by 4-15% SDS/PAGE Ready Gels under both reducing and non-reducing conditions. Supernatants were taken from trophozoites at mid-log phase.

For fast protein liquid chromatography (FPLC) (Amersham Pharmacia Biotech, Piscataway, NJ), culture supernatants of mannose-stimulated *Acanthamoeba* trophozoites were concentrated ten-fold using Ultrafree-15 centrifuge concentrators with a molecular cut-off of five kDa (Millipore, Bedford, MA). Samples were centrifuged at 3,000 x g for 20 minutes and passed in 0.5 ml volumes over a Superdex 200 (Amersham Pharmacia Biotech) column using PBS (pH. 7.2). Fractions were collected every 0.5 ml and examined by 4-15% SDS/PAGE and fractions containing the mannose-induced cytolytic protein were pooled, concentrated ten-fold, and buffer exchanged three times into 10 mM Tris buffer (pH 8.0) using Ultrafree 0.5 concentrators. Two hundred microliters, containing 1.0 mg of protein, were applied to a DEAE ionic-exchange column using 10 mM Tris buffer, pH 8.0 (Buffer A).

Adsorbed protein was eluted using a gradient of 10 mM Tris buffer, pH 8.0 with 1M NaCl (Buffer B). Fractions were examined for the ~133 kDa protein by 4-15% SDS/PAGE. An initial 15% buffer B step removed contaminating proteins, and the ~133 kDa protein was eluted between 15-30% of buffer B run at 0.1 ml/min. Fractions containing the ~133 kDa protein were pooled and concentrated ten-fold and washed three times with PBS (pH 7.2) to buffer exchange. Protein test samples were adjusted to 1.5, 7.8, and 15.6 μg in 25 μl of PBS (pH 7.2) and immediately used in cytotoxicity assays.

PRODUCTION OF CHICKEN ANTI-MIP-133 ANTISERUM

Chicken anti-MIP-133 antiserum was prepared by Aves Labs, Inc. (Aves Labs, Inc.) (Tigard, OR) as described on their company website (www.aveslabs.com). Briefly, four samples containing 100 μg of MIP-133 were excised from 4-15% SDS/PAGE gels, frozen at 20° C, and sent to Aves Lab, Inc. on dry ice. One chicken was immunized with 100 μg of MIP-133 every two weeks. One week after the fourth injection, six eggs were collected from the immunized chicken. Control eggs are taken from the same chicken prior to the first immunization with MIP-133. The yokes are removed from the eggs and the IgY fraction was purified. We received 50 ml of anti-MIP-133 IgY (50 mg IgY/ml) in PBS and 10 ml of pre-immunized IgY (10 mg/ml) in PBS.

IgY ELISA AND WESTERN BLOT

A conventional ELISA was used to demonstrate the specificity of the chicken anti-MIP-133 antibody. Briefly, 96-well plates were coated with 50 μg of MIP-133 and incubated overnight at 37° C in carbonate buffer. Plates were washed four times with PBS containing 0.05% Tween-20 (wash buffer; Sigma), then blocked with 0.5% BSA in PBS for 1 hour at room temperature. All subsequent antisera were diluted with blocking buffer and incubated at room temperature. Chicken anti-MIP-133 antiserum (Aves Labs, Inc.) was added at either a 1:50, 1:75, or 1:100 dilution for one hour at 4° C and washed three times in PBS. HRP conjugated goat anti-chicken IgY (Aves Labs, Inc.) was added at a dilution of 1:10,000 and incubated for 1 hour at 37° C. Plates were developed by adding 1.0 mM 2,2'-azinobis(3-ethyl-benzthiazoline-6-sulfonic acid) (Sigma) containing 0.003% H_2O_2 and incubated for 30 minutes at room temperature. After development, 100 μl of 10% SDS (Sigma) were added per well prior to reading on a microplate reader at 405 nm.

Western blot analysis was carried out using conventional techniques. Briefly, 30 μg of 10-fold concentrated crude supernatant taken from *A. castellanii* trophozoites grown in mannose were resolved using 4-25% ready gels. Gels were transferred to Trans-Immun-Blot PVDF membranes (Bio-Rad, Hercules, CA) using a Bio-Rad minitransfer apparatus. Blots were blocked in 5% dry milk in PBS (blocking buffer) overnight at 4° C prior to addition of 1:200 chicken anti-MIP-133 antiserum for one hour at room temperature. After one hour, membranes were washed in PBS and incubated in 1:2,000 rabbit anti-chicken IgG that was conjugated with alkaline

phosphatase (Sigma). After one hour, the membrane was washed three times in PBS and developed using NBT/BCIP stock solution (Roche, Mannheim, Germany) as recommended by the manufacturer.

ASSAY FOR CYTOPATHIC EFFECT (CPE)

The MIP-133 protein was added at 1.5, 7.8, and 15.6 μg of protein (in 25 μl PBS) to 96-well plates with confluent monolayers of the respective target cells (see Table 1 above) and incubated for 18 hours at 35°C. Each well contained 200 μl of the respective required growth medium. Inhibition experiments involved incubating the protein samples with either a 1:75 dilution of chicken anti-MIP-133 antiserum or chicken preimmune control serum, 1:50 dilution of pooled enteric washes from orally immunized Chinese hamsters (described below in the Collection of Chinese Hamster Antibodies section) or from control (PBS) immunized hamsters, or 1:50 and 1:100 dilutions of serum samples from intramuscularly immunized Chinese hamsters (described below in the Collection of Chinese Hamster Antibodies section). Additional control wells consisted of untreated target cells. Following incubation, all wells were washed three times with their respective growth medium and stained with Giemsa stain (Shandon, Inc., Pittsburgh, PA). After staining, the wells were washed three times with PBS (pH 7.2) and solubilized in 0.1 ml of 5% lauryl sulfate(SDS) in PBS. Solubilized cells were transferred to a new 96-well plate, and the optical density (OD) was read at 590 nm in a Molecular Devices Microplate Reader. Percent cytopathic effect (CPE) was calculated according to the following formula: % CPE =

100 - [(OD of experimental well - OD of supernatant alone/OD of control cells alone) × 100]. Assays were performed in triplicate.

PROTEIN INHIBITION AND DEGRADATION

Inhibition of the CPE was determined by incubating the purified protein test sample (15.6 μg in 25 μl PBS) in either 0.1 mM or 1.0 mM of phenylmethylsulfonyl fluoride (PMSF) (Sigma), 1 mM 1, 10-phenanthroline (Sigma), or 1 μM or 10 μM of cystatin (Sigma) for 30 minutes prior to use in CPE assays using Chinese hamster epithelial cells as target cells. Controls included ten-fold concentrated PYG containing 100 mM methyl-α-D-mannopyranoside or the untreated protein test sample. All assays were performed in triplicate.

To confirm that the MIP-133 cytolytic activity was due to the protein itself, protein degradation was performed by incubating the protein test samples with either pepsin (5mg/ml, Sigma) or proteinase K (5mg/ml, Sigma) for 4 hours at 37° C, or incubating the protein test samples at 100° C for 30 minutes. Control treatments included PBS (pH 7.2), 37° C for 4 hours, and pepsin or proteinase K alone applied directly to target cells. All treated samples were immediately used in CPE assays with HCORN target cells. All assays were performed in triplicate.

To confirm that MIP-133 had been effectively degraded by both pepsin and proteinase K, additional samples of MIP-133 were incubated with pepsin, proteinase K, and PBS for 18 hours before being added to a 96-well plate. These samples were

dried overnight and tested for detectable MIP-133 by ELISA using the IgY ELISA protocol mentioned above.

ZYMOGRAPHY

It is often useful to test for proteolytic activity when characterizing proteins. Among the possible methods, zymogram gels are a popular approach. The gels are cast with gelatin and serve as substrates for assessing protease activity. A positive result following renaturation and staining is distinguished by a clear band in a darkly stained gel.

Zymography overlays consisted of running the purified protein test sample (15.6 μg) on 4-15% SDS/PAGE ready gels at 4° C, and then soaking the gels in 1x zymogram renaturation (Bio-Rad) buffer at room temperature for 30 minutes. Protein test samples were either run untreated, or pretreated with with 1 mM PMSF or 10 μM cystatin for 30 minutes prior to loading. After 30 minutes, the gel was overlayed on top of a 10% gelatin zymogram gel (Bio-Rad) and incubated for two hours at 35° C. After incubation, gels were stained with bio-safe Coomassie G250 stain (Bio-Rad).

Dot zymography was performed by cutting holes in 10% gelatin zymogram gels with a 3 mm trephine. Test samples included 1.5 and 7.8 μg (in 10 μl) of MIP-133. Protease inhibition included pretreatment of 7.8 μg of MIP-133 with 1 mM PMSF or 10 μM cystatin for 30 minutes prior to addition to the zymogel. Proteolytic activity was determined by comparison with a standard curve generated by using

serial dilutions of collagenase (Sigma). Additional controls included undiluted PYG and PBS. All samples were in 10 μl volumes. Samples were applied in the 3 mm wells and incubated for 18 hours at 35° C. After incubation, gels were stained with bio-safe Coomassie G250 stain.

CONTACT LENS PREPARATION

Contact lenses were prepared from Spectra/Por dialysis membrane tubing (Spectrum Medical Industries, Los Angeles, CA) using a 3-mm trephine prior to heat sterilization. Lenses were placed in sterile 96-well microtiter plates (Costar, Cambridge, MA.) and incubated with $4x10^5$ (total volume in each well was 200 μl) *A. castellanii* trophozoites at 35°C for 24 hours. Attachment of amoebae to the lenses was verified microscopically before infection.

IN VIVO CORNEAL INFECTIONS

Acanthamoeba keratitis was induced as described previously (74, 105, 198). Briefly, Chinese hamsters were anesthetized with ketamine (100 mg/kg) (Fort Dodge Laboratories, Fort Dodge, IA) injected peritoneally. Prior to manipulation, the corneas were anesthetized by topical application of Alcain (Alcon Laboratories, Fort Worth, TX). Approximately 25 percent of the cornea was abraded using a sterile cotton applicator before placing the amoebae-laden lens onto the center of the cornea.

The eyelids were then closed by tarsorrhaphy using 6-0 Ethilon sutures (Ethicon, Somerville, NJ). The contact lenses were removed three to four days post infection and the corneas were visually inspected by microscopy for severity of disease. Visual inspections were recorded daily during the times indicated. The infections were scored on a scale of 0-5 based on the following parameters: corneal infiltration, corneal neovascularization, and corneal ulceration. The pathology was recorded as follows: 0 = no pathology, 1 = ≤ 10% of the cornea involved, 2 = 10-25%, 3 = 25-50%, 4 = 50-75%, and 5 = 75-100% as described previously (Fig. 5) (105). Any animals receiving a score of at least 1.0 for any parameter were scored as infected. In Chinese hamsters, *Acanthamoeba* keratitis resolves at approximately three weeks. At this time, there is a conspicuous absence of corneal opacity, edema, epithelial defects, and stromal necrosis and inflammation. Whole eye photos were taken by camera-enhanced light microscopy (Stemi 2000-C; Carl Zeiss MicroImaging, Thornwood, NY).

HISTOLOGICAL EXAMINATION

Infected eyes were removed and fixed in 10% Carson's formalin for 24 hours. Specimens were then embedded in paraffin, cut into 4 μm sections using a Reichert Histostat Rotary microtome (Reichert Scientific Instruments, Buffalo, NY) and placed on polysine hydrobromide precoated slides (Polysciences, Warrington, PA). Sections were stained with hematoxylin and eosin, covered with a coverslip and

Figure 5. Clinical photos and histology of Chinese hamsters infected with *Acanthamoeba castellanii*. Digital whole eye photos (left) were taken at 10X. Histological specimens were embedded in paraffin, cut into 4 mm sections, and stained with hematoxylin and eosin. Sections were photographed at 20 X. Note increased stromal edema and increased inflammation as clinical scores increase. Bar = 70 μm.

Figure 5

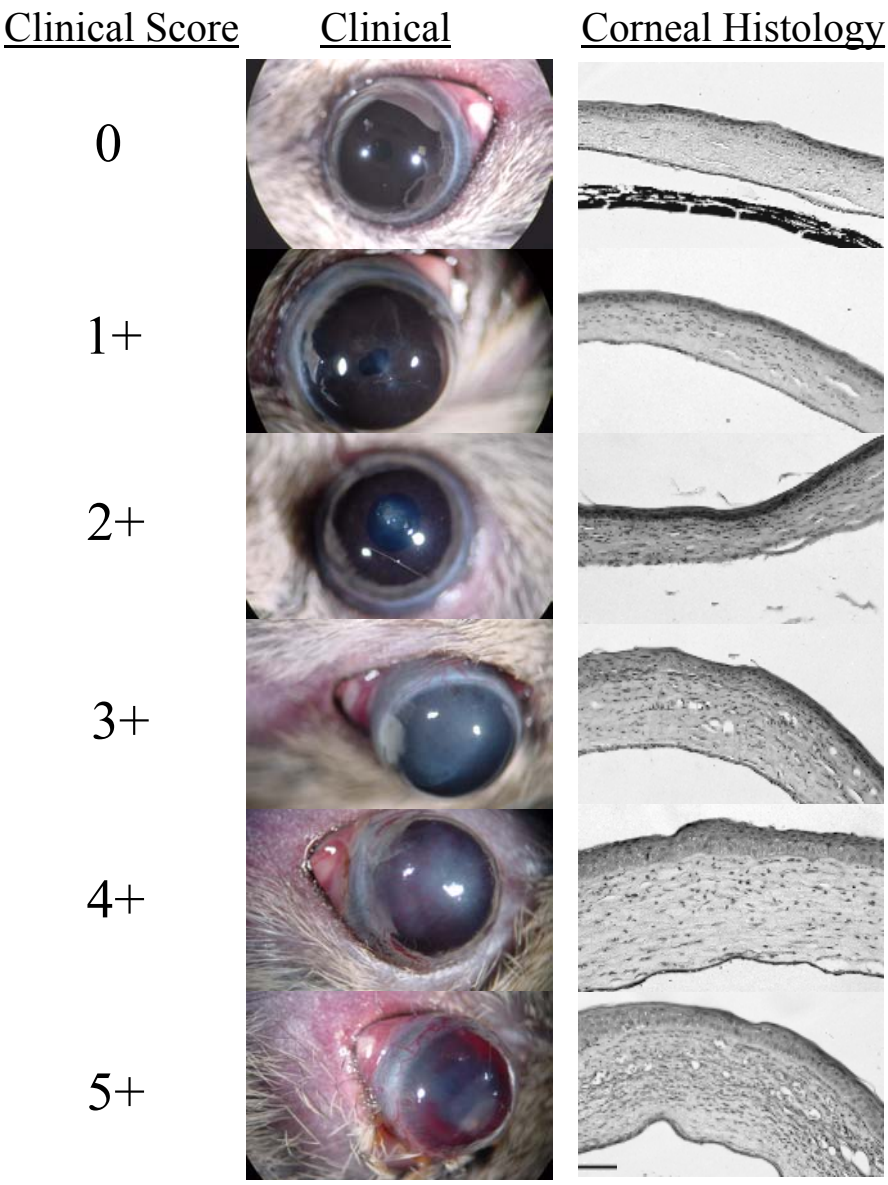

examined by light microscopy. Pictures were taken by camera-enhanced light microscopy (Fig.5) (BX50; Olympus Optical, Tokyo, Japan).

EXAMINATION OF CYTOPATHIC MECHANISMS BY FLOW CYTOMETRY

A flow cytometric assay was used to detect and quantify apoptosis induced by MIP-133. The experiment was carried out by using TACS^{TM}Annexin V–FITC kit (R&D systems) following the manufacturer's instruction. Briefly, HCE cells were grown to ~90% confluency in 24 well plates. The cells were then incubated with either 1.7 μg MIP-133 alone, or in combination with 20 uM Z-DEVD-FMK caspase-3 inhibitor (BD Pharmingen, San Diego, CA), caspase-9 inhibitor Z-LEHD-FMK (BD Pharmingin), caspase-10 inhibitor Z-AEVD-FMK (Pharmingin), the control inhibitor Z-FA-FMK, or staurosporine (Positive control for apoptosis; 3ug/ml; Sigma) for 18 hours. Cells were trypsinized, washed twice with PBS, stained with annexin-V (1μL) and PI (10μL) for 15 minutes, and apoptosis was quantified by flow cytometry at 488nm wavelength. The Annexin V apoptotic detection kit relies on the specific staining of both annexin V and propidium iodide. During apoptosis, the cell membrane's phospholipid asymmetry changes; phosphatidylserine (PS) is exposed on the outer membrane while membrane integrity is maintained. Annexin V specifically binds PS. Apoptotic cells stain with annexin V that has been conjugated to fluorescein; necrotic cells stain with annexin V and propidium iodide (PI), and live cells stain with neither. Cells that stain with PI were gated out. For each sample,

10,000 ungated events were acquired and the results were analyzed with CellQuest software (BD Biosciences, Franklin Lakes, NJ). The results are expressed as percent apoptosis.

PREPARATION OF CLODRONATE AND CARBOXYFLUORESCEIN LIPOSOMES

Multilamellar liposomes were prepared as described earlier (199, 200). Briefly, 8 mg cholesterol and 86 mg phosphatidylcholine (Lipoid GmbH, Ludwigshafen, Germany) were dissolved in 10 ml of chloroform in a round-bottomed flask. After low-vacuum rotary evaporation at 37° C, a thin film was then dispersed by gentle rotation for 10 minutes in PBS for the preparation of PBS-containing liposomes. Liposomes were washed twice by centrifugation in PBS at 100,000 x *g* for 30 minutes and resuspended in 4 ml of PBS that containing either 20 mg of clodronate (199)(Roche Diagnostics, Mannheim, Germany) or 2 ml of 70 mM carboxyfluorescein (10, 45, 191)(CF; Sigma) in 10mM Tris, pH 7.35. Untrapped clodronate or CF was removed by centrifugation of the liposome suspension in PBS. All liposomes were stored at 4° C and used within 7 days of preparation. Clodronate liposomes were tested for *in vitro* toxicity against macrophages prior to use. Additionally, clodronate liposomes were tested for toxicity to Langerhan's cells *in vitro*, and were found to have no affect on Langerhan's cell viability (data not shown). All liposomes, regardless of their components, ranged in size from 100 nm to 3 μm.

EXAMINATION OF CYTOPATHIC MECHANISMS BY LIPOSOME PERFORATION

The ability of MIP-133 to permeabilize liposomes was assayed by measuring the release of trapped CF (10, 191). 1.5, 7.8, or 15.6 μg of MIP-133 (in 25 μl PBS) was incubated with 100 μl of the CF-encapsulated liposome suspension (described above) at 37°C for 18 hours. The total volume of the suspension was increased to 2 ml by adding 140 mM NaCl-10mM Tris-HCl buffer (pH 7.2). After 18 hours, the suspensions were mixed by inversion and released CF was measured at 520 nm using a Beckman DU-64 spectrophotometer (Beckman Instruments, Fullerton, CA). At the conclusion of the experiment, maximum release was determined by sonicating the liposomes three times for 1 minute with a Fisher model 300 sonic dismembrator (Fisher, Farmingdale, New York) set at 40%.

MIGRATION ASSAY

An *in vitro* migration assay was utilized to determine the contribution of MIP-133 in the invasion of extracellular matrices by *Acanthamoebae* trophozoites. The assays were performed in 24-well transwells (6.5-mm diameter, 3.0 μm pore size, Costar, Corning Inc., Corning, NY). The top and bottom chambers were separated by a membrane that was coated with 100 μl Matrigel (Collaborative Biomedical

Products, Bedford, MA) that was diluted 1:3 in HBSS. Excess Matrigel was removed after 10 minutes, and the membranes were allowed to dry at room temperature. 1 x 10^5 *Acanthamoeba* trophozoites were placed in the top chamber in 100 µl PYG. Plates were incubated at 37° C for two hours, and *Acanthamoebae* were then counted in the bottom chamber by light microscopy (100 x). Inhibition assays involved incubating *A. castellanii* with either 1:75 or 1:100 dilutions of chicken anti-MIP-133 antiserum, chicken pre-immune serum, 1.0 mM of phenylmethylsulfonyl fluoride (PMSF; Sigma), or 10 µM of cystatin (Sigma) for 30 minutes prior to addition to the upper chambers. All experiments were performed in triplicate.

COLLAGEN DIGESTION ASSAY

Collagen digestion assays were performed in 96-well microtiter plates as a means of determining the capacity of MIP-133 to degrade types I and IV collagen, the predominant collagen species found in the human cornea. Microtiter plates were coated with either 10 µg of human collagen type I (Sigma) or type IV (US Biological, Swampscott, MA) in 50 µl PBS (64). Plates were incubated at 37° C overnight to dry. After drying, plates were washed three times with PBS and then incubated with either 15.6 µg (in 25 µl PBS) of MIP-133, PBS, or 0.1 mg (in 25 µl PBS) of *Clostridium histolyticum* collagenase (Sigma) for 24 or 72 hours at 37° C. Well volumes were increased to 100 µl by adding PBS. Wells were then washed three

times with PBS, incubated with either 1:500 mouse anti-collagen type IV IgG or 1:2000 mouse anti-collagen type I IgG (Sigma) as the primary antibody for one hour. Plates were then washed three times in PBS and incubated with 1:20,000 goat anti-mouse IgG conjugated with horseradish peroxidase (HRP) (Southern Biotechnology Associates, INC., Birmingham, AL) for one hour. Plates were washed three times in PBS and read at OD 405 nm in a Molecular Devices Microplate Reader (Menlo Park, CA). Inhibition studies involved coincubating MIP-133 with the chicken anti-MIP-133 antiserum diluted 1:75 or control antiserum diluted 1:75. All experiments were performed in triplicate.

IMMUNIZATIONS

For oral immunizations, Chinese hamsters received one ml of 0.1 M sodium carbonate (pH 9.6, Sigma) by gavage tube prior to administration of either 100 μg of MIP-133 (in 100 μl of PBS) plus 10 μg of neutralized cholera toxin (Sigma), 200 μg of MIP-133 plus 20 μg of neutralized cholera toxin, or 400 μg of MIP-133 plus 40 μg of neutralized cholera toxin (105). Immunizations were administered once a week for four weeks prior to infection with *A. castellanii*. Control groups included animals immunized with equivalent doses of neutralized cholera toxin alone or untreated prior to infection.

Intramuscularly immunized animals received either 100 μg, 200 μg, or 400 μg of MIP-133 (in 50 μl of PBS) mixed in 50 μl Freund's complete adjuvant for the initial immunization. Subsequent immunizations were performed using Freund's incomplete adjuvant. Immunizations were administered once a week for four weeks prior to infection with *A. castellanii*. Control groups included animals immunized with equivalent doses of PBS or untreated prior to infection.

COLLECTION OF CHINESE HAMSTER ANTIBODIES

Oral immunization is an effective method for inducing IgA antibodies that are expressed in mucosal secretions including the tears, saliva, and enteric mucosa (105, 107). The volume of tears produced by Chinese hamsters is infinitesimal. However, significant quantities of IgA antibodies can be isolated from enteric washes from orally immunized hamsters (107). Accordingly, enteric washes were assessed for the presence of anti-MIP-133 IgA antibodies following oral immunization. Enteric washes were collected as stated previously (106). Briefly, the enteric washes were collected from Chinese hamsters after being anesthetized with ketamine and euthanized by cervical dislocation. Approximately 20 cm of the small intestine were removed and 10 ml of PBS were injected through the intestinal lumen using an 18-gauge needle. The enteric washes were collected and centrifuged at 700 x *g* to remove sediments. Protease inhibitor cocktail tablets (Boehringer-Mannheim,

Indianapolis, IN) were added to the pooled enteric washes at one tablet per 10 ml. The enteric washes were stored at -80° C until used.

Serum samples from intramuscularly immunized Chinese hamsters were collected via cardiac puncture. Sera was isolated and immediately used for detection of MIP-133 specific IgG.

ANTIBODY TITRATIONS FOR IMMUNIZED ANIMALS

A conventional ELISA was used to titrate anti-MIP-133 antibodies in immunized animals. 96-well assay plates were coated with 50 μg of MIP-133 overnight at 37° C in carbonate buffer. Plates were washed four times with PBS containing 0.05% Tween-20 (wash buffer; Sigma), then blocked with 0.5% BSA in PBS for one hour at room temperature. Serum samples and enteric washes were diluted in blocking buffer and incubated in MIP-133 coated plates (50 μg; as mentioned in the IgY ELISA section) at room temperature. For IgA detection, enteric washes were added at a dilution of 1:2 for one hour and then washed three times in PBS. Rabbit anti-Chinese hamster IgA hyperimmune serum (107) was then added at a dilution of 1:2 and incubated for two hours at 37° C. Plates were washed three times in PBS, and 50 μl of 1:1000 goat anti-rabbit IgG conjugated with HRP (Santa Cruz Biotechnology) was added to each well. For IgG detection, the serum samples were diluted 1:100 for one hour prior to incubation at 37°C. Plates were then washed

three times in PBS and hamster IgG was detected by goat anti-hamster IgG conjugated to HRP (1:10,000; Accurate).

Plates were developed by adding 1.0 mM 2,2'-azinobis(3-ethyl-benzthiazoline-6-sulfonic acid) (Sigma) containing 0.003% H_2O_2 and incubating for 30 minutes at room temperature. After development, 100 µl of 10% SDS (Sigma) were added per well prior to reading on a microplate reader at 405 nm.

IN VIVO **LIPOSOME TREATMENT**

Both clodronate and PBS containing liposomes were administered via subconjunctival injection on days -8, -6, -4, and -2 of infection. 50 µl of the liposome preparation were injected in four quadrants of the eye encircling the entire conjunctiva. Our laboratory has previously shown that this protocol depletes virtually all of the conjunctival macrophages in the Chinese hamster (199). *Acanthamoeba* infections were produced via contact lens placement one day after the final injection of liposomes.

Clodronate liposome treated animals were orally immunized on days 5, 12, 19, and 26 days post infection using 400 µg of the MIP-133 protein as described above.

CHAPTER THREE
Results

EFFECTS OF MANNOSE BINDING ON *ACANTHAMOEBA* TROPHOZOITES

Effects of Mannose on Trophozoite Proliferation, Cyst Development and Excystment

Before examining the effects that mannose has on *A. castellanii's* pathogenic cascade, it was important to determine how it might affect the growth of the organism.

A. castellanii cultures grown in medium that contained mannose consistently produced approximately 50% fewer trophozoites than cultures not containing mannose (Fig. 6A, B). Trophozoites grown in 100 mM galactose or 100 mM lactose were not significantly different from amoebae grown in PYG alone (Fig. 6A). Stationary phases were reached at the same time in both groups (~125 hours).

Upon reaching stationary phase, cultures stimulated with mannose produced nearly 3-fold more cysts (Fig. 6B). This increase was sustained during the remaining times that were monitored. Moreover, the mannose cultures produced cysts approximately 24 hours earlier than cultures grown without mannose. The results indicate that mannose induced encystment.

Figure. 6. Effects of mannose on *A. castellanii* proliferation, encystment and excystment. (A) Trophozoites grown in PYG, PYG with 100 mM methyl-α-D-mannopyranoside (Man), lactose (Lac), or galactose (Gal). Samples were examined spectrophotometrically at optical density 480. (B) Trophozoites grown in PYG or PYG with 100 mM methyl-α-D-mannopyranoside. Samples were examined for trophozoites (Trophs) and cysts by compound microscopy. (C) Cysts were incubated in PYG, PYG with 100 mM methyl-α-D-mannopyranoside, PBS, and examined by compound microscopy. The results shown are representative of three separate experiments.

Figure 6

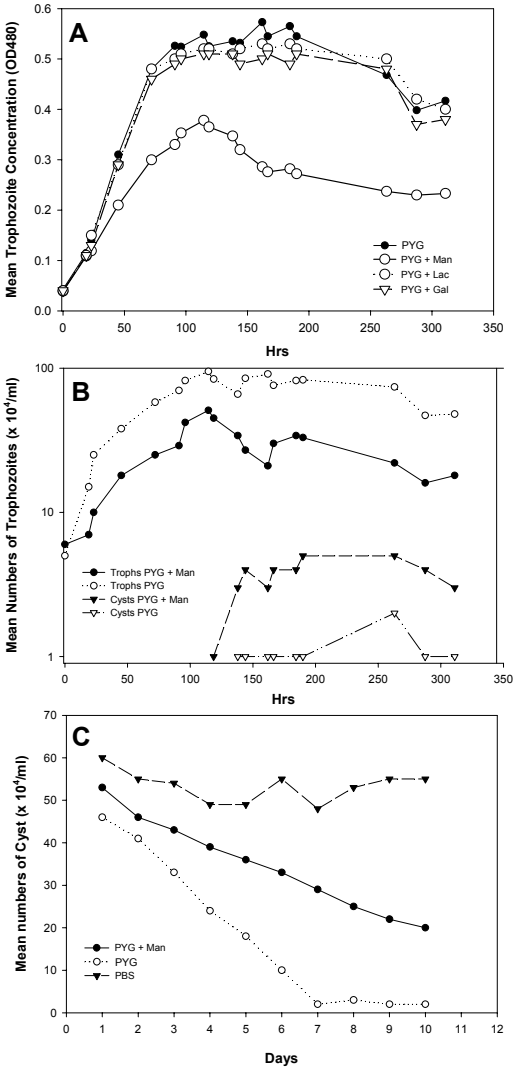
A
Mean Trophozoite Concentration (OD480)
Hrs
PYG
PYG + Man
PYG + Lac
PYG + Gal
B
Mean Numbers of Trophozoites (x 10⁴/ml)
Hrs
Trophs PYG + Man
Trophs PYG
Cysts PYG + Man
Cysts PYG
C
Mean numbers of Cyst (x 10⁴/ml)
Days
PYG + Man
PYG
PBS

To assess whether the presence of mannose affected excystment, cultures containing 100% cysts were placed in PYG, PYG with 100 mM methyl-α-D-mannopyranoside, or PBS (Fig. 6C). *Acanthamoeba* cysts in PYG displayed a consistent reduction in the number of cysts until approximately day 7, when they became too few to count, while the numbers of trophozoites increased proportionately. By contrast, cysts incubated in PYG with mannose exhibited a slower rate of excystment, and by day 10, approximately 50% of the cysts had excysted. Cyst populations in PBS remained constant throughout the times monitored.

Isolation of Mannose-Induced Cytolytic Factor

Crude supernatants from *A. castellanii* trophozoites that had been stimulated with 100 mM methyl-α-D-mannopyranoside for 48 hours produced 95% cytolysis to human corneal epithelial cells (HCE) as measured by ^{51}Cr release (fig 7). This was a 40% increase in cytolytic activity when compared to supernatants from trophozoite cultures not stimulated with mannose. Moreover, in agreement with a previous report (108), trophozoites treated with an unrelated sugar, lactose, did not demonstrate increased cytopathic activity against either human or Chinese hamster corneal epithelial cells (data not shown). It is noteworthy that human small intestinal epithelial cells (Fhs-74) cells were not susceptible to any of the supernatants tested (data not shown).

Figure 7. Chromium release assay of supernatants from mannose-stimulated *Acanthamoeba castellanii* trophozoites against human corneal epithelial cells. 2×10^6 ^{51}Cr-labeled human corneal epithelial cells were plated into 96-well flat-bottomed microtiter plates. Plates were centrifuged at 700 x g for five minutes and washed with complete KGM medium three times. Then 200 μl of 0.22 μm filter-sterilized supernatant from *A. castellanii* stimulated with 100 mM mannose for 48 hours were added to each well for 18 hours at 35° C. After 18 hours, plates were centrifuged at 700 x g for five minutes and the supernatants were removed from each well and counted on a gamma counter. Controls included KGM medium, PYG alone, PYG with 100 mM mannose, and supernatant from *A. castellanii* trophozoites grown in PYG for 48 hours. Total release was determined by solubilizing the cells with detergent. All experiments were performed in triplicate.

Figure 7

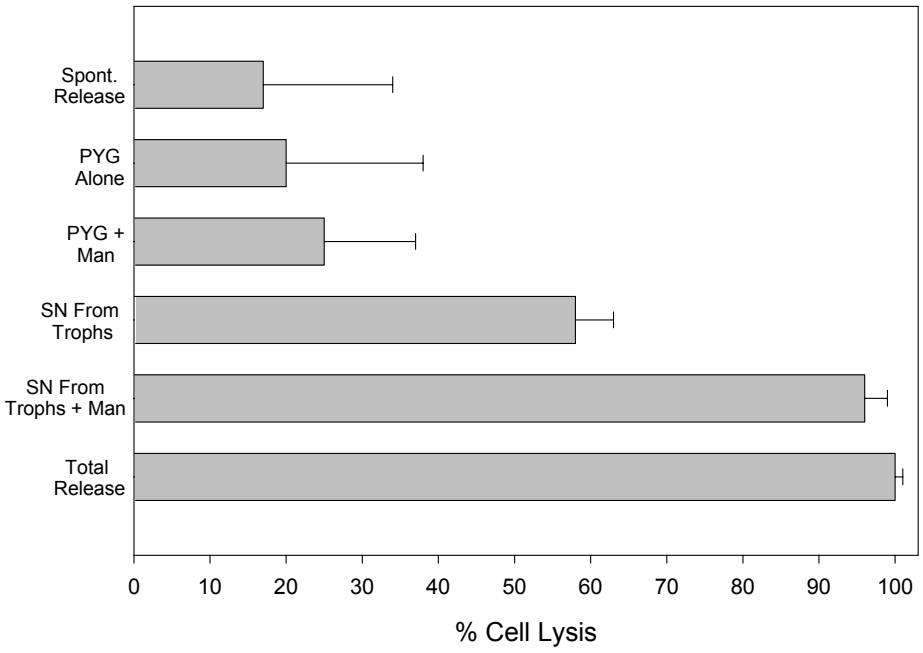
Spont. Release
PYG Alone
PYG + Man
SN From Trophs
SN From Trophs + Man
Total Release
0
10
20
30
40
50
60
70
80
90
100
% Cell Lysis

Size fractionated supernatants displayed killing of the HCE and HCORN cells in both upper fractions from the 50 and 100 kDa membrane concentrators (Fig. 8A, B). Unfractionated 10x concentrated supernatants from mannose-stimulated trophozoites displayed approximately 90% CPE, while 10x concentrated PYG supplemented with mannose did not produce cell death. In contrast, small intestinal epithelial cells (Fhs-74) cells were not killed by either the upper or lower fractions tested (Fig. 8C).

Initial examination involved SDS/PAGE analysis of concentrated supernatants. Mannose-stimulated supernatants contained two new bands at approximately 133 kDa and 70 kDa (Fig. 9). Both the 133 kDa and 70 kDa bands appeared under non-reducing and reducing conditions. Supernatants from *A. castellanii* grown without mannose did not produce the two bands (Fig. 9). Lane A reflects the large amount of proteins from the proteose peptone and yeast extracts that are present in PYG medium. Notice how the *Acanthamoebae* effectively utilize the medium proteins after 48 hour (Fig 9; Lanes B and C).

Initial purification of the 133 kDa mannose-induced protein (MIP-133) via Superdex 200 size-exclusion FPLC chromatography generated high yields of the protein as seen by SDS/PAGE analysis (Fig. 10A). Further separation via DEAE ionic exchange produced a single band between a 15-30% elution gradient (Fig. 10B; Lanes 3-8). Fractions collected between 0–14% (Fig. 10B; Lanes 1-2) and 31–100% (data not shown) did not contain the 133 kDa protein.

Comment:

Figure. 8. Molecular weight estimation of cytopathic factors in supernatants derived from *A. castellanii* trophozoites stimulated with 100 mM methyl-α-D-mannopyranoside. Supernatants were collected at mid-log phase as described in the *Materials and Methods* section, and size fractionated with centrifuge concentrators having a molecular mass cut-off of either 50 or 100 kDa. Fractions were added to human corneal epithelial (HCE) cells (A), hamster corneal epithelial (HCORN) cells (B), or human small intestine epithelial (Fhs-74) cells (C) for 18 hours and CPE was assessed spectrophotometrically. Each bar shows the mean ± SE of triplicate counts.

Figure 8

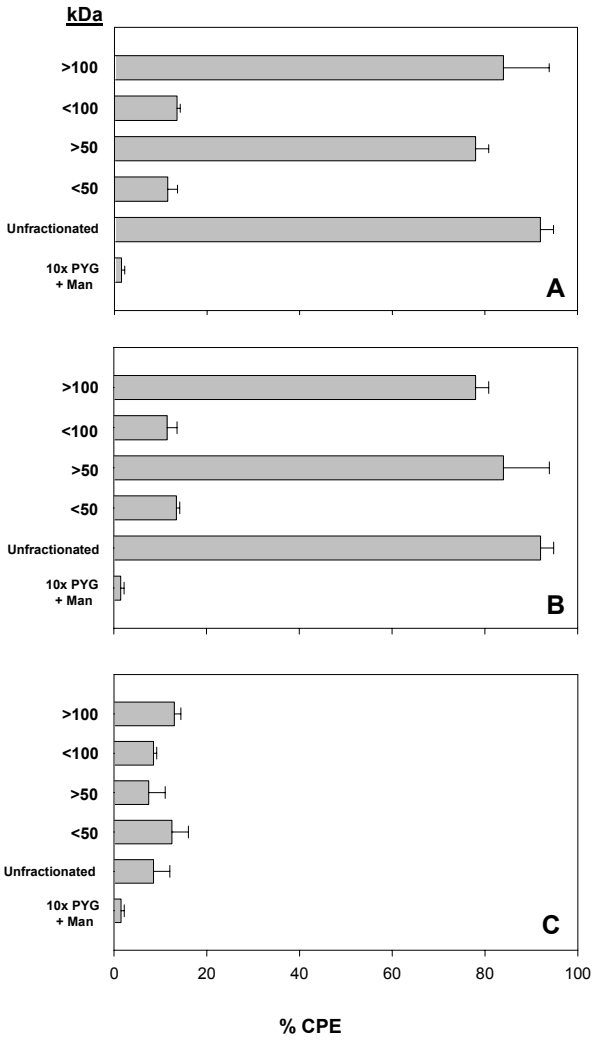
kDa
>100
<100
>50
<50
Unfractionated
10x PYG
+ Man
A
>100
<100
>50
<50
Unfractionated
10x PYG
+ Man
B
>100
<100
>50
<50
Unfractionated
10x PYG
+ Man
C
0
20
40
60
80
100
% CPE

Figure. 9. Protein analysis of *Acanthamoeba* supernatants. Lanes: L = MW ladder: A = PYG concentrated ten-fold: B = supernatants from trophozoites grown in PYG alone and concentrated ten-fold: C = supernatants from trophozoites grown in PYG supplemented with 100 mM methyl-α-D-mannopyranoside and concentrated ten-fold. Supernatants were collected at mid-log phase.

Figure 9

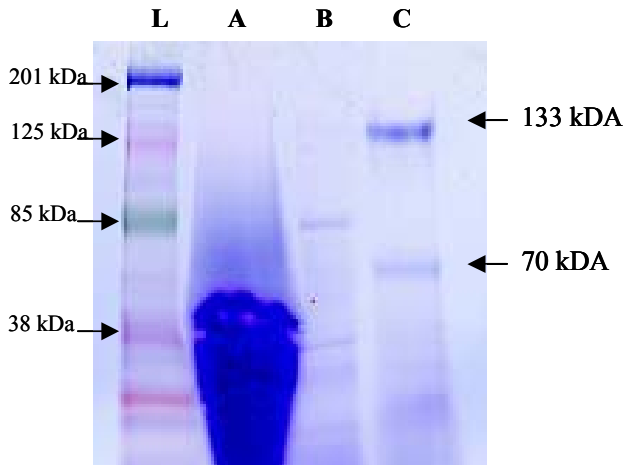

Figure. 10. Purification of the 133 kDa protein. Supernatants from trophozoite cultures were grown in 100 mM methyl-α-D-mannopyranoside and isolated by size over Superdex 200 columns, pooled, and separated by DEAE ion exchange as described in the *Materials and Methods* section. A) MW ladder (Lane L), supernatant concentrated 10x (Lane 1), unconcentrated supernatant (Lane 2), single fraction of 133 kDa protein from Superdex 200 column (lane 3), and pooled fractions of 133 kDa protein from superdex200 column (lane 4). B) MW ladder (lane L), individual fractions eluted from DEAE resin representing the 15% clearance step (lanes 1-2), and fractions eluted by 15-30% gradient at 0.1 ml/min (lanes 3-8).

Figure 10

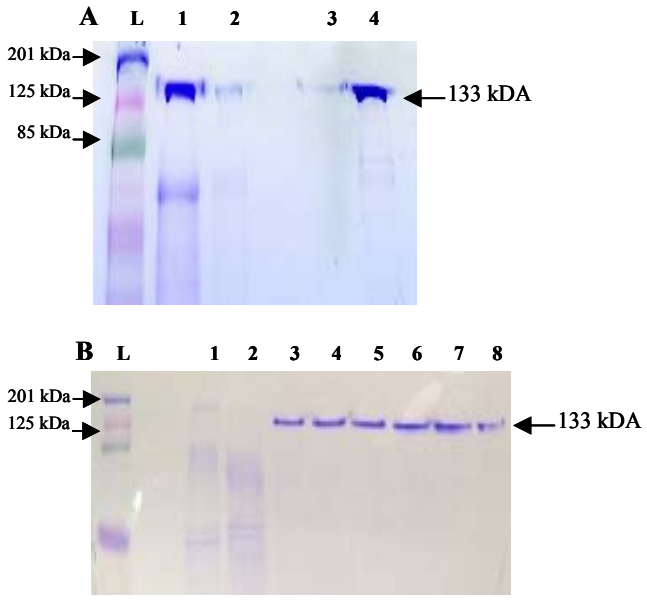
A
L
1
2
3
4
201 kDa
125 kDa
85 kDa
133 kDA
B
L
1
2
3
4
5
6
7
8
201 kDa
125 kDa
133 kDA

In vitro CPE Analysis of the Purified 133 kDa Protein

To test the cytopathic activity of the purified protein, samples were adjusted to 1.5, 7.8, and 15.6 μg of protein in 25 μl of PBS (pH 7.2).

The human corneal epithelial cells were killed by the 133 kDa protein in a dose-dependent manner (Fig. 11A). The lowest concentration tested (1.5 μg) killed approximately 20% of the corneal cells, while the higher concentrtion (15.6 μg) killed approximately 90% of the target cells. Microscopic examination revealed piecemeal death of individual corneal cells, as opposed to entire layers of cells lifting up off the bottom of the wells (Fig. 12, Column A). In contrast to the human corneal epithelial cells (HCE), hamster corneal epithelial cells (HCORN) were extensively killed by all three concentrations of the protein tested (Fig. 11B and Fig. 12, Column B). As before, the human intestinal epithelial cells (Fhs-74) were not susceptible to any of the protein samples tested (Fig. 11C and Fig. 12, Column C). Fractions collected by DEAE ionic exchange and eluted between 0-14% and 31-100%, did not induce significant CPE (data not shown). In all three treatment groups, the PBS control did not kill any of the cell lines tested.

Figure. 11. CPE assays using the purified 133 kDa mannose-induced protein. Test samples were adjusted to 1.5, 7.8, and 15.6 μg of protein in 25 μl of PBS before addition to HCE (A), HCORN (B), or Fhs-74 (C) cells in 96 well microtiter plates. Plates were incubated at 37° C for 18 hours. CPE was assessed spectrophotometrically. Each bar shows the mean ± SE of triplicate counts. ** and ***, significantly different from untreated controls ($P < 0.01$ and $P < 0.001$, respectively).

Figure 11

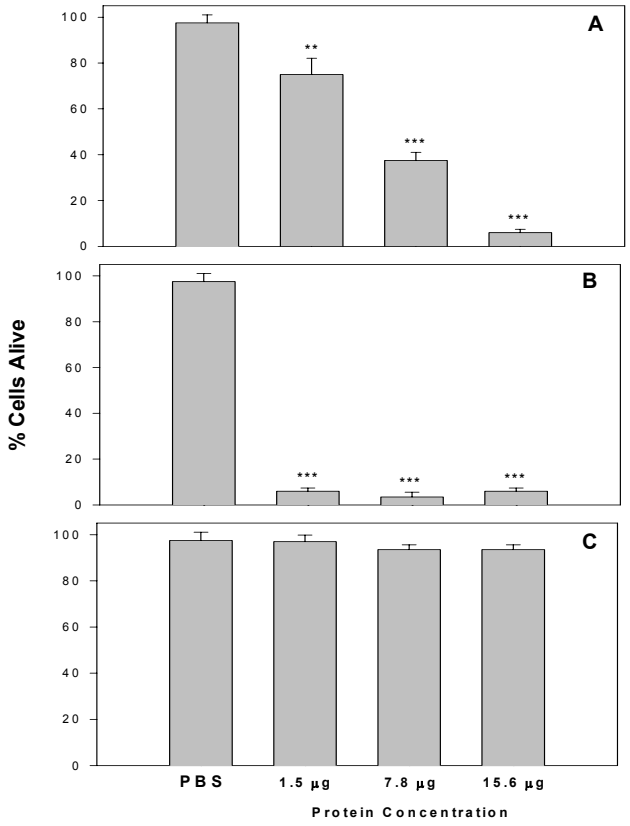
A
B
C
100
80
60
40
20
0
**
***
***
***
***
***
% Cells Alive
PBS
1.5 µg
7.8 µg
15.6 µg
Protein Concentration

Figure. 12. Light microscopy photographs of target cells incubated with the purified MIP-133. Target cells examined were HCE (Column A), HCORN (Column B) and Fhs-74 cells (column C). Cell were then treated with either PBS (Con Row) or 1.5 μg (Row 1), 7.8 μg (Row 2), or 15.6 μg (Row 3) of MIP-133 at 37° C for 18 hours. Photographs were taken at 10x magnification. Photos are representatives of triplicate experiments.

Figure 12

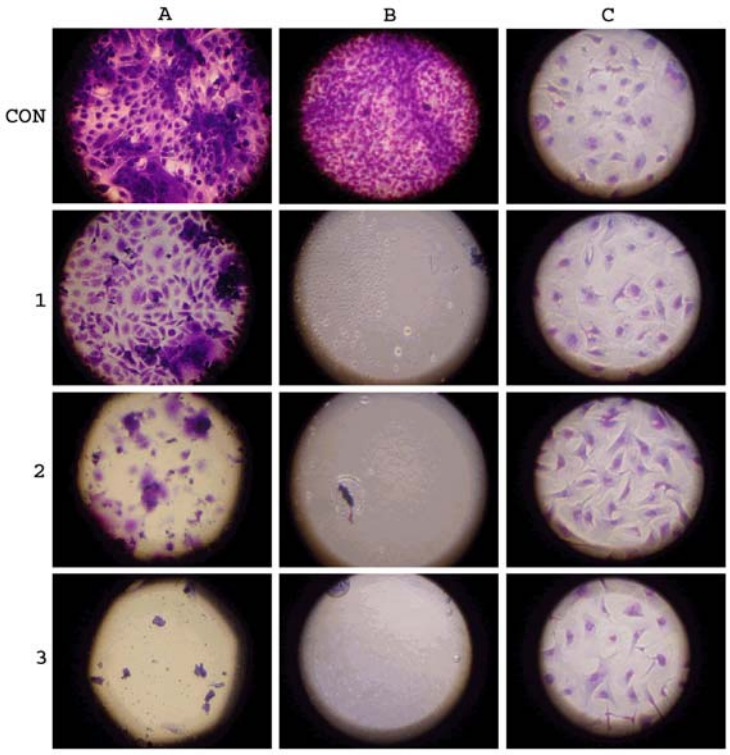

Previous studies in our lab have shown that the CPE produced by crude mannose-stimulated supernatants of *A. castellanii* could be inhibited by the serine protease inhibitor PMSF (108). Figure 13A shows that the 0.1 mM PMSF treatment inhibited the cytolytic function of the 133 kDa protein by 20%, while the higher dose (1 mM) inhibited CPE by approximately 60%. Treatment with 1 mM 1, 10-phenanthroline inhibited CPE of Chinese hamster corneal epithelial cells (HCORN) by 70%, and in combination with 1 mM PMSF, completely inhibited CPE. PMSF and 1, 10-phenanthroline alone did not affect the viability of the HCORN cells (data not shown). In contrast, cystatin did not inhibit the cytolytic activity of MIP-133 (Fig. 13B).

To determine whether proteases could reduce the CPE of MIP-133, the test samples were digested with either pepsin or proteinase K. Figure 13C shows that both pepsin and proteinase K significantly ($P<0.001$) reduced the CPE of HCORN cells by 80% and 70% respectively. Proteinase K and pepsin alone did not affect cell viability (data not shown). The cytolytic activity of the samples incubated at 100° C for 30 minutes was reduced by approximately 90%. PBS treatment did not significantly reduce the cytolytic activity of the protein as compared to the untreated control.

Figure. 13. Effects of protease inhibitors and protease degradation on CPE produced by MIP-133. A) Serine protease inhibition. Purified MIP-133 was pretreated with either 0.1 mM or 1 mM PMSF, 1 mM 1, 10-phenanthroline (1, 10-P), or 1 mM PMSF and 1 mM 1, 10-phenanthroline combined, for 30 minutes prior to addition to HCORN cells. B) Cysteine protease inhibition. Purified MIP-133 was pretreated with 1 μM or 10 μM cystatin for 30 minutes prior to addition to HCORN cells. C) Protein degradation was assessed by incubating MIP-133 with either 10 μg pepsin or 10 μg proteinase K at 37° C for 4 hours prior to addition to HCORN cells. As an additional control, MIP-133 was heated at 100° C for 30 minutes prior to addition to HCORN cells. CPE was assessed spectrophotometrically as mentioned in *Materials and Methods*. Each bar shows the mean ± SE of triplicate counts. * and ***, significantly different from treatments with protein test samples ($P < 0.05$ and $P < 0.001$, respectively).

Figure 13

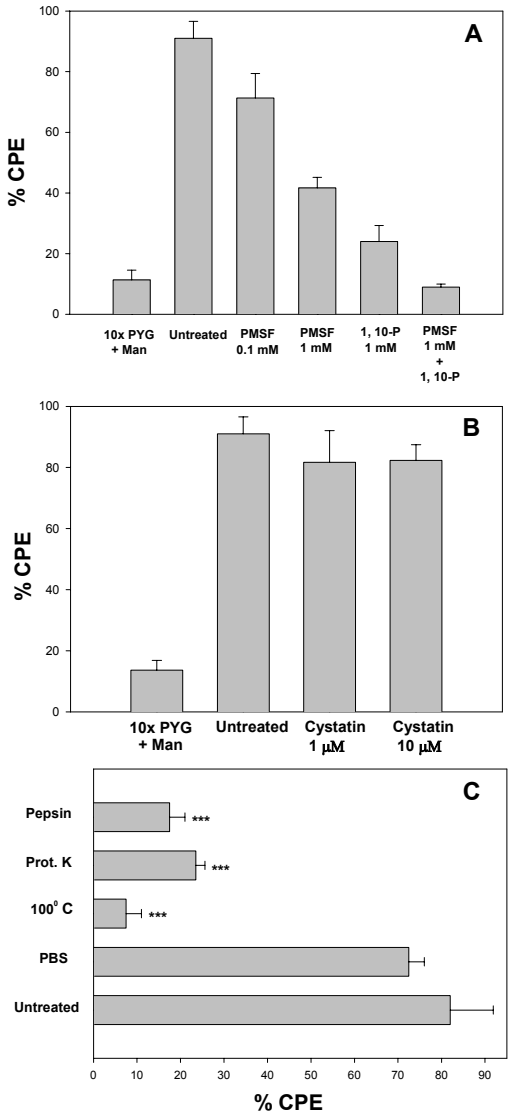
A
% CPE
100
80
60
40
20
0
10x PYG + Man
Untreated
PMSF 0.1 mM
PMSF 1 mM
1, 10-P 1 mM
PMSF 1 mM + 1, 10-P
B
% CPE
10x PYG + Man
Untreated
Cystatin 1 μM
Cystatin 10 μM
C
Pepsin
Prot. K
100° C
PBS
Untreated
***
0
10
20
30
40
50
60
70
80
90
% CPE

CYTOPATHIC MECHANISM AND IMMUNOGENICITY OF MIP-133

Mechanism of cell death in vitro

MIP-133 has been shown to be very effective at killing both human and hamster corneal epithelial cells *in vitro,* the first mechanistic barrier that the amoebae must surpass. Although MIP-133 can be effectively blocked by serine protease inhibitors, it is unknown how the protein kills corneal epithelial cells.

Other pathogenic amoebae, such as *Entamoeba histolytica*, kill target cells by elaborating protein molecules, called amoebapores, that disrupt mammalian cell membranes culminating in osmotic lysis (109, 110). Accordingly, experiments were performed to determine if MIP-133 produced similar lysis of the cell membrane. Other investigators have used liposomes loaded with carboxyfluorescein as a model of detecting protein-mediated cell lysis (10, 45, 191). Carboxyfluorescein encapsulated liposomes were incubated with 1.5, 7.8, or 15.6 μg of MIP-133 for 18 hours at 37° C. The quantity of released carboxyfluorescein was assessed spectrophotometrically as a measure of membrane disruption. The results indicated that none of the three concentrations of MIP-133 induced significant release of carboxyfluorescein (Fig 14).

Figure. 14. Lipid perforation assay. Carboxyfluorescein-encapsulated liposomes were prepared as described in the *Materials and Methods*. Untrapped carboxyfluorescein (CF) was removed by centrifugation of the liposome suspension in PBS. 1.5, 7.8, or 15.6 μg (in 25 μl PBS) of MIP-133 was incubated with 100 μl of the carboxyfluorescein encapsulated liposomes at 37° C for 18 hours. The total volume of the suspension was increased to 2 ml by adding 140 mM NaCl-10mM Tris-HCl buffer (pH 7.2). After 18 hours, liposome perforation was assessed spectrophotometrically. Maximum fluorescein release was produced by sonication. Each bar shows the mean ± SE of triplicate counts.

Figure 14

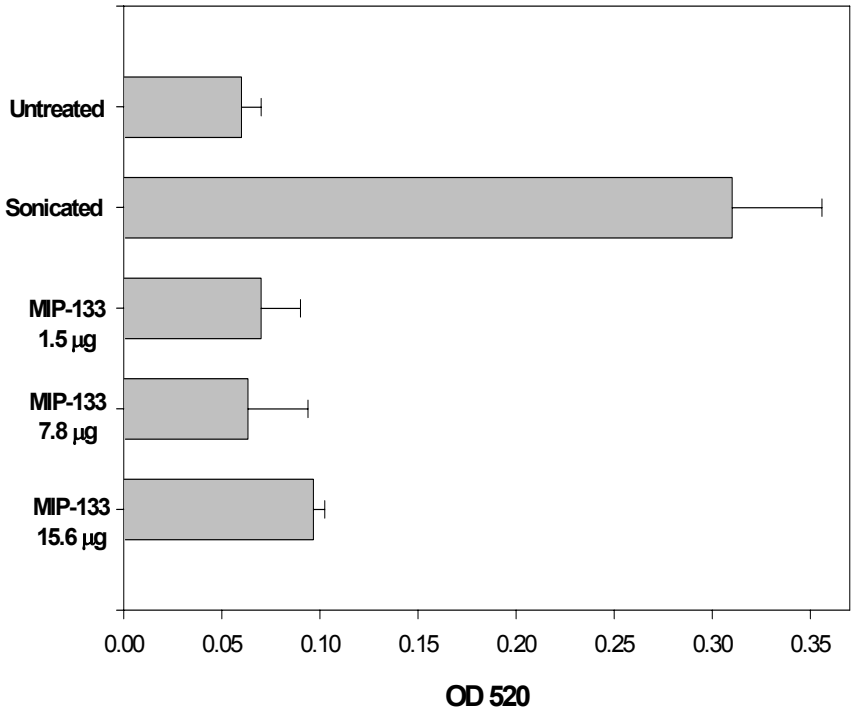
Untreated
Sonicated
MIP-133
1.5 µg
MIP-133
7.8 µg
MIP-133
15.6 µg
0.00
0.05
0.10
0.15
0.20
0.25
0.30
0.35
OD 520

Our lab has previously demonstrated that *Acanthamoeba* trophozoites induce apoptosis of various mammalian cells (8). Therefore, it was important to determine if MIP-133 killed corneal epithelial cells by an apoptotic mechanism. Human corneal epithelial cells (HCE) were incubated with of MIP-133 (1.7 μg/200 μl culture medium) at 37° C for 18 hours and tested for apoptosis using the Annexin V flow cytometry assay. HCE cells treated with MIP-133 displayed a 3-fold increase in apoptosis over untreated cells (Fig. 15). Incubation with a caspase-3 inhibitor (Z-DEVD-FMK) completely abrogated MIP-133-mediated apoptosis. By contrast, the control inhibitor did not affect apoptosis. Moreover, incubation of HCE cells with the caspase-9 (Z-LEHD-FMK) and -10 inhibitors (Z-AEVD-FMK) significantly reduced MIP-133-mediated apoptosis (Fig. 16). The caspase-9 inhibitor reduced apoptosis by approximately 45%, while the caspase-10 inhibitor nearly abrogated apoptosis. The control inhibitor did not reduce apoptosis.

Figure. 15. Effects of caspase-3 inhibition on MIP-133-mediated apoptosis. Human corneal epithelial cells (HCE) were treated with 1.7 μg MIP-133 either alone, or with 20 μM of the caspase-3 inhibitor Z-DEVD-FMK (cas-3 Inh), or the control inhibitor Z-FA-FMK (con Inh). HCE cells were examined by Annexin V flow cytometry as described in the *Materials and Methods* section. Additional controls included untreated cells and cells treated with 3 μg/ml staurosporine (STS) as a positive control. Bars represent the means ± SE of triplicate experiments. *** = significantly different from untreated controls ($P < 0.001$).

Figure 15

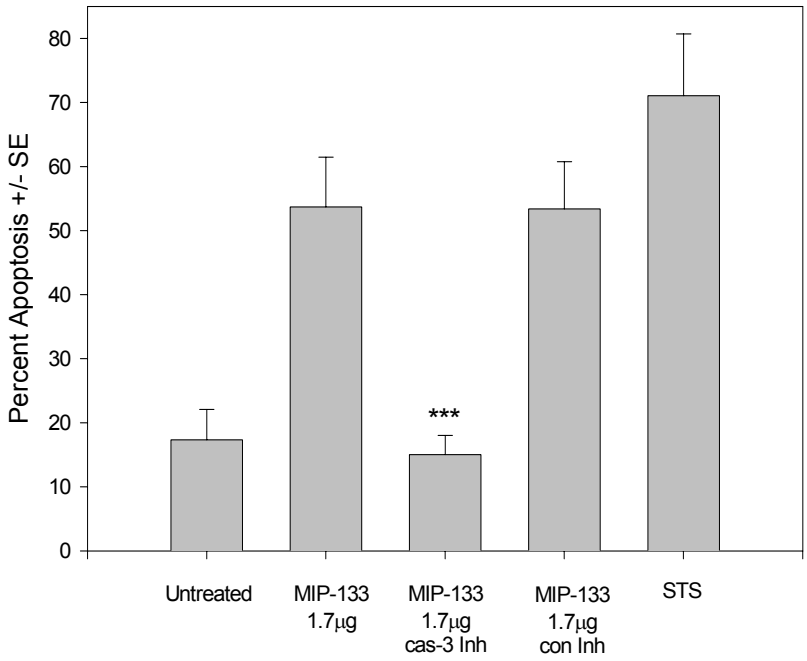
Percent Apoptosis +/- SE
80
70
60
50
40
30
20
10
0
***
Untreated
MIP-133 1.7μg
MIP-133 1.7μg cas-3 Inh
MIP-133 1.7μg con Inh
STS

Figure. 16. Effects of caspase-9 and caspase-10 inhibition of MIP-133-mediated apoptosis. Human corneal epithelial cells (HCE) were treated with 1.7 μg MIP-133 either alone, or with 20 μM of the caspase-9 inhibitor Z-LEHD-FMK (cas-9 Inh), caspase-10 inhibitor Z-AEVD-FMK (cas-10 Inh), or the control inhibitor Z-FA-FMK (con Inh). HCE cells were examined by Annexin V flow cytometry as described in the *Materials and Methods* section. Additional controls included untreated cells and cells treated with 3 μg/ml staurosporine (STS) as a positive control. Bars represent the means ± SE of triplicate experiments. *** = significantly different from untreated controls ($P < 0.001$).

Figure 16

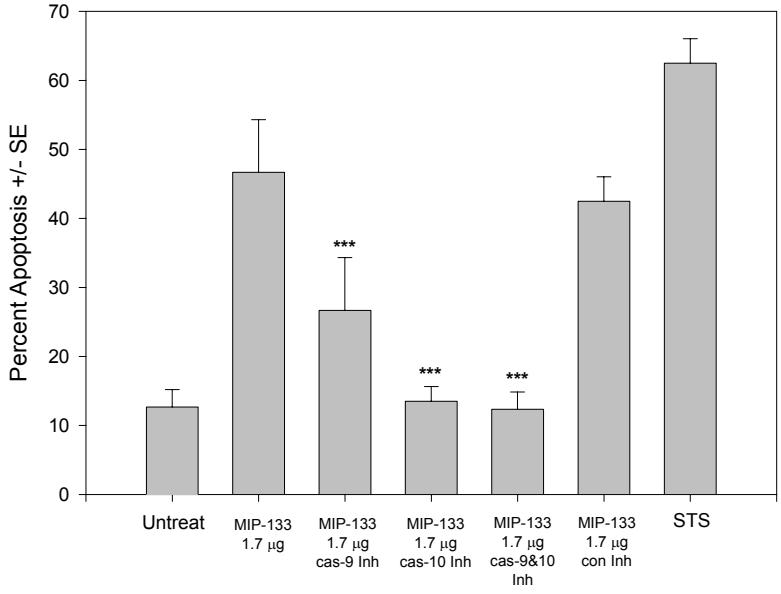
Percent Apoptosis +/- SE
70
60
50
40
30
20
10
0
***
***
***
Untreat
MIP-133 1.7 μg
MIP-133 1.7 μg cas-9 Inh
MIP-133 1.7 μg cas-10 Inh
MIP-133 1.7 μg cas-9&10 Inh
MIP-133 1.7 μg con Inh
STS

Correlation of MIP-133 Production with Pathogenic and Non-Pathogenic Strains of *Acanthamoeba*

Acanthamoeba spp. can exist in a wide range of habitats as free-living amoebae or as facultative pathogens. The *A. castellanii* used in the present studies was an ocular isolate from a diseased eye (ATCC 30868). Therefore, it was important to determine if MIP-133 production was restricted to pathogenic strains of *Acanthamoeba* spp. and correlated with pathogenic potential, or if it was also produced by non-pathogenic environmental isolates of *Acanthamoeba* spp.

None of the *Acanthamoeba* soil isolates grown in the presence of mannose produced MIP-133 as detected by SDS/PAGE (Fig 17A). *A. castellanii*, the positive control, produced significant amounts of the MIP-133. Moreover, all three of the soil isolates produced either no disease, or significantly less disease as compared to the standard ocular isolate of *A. castellanii* (Fig. 17B). Both *A. astronyxis* and *A. castellanii neff* produced symptoms similar to the sterile contact lens control. However, *A. hatchetti* did produce a significant infection, even though this strain did not produce detectable MIP-133 protein.

By contrast, the clinical isolates of *Acanthamoeba* produced the MIP-133 protein when grown in mannose (Fig. 18A). All three clinical isolates tested produced similar levels as compared to *A. castellanii* (Fig. 18B). Additionally, when tested in vivo, the clinical isolates produced severe *Acanthamoeba* keratitis. *A. culbertsoni* produced clinical symptoms more severe than *A. castellanii*.

Figure. 17. Correlation between MIP-133 production and ability of *Acanthamoeba* soil isolates to cause keratitis. A) *Acanthamoeba* spp. were grown for 48 hours at 35° C in PYG containing 100 mM methyl-α-D-mannopyranoside. Supernatants were collected, filter sterilized, concentrated 10-fold, and analyzed by SDS/PAGE. Lanes: L = MW ladder; 1 = *A. hatchetti* (soil isolate); 2 = *A. astronyxis* (soil isolate); 3 = *A. castellanii neff* (soil isolate); 4 = *A. castellanii* (clinical isolate). The arrow points at ~133 kDa. B) Ability of *Acanthamoeba* spp. to cause keratitis in Chinese hamsters. Animals were infected with *Acanthamoeba*-laden lenses as described in the *Materials and Methods* section. The results are representative of three separate experiments (N=8 each group).

Figure 17

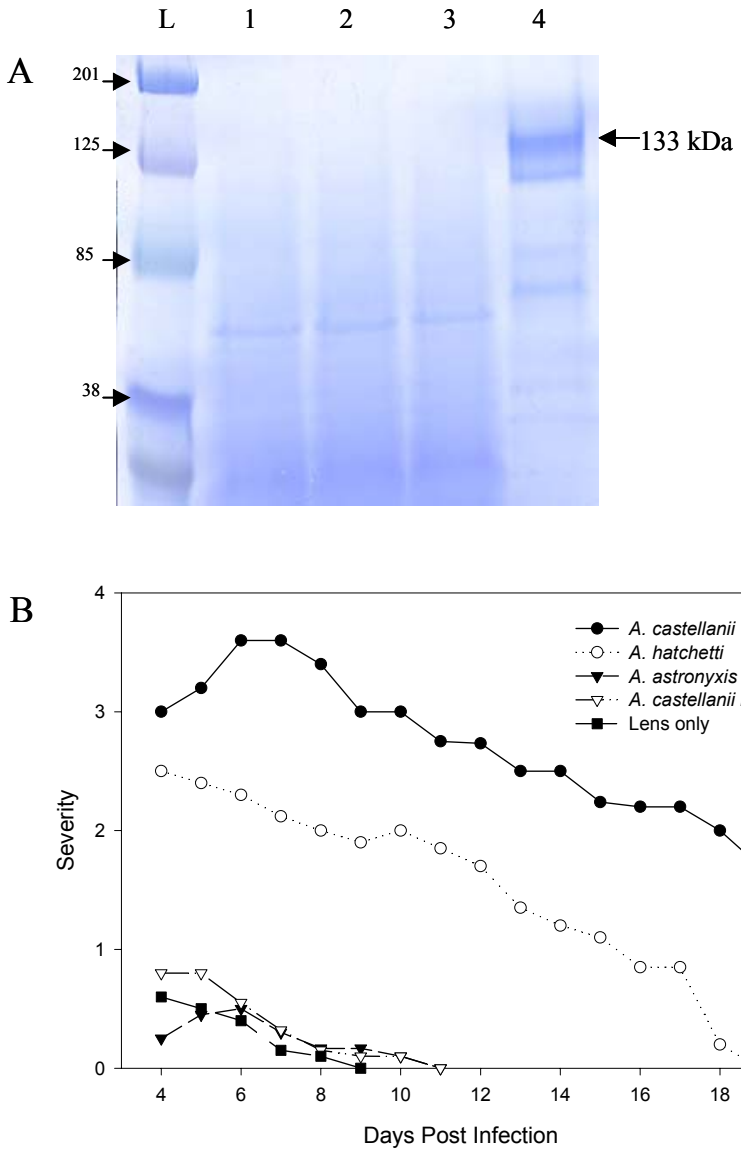
A
L
1
2
3
4
201
125
85
38
133 kDa
B
A. castellanii
A. hatchetti
A. astronyxis
A. castellanii neff
Lens only
Severity
Days Post Infection
0
1
2
3
4
4
6
8
10
12
14
16
18
20

Figure. 18. Correlation between MIP-133 production and ability of clinical isolates of *Acanthamoeba* to cause keratitis. A) *Acanthamoeba* spp. were grown for 48 hours at 35° C in PYG containing 100 mM methyl-α-D-mannopyranoside. Supernatants were collected, filter sterilized, concentrated 10-fold, and analyzed by SDS/PAGE. Lanes: L = MW ladder; 1 = *A. culbertsoni*; 2 = *A. polyphaga*; 3 = *A. rhysodes*; 4 = *A. castellanii*. The arrow points at ~133 kDa. B) Ability of *Acanthamoeba* spp. to cause keratitis in Chinese hamsters. Animals were infected with *Acanthamoeba* laden lenses as described in the *Materials and Methods* section. The results are representative of three separate experiments (N=8 each group).

Figure 18

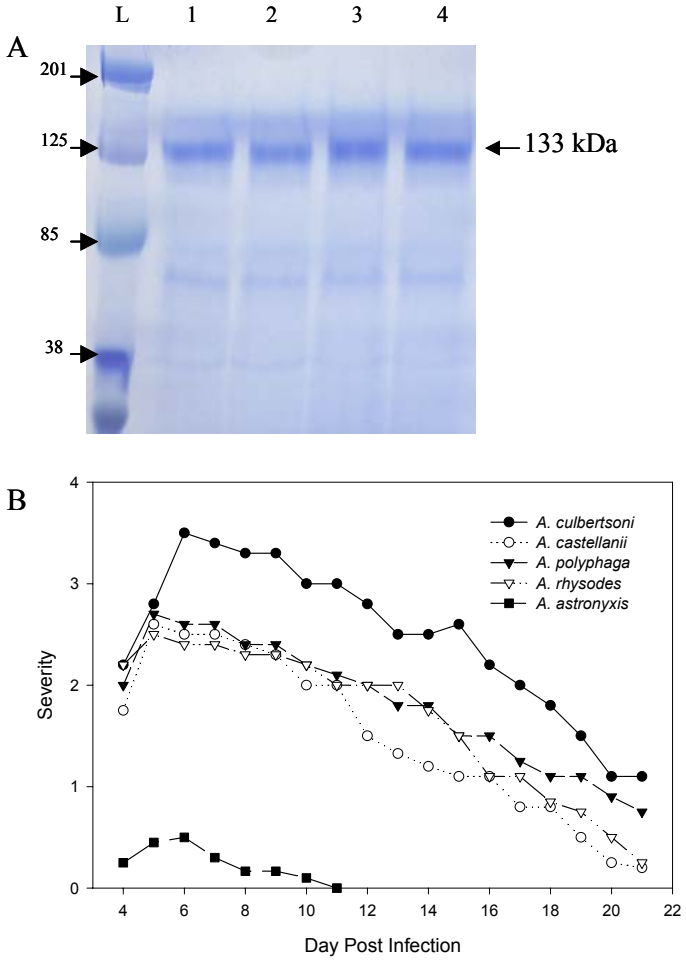
A
L
1
2
3
4
201
125
85
38
133 kDa
B
A. culbertsoni
A. castellanii
A. polyphaga
A. rhysodes
A. astronyxis
Severity
Day Post Infection
0
1
2
3
4
4
6
8
10
12
14
16
18
20
22

The *in vitro* characterization of MIP-133 indicated that it is a serine protease. Other serine proteases, such as urokinase-type plasminogen activator and tissue-type plasminogen activator, are known to facilitate tumor cell invasion of basement membranes and extracellular matrices (65, 97, 155). Therefore, experiments were performed to determine if MIP-133 secretion correlated with trophozoite invasiveness through an artificial extracellular matrix (Matrigel). All three of the soil isolates tested were ineffectual in migrating through the collagenous Matrigel (Fig. 19A). By contrast, all of the clinical isolates were capable of migrating through the Matrigel at approximately equal levels as compared to the original standard ocular isolate of *A. castellanii* (Fig. 19B).

An antibody was generated in chickens to confirm the role of MIP-133 in the pathogenesis of *Acanthamoeba* keratitis. The specificity of the chicken anti-MIP-133 was confirmed by western blot (Fig. 20A). Preimmune serum did not bind to the mannose-stimulated protein (data not shown). The strength of the anti-MIP-133 antiserum was confirmed by ELISA and showed reactivity of the anti-MIP-133 antiserum to MIP-133 at 1:50, 1:75, and 1:100 dilutions (Fig. 20B). As with the western blot, the preimmune serum did not react with MIP-133 in the ELISA. Furthermore, ELISA analysis of MIP-133 after pepsin and proteinase K digestion confirmed that most of the MIP-133 reactivity with the chicken anti-MIP-133 antiserum was degraded after 18 hours of incubation with these enzymes (Fig. 21).

None of the soil isolates produced MIP-133 either constitutively or after cultivation in 100 mM mannose (Fig. 22A). By contrast, all of the clinical isolates of

Figure. 19. Invasiveness of soil and clinical isolates of *Acanthamoeba* through a collagenous matrix. 1 x 10^5 *Acanthamoeba* trophozoites from either soil (A) or clinical isolates (B) were placed in the upper chambers of 3.0 μm pore size transwells coated with Matrigel. After 2 hours, trophozoites were counted in the bottom chamber. Bars indicate means ± SE of 10 random high powered fields (100X).

Figure 19

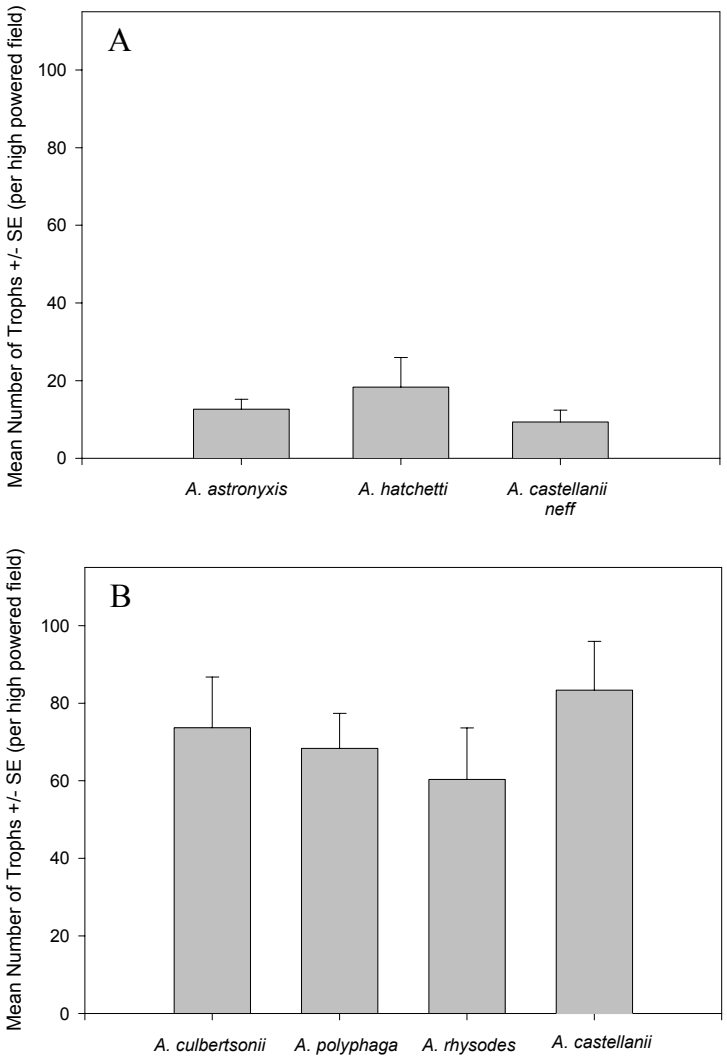
A
Mean Number of Trophs +/- SE (per high powered field)
100
80
60
40
20
0
A. astronyxis
A. hatchetti
A. castellanii neff
B
Mean Number of Trophs +/- SE (per high powered field)
100
80
60
40
20
0
A. culbertsonii
A. polyphaga
A. rhysodes
A. castellanii

Figure. 20. Specific binding of the chicken anti-MIP-133 antiserum. A) Western Blot. Crude supernatants taken from *A. castellanii* trophozoites grown in 100 mM mannose for 48 hours at 35° C were resolved by SDS/PAGE and transferred to PVDF membranes. Membranes were first incubated with chicken anti-MIP-133 antiserum, followed by rabbit anti-chicken IgG-alkaline phosphatase as described in the *Materials and Methods* section. The membranes were then washed and developed using NBT/BCIP stock solution. Arrow indicates the 133 kDa band. B) ELISA. 96-well plates were coated with 50 μg of MIP-133 and allowed to dry. After drying, wells were blocked and incubated with 1:50, 1:75, or 1:100 of either the chicken anti-MIP-133 antiserum or pre-immune chicken serum. Wells were then washed and incubated with goat anti-chicken IgY-horse radish peroxidase. ELISA plates were developed and read at 405 nm. Bars represent the means ± SE of triplicate experiments. *** = significantly different from pre-immune serum of same dilution ($P < 0.001$).

Figure 20

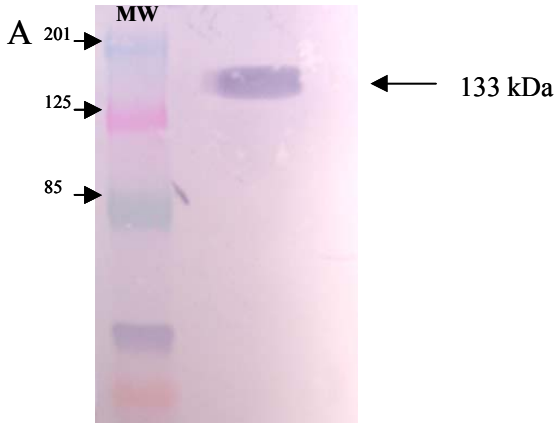
A
MW
201
125
85
133 kDa

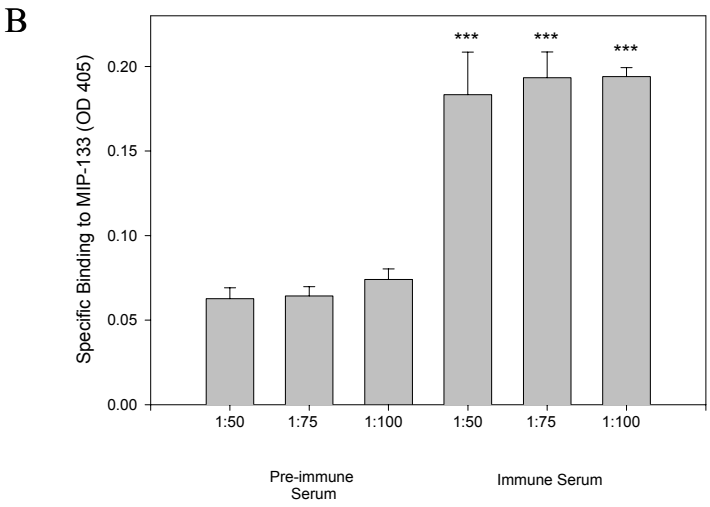
B
Specific Binding to MIP-133 (OD 405)
0.00
0.05
0.10
0.15
0.20
***
***
***
1:50
1:75
1:100
1:50
1:75
1:100
Pre-immune Serum
Immune Serum

Figure 21. Detection of MIP-133 after pepsin and proteinase K digestion. Protein degradation was assessed by incubating 15.6 μg of MIP-133 with either 10 μg pepsin or 10 μg proteinase K at 35° C for 18 hours prior to addition to a 96-well plate. Control samples were incubated with PBS. Plates were allowed to dry overnight and were analysed by ELISA. Each bar shows the mean ± SE of triplicate counts. * and *** significantly different from treatments with protein test samples($P < 0.05$ and $P < 0.001$, respectively).

Figure 21

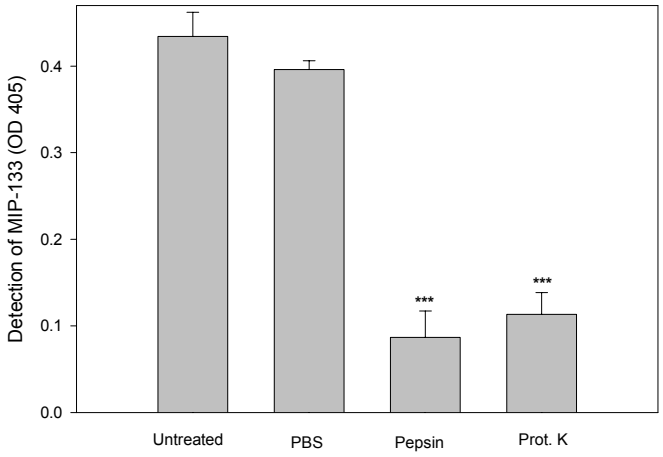
Detection of MIP-133 (OD 405)
0.0
0.1
0.2
0.3
0.4
***
***
Untreated
PBS
Pepsin
Prot. K

Figure. 22. Production of MIP-133 as a result of mannose stimulation. *Acanthamoeba* spp. were grown in PYG containing 100 mM methyl-α-D-mannopyranoside. Supernatants were collected at mid-log phase, filter sterilized, concentrated 10-fold, and analyzed by ELISA. A) The results of 3 soil isolates (*A. hatchet*, *A. astronyxis*, and *A. castellanii neff*) and one clinical isolate (*A. castellanii*). B) The results of 4 clinical isolates (*A. culbertsoni*, *A. polyphaga*, *A. rhysodes*, and *A. castellanii*). Each bar shows the mean ± SE of triplicate counts.

Figure 22

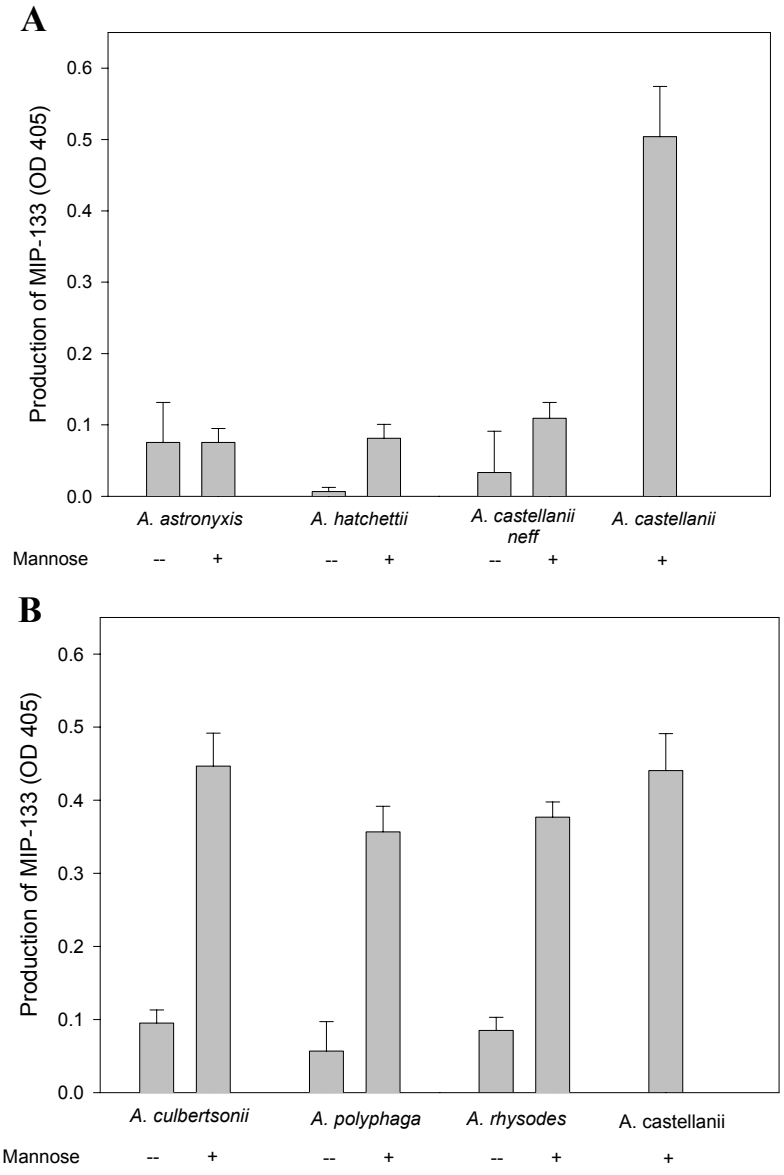
A
Production of MIP-133 (OD 405)
0.0
0.1
0.2
0.3
0.4
0.5
0.6
A. astronyxis
A. hatchettii
A. castellanii neff
A. castellanii
Mannose
-- + -- + -- + +
B
Production of MIP-133 (OD 405)
0.0
0.1
0.2
0.3
0.4
0.5
0.6
A. culbertsonii
A. polyphaga
A. rhysodes
A. castellanii
Mannose
-- + -- + -- + +

Acanthamoeba produced MIP-133 after mannose stimulation, but not when cultured in the absence of mannose (Fig. 22B).

THE ROLE OF MIP-133 IN THE SUBSEQUENT STEPS OF THE PATHOGENIC CASCADE OF *ACANTHAMOEBA* KERATITIS

MIP-133 Effectively Degrades the Collagen Matrixes that Comprise Bowman's Membrane and the Stroma

The pathogenesis of *Acanthamoeba* keratitis begins with the trophozoites binding to the mannose on the corneal epithelium surface via a mannose-binding receptor (217). This is a critical step in the initiation of keratitis, that is followed by the rapid destruction of the corneal epithelial cell layer. Immediately after destroying the corneal epithelial cells, trophozoites penetrate Bowman's membrane and invade the stroma. MIP-133 was shown to effectively kill corneal cells, and we hypothesized that MIP-133 also played an important role in facilitating the invasion of the trophozoites into the stroma. Therefore, experiments were performed to investigate whether MIP-133 had proteolytic activity against the types of collagen that comprise the matrices of the cornea.

MIP-133 was incubated with zymography gels impregnated with gelatin to test for proteolytic activity. The zymography overlay using 15.6 μg of MIP-133 (in 25 μl PBS) displayed lytic ability against the gelatin in the zymogels (Fig. 23A). Within two hours, lytic zones could be readily visualized. Dot zymography using 1.5

and 7.8 μg of MIP-133 (both in 10 μl PBS) displayed 7 mm and 10 mm lysis diameters respectively (Fig. 23B). Proteolytic activity was comparable to 0.1 mg (in 10 μl PBS) of collagenase (approximately 41 units) under the conditions tested (data not shown). All samples pretreated with PMSF displayed 100% inhibition of lysis. Samples pretreated with cystatin produced the same lysis as the untreated protein samples on the overlay and the dot zymography (10 mm). Neither the PYG nor the PBS control was found to degrade gelatin.

Bowman's membrane and the corneal stroma are comprised almost entirely of collagen (Types IV and I respectively). To determine the effect of MIP-133 on these corneal components, we performed experiments to ascertain the ability of MIP-133 to specifically degrade types IV and I collagen.

MIP-133 was efficient at degrading both human types I and IV collagen (Fig. 24). At 24 hours, type IV collagen was more efficiently degraded compared to type I. However, by 72 hours, both forms of collagen were nearly completely degraded. Degradation of collagen was similar to the collagenase control at both the 24 and 72 hour time points tested. The PBS control did not show lytic activity against either collagen.

Figure. 23. Proteolytic activity of MIP-133. A) 15.6 μg (in 25 μl PBS) of MIP-133 was electrophoresed in 4-15% SDS/PAGE ready gels and then overlaid onto 10% gelatin zymogels for 2 hours. Lanes: 1 = untreated protein sample; 2 =, pretreatment with 10 μM cystatin; 3 = pretreatment with 1 mM PMSF. B) 10% gelatin zymogels, with 3 mm cut-outs were incubated with 1.5 and 7.8 μg (in 10 μl PBS) of the purified protein. Some samples were pretreated with 1 mM PMSF or 1 μM cystatin for 30 minutes prior to addition. Additional controls included straight PYG and PBS.

Figure 23

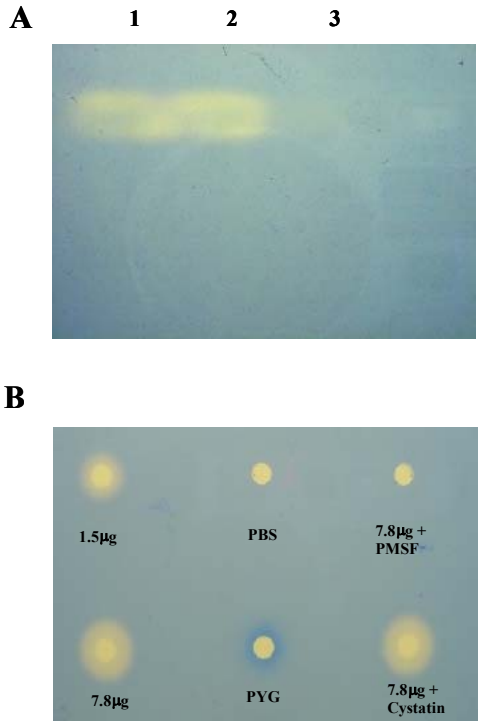

Figure. 24. Collagenolytic activity of MIP-133. 10 μg of human collagen types I and IV were incubated and dried onto 96-well plates. Wells were treated with either 15.6 μg (in 25 μl PBS) of MIP-133, PBS, or 0.1 mg (in 25 μl PBS) of collagenase (Col) for 24 hours (A) and 72 hours (B). Well volumes were increased to 100 μl with the addition of PBS. Sample wells were then washed 3 times with PBS, incubated with mouse anti-collagen type IV IgG or mouse anti-collagen type I IgG as the primary, followed by goat anti-mouse IgG-HRP as described in the *Materials and Methods* section. Plates were developed and read at OD 405 nm. Bars represent the means ± SE of triplicate experiments. *, ** and ***, significantly different from PBS treated controls ($P < 0.05$, $P < 0.01$ and $P < 0.001$, respectively).

Figure 24

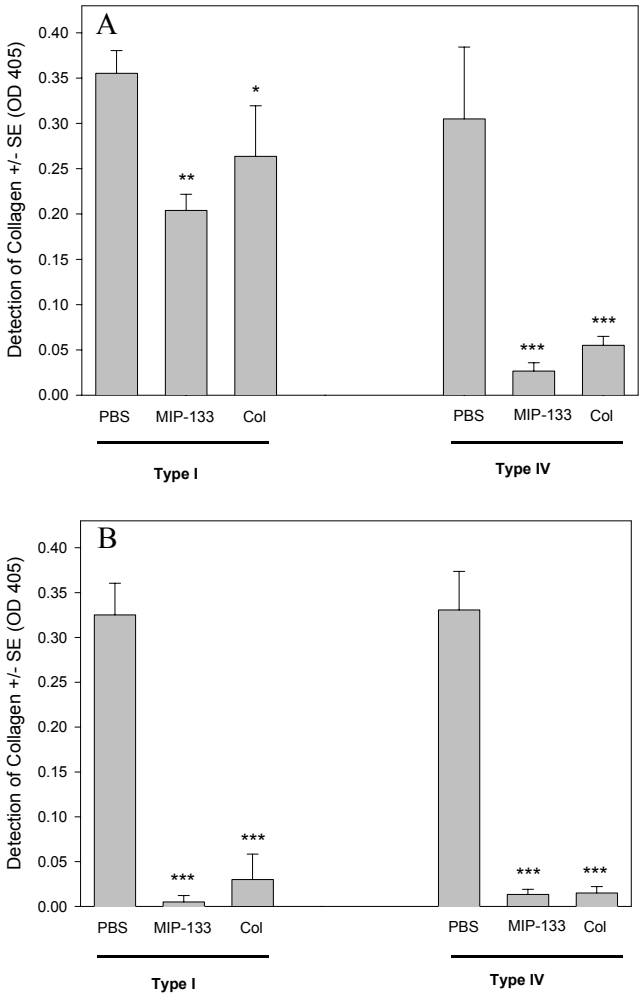
A
Detection of Collagen +/- SE (OD 405)
0.40
0.35
0.30
0.25
0.20
0.15
0.10
0.05
0.00
**
*
***
***
PBS
MIP-133
Col
PBS
MIP-133
Col
Type I
Type IV
B
Detection of Collagen +/- SE (OD 405)
0.40
0.35
0.30
0.25
0.20
0.15
0.10
0.05
0.00
***
***
***
***
PBS
MIP-133
Col
PBS
MIP-133
Col
Type I
Type IV

Specificity of MIP-133 Induced CPE Against Ocular Derived Cell

MIP-133 kills corneal epithelial cells from both human and Chinese hamsters, two mammalian species that are susceptible to *Acanthamoeba* keratitis. Following the destruction of the corneal epithelial layer, MIP-133 degrades collagen types IV and I that comprise the bulk of Bowman's membrane and the corneal stroma. Even though the corneal epithelial cells were destroyed, our experiments demonstrated that human small intestinal cells were resistant to MIP-133-mediated killing. These results suggested that MIP-133-mediated killing might be specific to corneal cells. To investigate this hypothesis, we performed experiments to ascertain the specificity of MIP-133 killing to corneal cells.

All of the human corneal cells in the pathogenic cascade of *Acanthamoeba* keratitis (corneal epithelium, stromal keratocytes, and corneal endothelium) were killed by MIP-133 (Table 2). Additionally, rabbit stromal cells and Chinese hamster corneal epithelial cells were also susceptible to MIP-133-mediated killing (Table 2). The capacity of MIP-133 to kill corneal endothelial cells was a surprise. We have shown that *Acanthamoeba* trophozoites are attracted to corneal endothelial cells components, however, there is no compelling evidence that trophozoites ever penetrate this layer and invade the eye (197). The possibility that trophozoites might be capable of invading beyond the cornea was intriguing, therefore we performed experiments to determine whether MIP-133 had any effect on intraocular cell lines. The results demonstrated that MIP-133 was capable of killing both human ciliary

Table. 2. MIP-133-induced CPE assays on corneal and intraocular cell lines. Test samples were adjusted to 1.5, 7.8, and 15.6 μg of protein in 25 μl of PBS before addition to corneal epithelial cells (HCE and HCORN), stromal cells (NHK and TRK), corneal endothelial cells (HCN), iris ciliary body cells (ICB), and retinal pigmented epithelial cells (RPE). Cells were incubated in 96 well microtiter plates for 18 hours at 35° C. CPE was assessed spectrophotometrically and percent death was calculated as described in the *Materials and Methods* section. Each numerical value represents the mean of triplicate counts.

Table 2

% MIP-133-Mediated Cell Death

Corneal Cells	**1.5 μg**	**7.8 μg**	**15.6 μg**
HCE	25	61	93
NHK	70	98	99
HCN	55	82	81
HCORN	98	99	99
TRK	85	96	97
Intraocular Cells	**1.5 μg**	**7.8 μg**	**15.6 μg**
ICB	17	57	77
RPE	6	57	82

body cells and retinal pigmented epithelial cells (Table 2). However, both cell lines displayed reduced susceptibility to MIP-133-mediated killing as compared to the corneal cells lines mentioned above.

Since MIP-133 kills corneal cells and intraocular cells, we hypothesized that other mammalian cells might also be susceptible to MIP-133. Therefore we performed experiments to ascertain whether MIP-133 would kill non-ocular cells. The results showed that human small intestine cells (FHs-74), liver cells (Chang cells), and smooth muscle cells (T/G HA-VSMC) were all resistant to MIP-133-mediated cell death (Table 3). These data are not surprising, as *Acanthamoeba* trophozoites are not known to cause disease in the liver, muscles, or small intestines. The mechanism for this apparent cell specificity, and thus, resistance to MIP-133 induced apoptosis, is unclear.

Earlier experiments showed that MIP-133 killed corneal epithelial cells via apoptosis in a caspase-dependent pathway. Inhibition of caspase-10 abrogated apoptosis by over 90%. The caspase-10 apoptotic cascade is induced by the activation of cell surface "death receptors" such as Fas, tumor necrosis factor-related apoptosis-inducing ligand-receptor (TRAIL), and tumor necrosis factor (TNF)-mediated apoptosis in a FADD dependent manner (148, 207). Therefore, cytotoxicity experiments were performed to determine whether MIP-133 interacted with any of these receptors. Ocular melanoma cells were chosen as a means of investigating the role of the TRAIL receptor. Cell lines with high (MEL 270) or low (OCM 1 and OCM 8) TRAIL receptor surface expression were susceptible to MIP-133-mediated killing (Table 4). Furthermore, two cell lines resistant to TRAIL-induced apoptosis

Table. 3. MIP-133-induced CPE assays on liver, smooth muscle, and small intestinal epithelial cells. Test samples were adjusted to 1.5, 7.8, and 15.6 μg of protein in 25 μl of PBS before addition to liver cells (CHANG), small intestinal epithelial cells (FHs), and smooth muscle cells (T/G HA-VSMC). Cells were incubated in 96 well microtiter plates for 18 hours at 35° C. CPE was assessed spectrophotometrically and percent death was calculated as described in the *Materials and Methods* section. Each numerical value represents the mean of triplicate counts.

Table 3

% MIP-133-Mediated Cell Death

Resist. Cell Lines	**1.5 μg**	**7.8 μg**	**15.6 μg**
Chang	0	0	0
Fhs	0	0	0
T/G HA-VSMC	0	10	11

Table. 4. MIP-133-induced CPE of ocular melanoma cells, splenocytes, mesenteric lymph node cells, and T-cells. Test samples were adjusted to 1.5, 7.8, and 15.6 μg of protein in 25 μl of PBS before addition to the cell lines indicated. Cells were incubated in 96-well microtiter plates for 18 hours at 35° C. CPE was assessed spectrophotometrically and percent death was calculated as described in the *Materials and Methods* section. Each numerical value represents the mean of triplicate counts.

Table 4

% MIP-133-Mediated Cell Death

Cell Lines	1.5 mg	7.8 mg	15.6 mg	Target Cell Properties
OM 431	10	93	93	Resistance to TRAIL-induced Apoptosis
MEL 202	44	72	79	"
MEL 270	20	75	91	TRAIL receptor +
OCM 1	95	96	95	TRAIL receptor -
OCM 8	2	90	88	" "
OMM-1	58	89	82	" "
OMM-1.5	31	66	88	" "
92-1	76	84	86	" "
Mel-290	5	82	90	" "
B6 Splenocytes	0	10	47	TNFR -
B6 Mesenteric Lymph node Cells	0	23	23	" "
Jurkat	20	7	30	Fas +

were also susceptible. A total of nine ocular melanoma cell lines were examined, and all were killed by MIP-133. To examine the role of TNFR2, CPE experiments were performed using spleen and mesenteric lymph node cells from TNFR2 knockout mice. Both cell preparations were susceptible to MIP-133-mediated killing. However, both were less susceptible than ocular melanoma cells. Finally, Fas-positive Jurkat cells actually displayed partial protection from MIP-133 mediated killing.

ANTIBODY-MEDIATED NEUTRALIZATION OF MIP-133 REDUCES PATHOGENIC PROPERTIES *IN VITRO* AND *IN VIVO*

In vitro inhibition of MIP-133

MIP-133 has been shown to be highly cytotoxic for human corneal epithelial cells *in vitro*. Degradation (via proteases) and inhibition (via serine protease inhibitors) of MIP-133 effectively eliminated *in vitro* CPE activity. However, to further characterize the role of MIP-133 *in vivo*, it is important to investigate the effects of mucosal immunity on MIP-133. Therefore, we performed experiments to ascertain whether anti-MIP-133 antibodies neutralized MIP-133 activity.

Figure 25 shows that the anti-MIP-133 antiserum was effective at blocking the cytotoxic activity of the MIP-133 protein. The cytotoxic effect of the 1.5 μg (in 25 μl culture medium) dose was completely abrogated, while the 7.8 μg (in 25 μl culture

Figure. 25. Inhibition of MIP-133-mediated CPE against HCE cells. MIP-133 samples were adjusted to 1.5, 7.8, and 15.6 μg of protein in 25 μl of PBS before addition to HCE cells in 96-well microtiter plates for 18 hours at 35° C. Protein samples were either used alone, or co-incubated with 1:75 chicken anti-MIP-133 antiserum (ImS) or the normal serum control (NS). All final volumes were 200 μl. CPE was assessed spectrophotometrically. Each bar shows the mean ± SE of triplicate counts. * and ***, significantly different from untreated controls ($P < 0.05$ and $P < 0.001$, respectively).

Figure 25

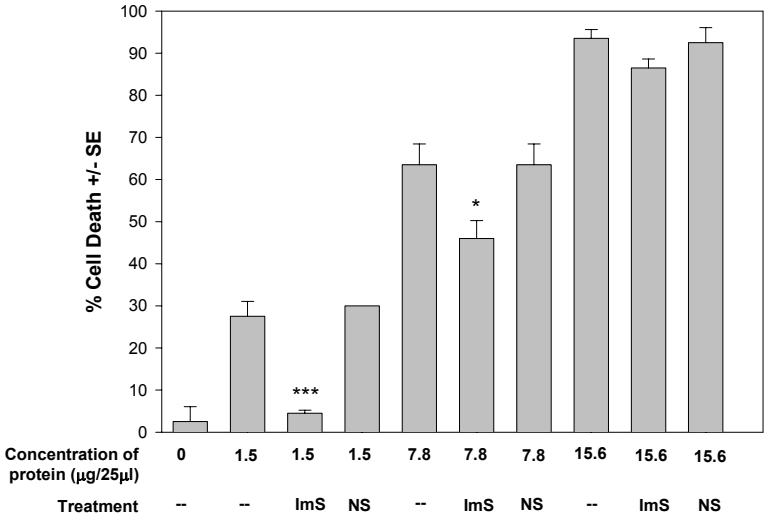
% Cell Death +/- SE
100
90
80
70
60
50
40
30
20
10
0
***
*
Concentration of protein (µg/25µl)
0
1.5
1.5
1.5
7.8
7.8
7.8
15.6
15.6
15.6
Treatment
--
--
ImS
NS
--
ImS
NS
--
ImS
NS

medium) dose was blocked by approximately 25%. However, the higher dosage (15.6 μg in 25 μl culture medium) was not inhibited by the antiserum. The preimmune serum control did not significantly reduce the cytolytic ability of the protein at any of the three doses tested.

After killing corneal epithelial cells, *Acanthamoeba* trophozoites penetrate Bowman's membrane and invade the corneal stroma. As anti-MIP-133 antiserum effectively neutralized the cytolytic activity of MIP-133 to corneal epithelial cells above, we suspected that the anti-MIP-133 antiserum might neutralize the collagenolytic activity of MIP-133. Therefore, we performed experiments to determine whether the anti-MIP-133 antiserum would impede trophozoite migration through a synthetic basement membrane (i.e., Matrigel) and prevent collagen degradation.

A. castellanii trophozoites incubated with the anti-MIP-133 antiserum displayed a significant decrease in their ability to migrate through the Matrigel matrix (Fig. 26). Trophozoites incubated with the serine protease inhibitor PMSF displayed similar reductions in the ability of the amoebae to migrate through the Matrigel. However, trophozoites incubated with the cysteine protease inhibitor cystatin did not show reduced migration. These results hinted at the possibility that the anti-MIP-133 antiserum was effective at neutralizing the collagenolytic activity of MIP-133.

Accordingly, we tested the ability of anti-MIP-133 antiserum to neutralize the collagenolytic activity of MIP-133. Incubating MIP-133 with the anti-MIP-133 antiserum completely (100%) abrogated the collagenolytic activity of MIP-133 at 24 hours (Fig. 27A). After 72 hours, anti-MIP-133 antiserum inhibited the

Figure. 26. Migration assay. 1 x 10^5 *A. castellanii* trophozoites were placed in the upper chambers of 3.0 µm pore size transwells coated with Matrigel. Trophozoites were treated with either 1:75 and 1:100 of either anti-MIP-133 antiserum (ImS) or the pre-immune normal serum control (NS). Additional controls included 1.0 mM phenylmethylsulfonyl fluoride (PMSF) and 10 µM cystatin (Cystat). After 2 hours, trophozoites were counted in the bottom chamber. Bars indicate means ± SE of 10 random high powered fields (100X). *** = significantly different from Medium control or normal serum control ($P < 0.001$).

Figure 26

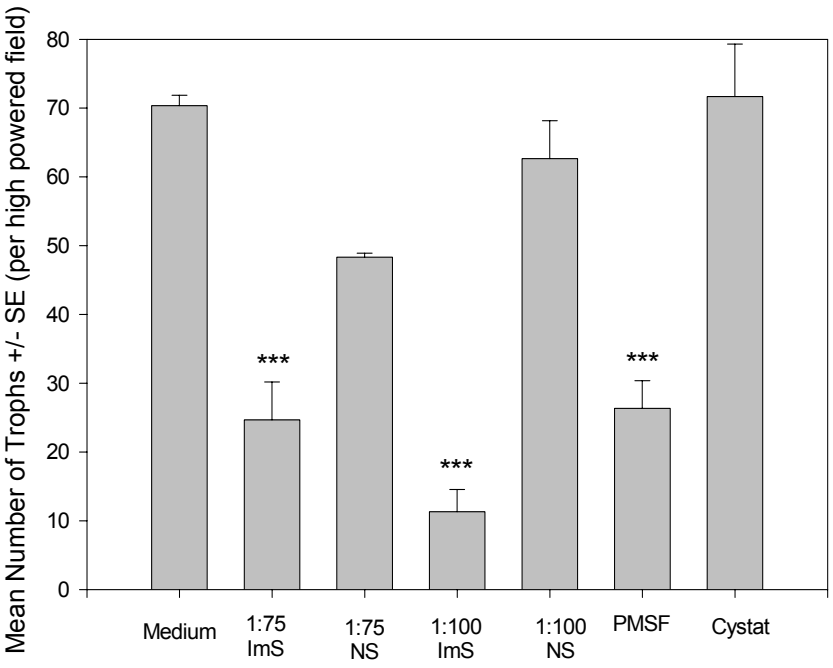
Mean Number of Trophs +/- SE (per high powered field)
80
70
60
50
40
30
20
10
0
***
***
***
Medium
1:75 ImS
1:75 NS
1:100 ImS
1:100 NS
PMSF
Cystat

Figure. 27. Anti-MIP-133 inhibition of MIP-133 collagenolytic activity and trophozoite migration. ELISA of 10 μg of human collagen types I and IV were incubated and dried onto 96-well plates. Wells were treated with either 15.6 μg of MIP-133, 15.6 μg of MIP-133 co-incubated with 1:75 chicken anti-MIP-133 antiserum (ImS), PBS, or 0.1 mg of collagenase (Col) for 24 hours (A) and 72 hours (B). Sample wells were then washed three times, incubated with mouse anti-collagen type IV IgG or mouse anti-collagen type I IgG as the primary, followed by goat anti-mouse IgG-HRP as described in the *Materials and Methods* section. Plates were then read at OD 405 nm. ***, significantly different from MIP-133 treatments ($P < 0.001$).

Figure 27

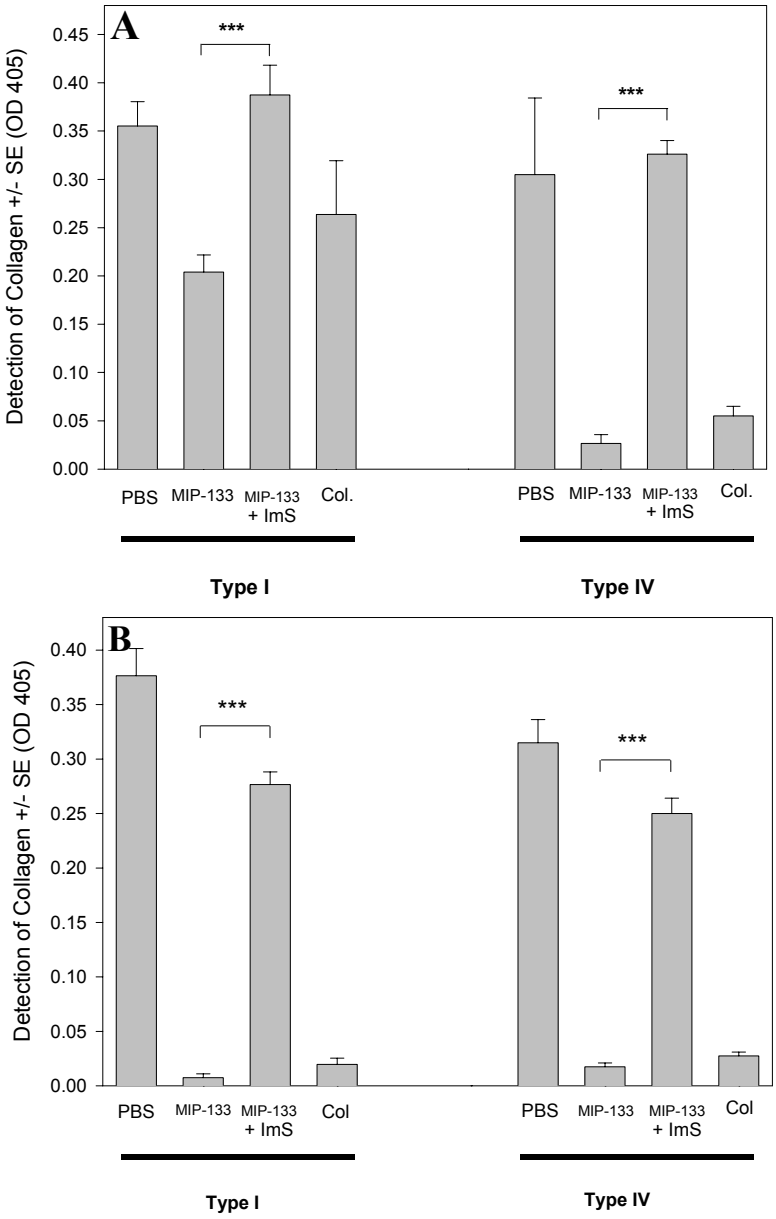
A
Detection of Collagen +/- SE (OD 405)
0.45
0.40
0.35
0.30
0.25
0.20
0.15
0.10
0.05
0.00
***
***
PBS
MIP-133
MIP-133 + ImS
Col.
PBS
MIP-133
MIP-133 + ImS
Col.
Type I
Type IV
B
Detection of Collagen +/- SE (OD 405)
0.40
0.35
0.30
0.25
0.20
0.15
0.10
0.05
0.00
***
***
PBS
MIP-133
MIP-133 + ImS
Col
PBS
MIP-133
MIP-133 + ImS
Col
Type I
Type IV

collagenolytic activity of MIP-133 on type I and type IV by 75% and 80% respectively (Fig. 27B). The collagenase control was not significantly different from the MIP-133 treatments.

Oral Immunizations against MIP-133 Provides Protection against *Acanthamoeba* Keratitis

Our laboratory has previously shown that oral immunization with antigens conjugated to neutralized cholera toxin is an effective method of inducing mucosal antibody responses, with the appearance of IgA antibodies in the tears and enteric washes of Chinese hamsters (105, 107). Furthermore, our lab has shown that protection against *Acanthamoeba* keratitis can be generated in both Chinese hamsters and pigs by oral immunization with *Acanthamoeba* surface antigens (6, 107, 198). We hypothesized that oral immunization with a protein that killed corneal epithelial cells, degraded Bowman's membrane, and dissolved the stroma, would also affect disease. Therefore, we performed experiments to immunize Chinese hamsters with MIP-133. Chinese hamsters were immunized either orally or intramuscularly with 100 μg, 200 μg, or 400 μg of MIP-133 once a week for four weeks prior to infection with *Acanthamoeba* trophozoites. The first intramuscular immunizations were administered with Freunds complete adjuvant, and the following three were with Freund's incomplete adjuvant. Oral immunizations were with neutralized cholera toxin. The results of a typical experiment are shown in Figure 28, and demonstrate that oral immunization with 400 μg of MIP-133 reduced the severity of corneal

infection by 30%, and shortened the duration of the disease by five days ($P < 0.01$). Immunization with lower doses of MIP-133 or with cholera toxin alone did not significantly affect the course of disease. Intramuscularly immunized animals displayed no significant difference in disease severity or duration from controls at any of the three immunization doses (data not shown).

Oral immunization is an effective method for inducing the production of secretory IgA antibody in a variety of mucosal secretions, including tears (107). The amount of IgA that can be collected from Chinese hamster tears is infinitesimal. However, significant quantities of IgA antibodies can be isolated from enteric washes from orally immunized hamsters (107). Accordingly, enteric washes were assessed for the presence of anti-MIP-133 IgA antibodies following oral immunization. Enteric washes from orally immunized Chinese hamsters and serum samples from intramuscularly immunized Chinese hamsters were tested by ELISA for the presence of mucosal IgA and serum IgG antibodies specific for MIP-133. Figure 29A shows that enteric washes from the orally immunized hamsters recognized MIP-133. By contrast, enteric washes taken from the PBS-treated animals did not specifically bind to MIP-133. IgG from serum samples also bound with high affinity to MIP-133 (Fig. 29B). PBS immunized animals did not display binding to the MIP-133 protein.

The anti-MIP-133 antibodies from immunized animals were tested for their ability to neutralize the cytopathic effects of MIP-133 *in vitro*. The enteric washes from immunized animals significantly inhibited the cytopathic activity of MIP-133 (Fig 30). Enteric washes from either PBS treated Chinese hamsters or

Figure. 28. Effect of oral immunization with MIP-133 on *Acanthamoeba* keratitis. Chinese hamsters were orally immunized with either 100 μg (A), 200 μg (B), or 400 μg (C) of MIP-133 with neutralized cholera toxin, or with cholera toxin alone, once a week for four weeks prior to infection with *A. castellanii* laden lenses as described in the *Materials and Methods* section. Lenses were removed four days post infection and corneas were evaluated for severity of keratitis at the times indicated. All of the animals orally immunized with 400 μg MIP-133 (C) displayed significantly milder disease than the cholera toxin and PBS control groups ($P < 0.01$). The results shown are representative of three separate experiments for each treatment (N=8 in each group for each experiment).

Figure 28

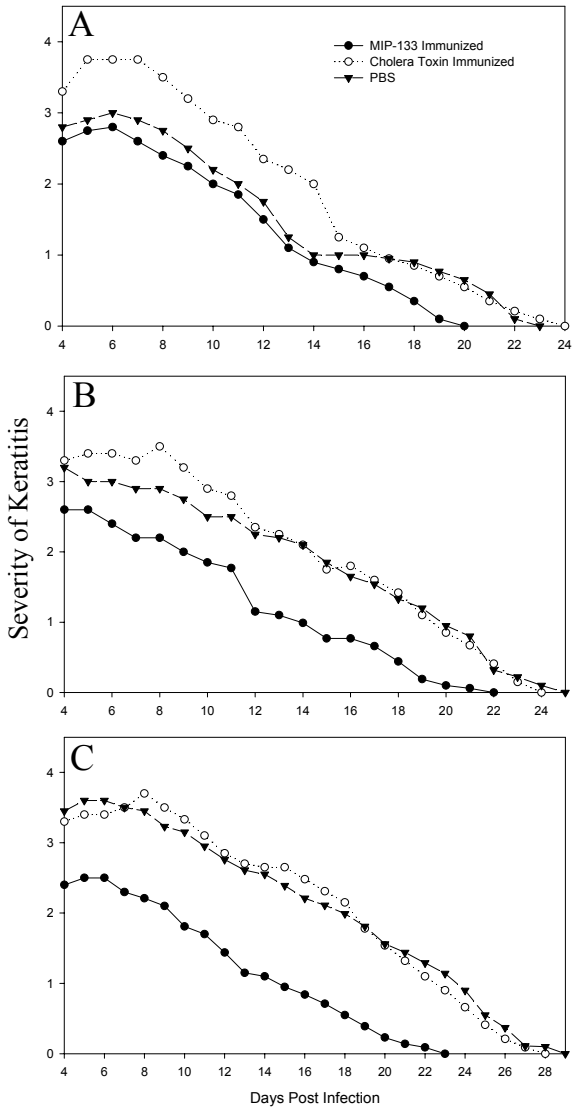
A
B
C
MIP-133 Immunized
Cholera Toxin Immunized
PBS
Severity of Keratitis
Days Post Infection

Figure. 29. Detection of IgA and IgG in Chinese hamsters immunized orally with MIP-133 conjugated to neutralized cholera toxin. A) IgA ELISA. 96-well plates were coated with 50 μg of MIP-133 and allowed to dry in carbonate buffer. After drying, wells were treated with blocking buffer and incubated with 1:2 pooled enteric wash from orally immunized hamsters. Wells were then washed and incubated with 1:2 rabbit anti-Chinese hamster IgA hyperimmune serum, washed three times in PBS, and incubated with 1:1,000 goat anti-rabbit IgG-horse radish peroxidase. ELISA plates were developed and read at 405 nm. Bars represent individual hamsters. B) IgG ELISA. 96-well plates were coated with 50 μg of MIP-133 and allowed to dry in carbonate buffer. After drying, wells were treated with blocking buffer and incubated with a 1:100 dilution of serum from orally immunized Chinese hamsters. Wells were then washed and incubated with goat anti-hamster IgG-HRP. Bars represent individual hamsters. ELISA plates were developed and read at 405 nm.

Figure 29

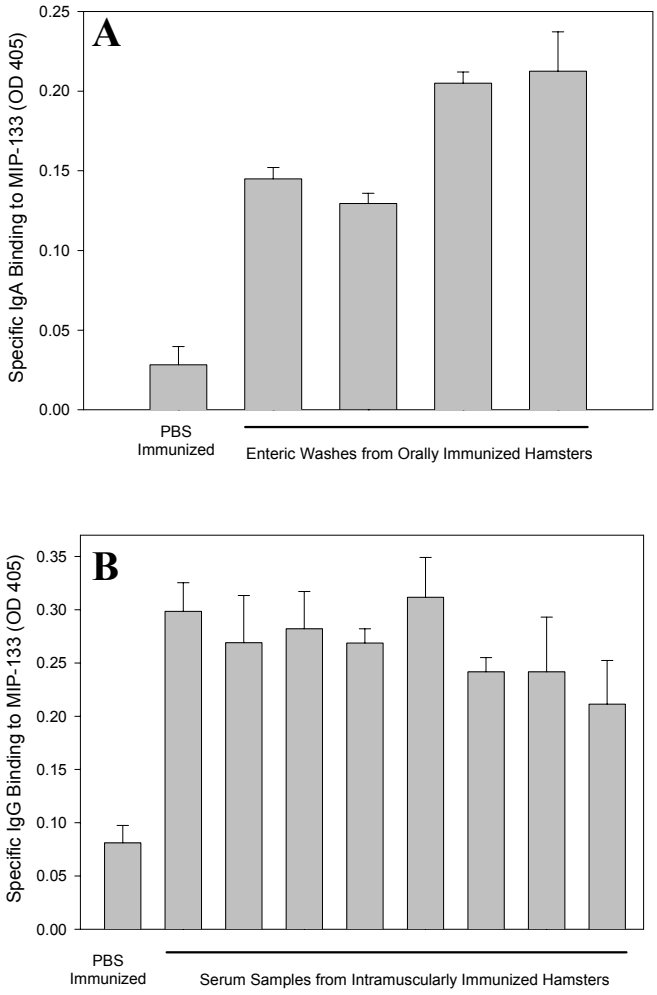
A
Specific IgA Binding to MIP-133 (OD 405)
0.25
0.20
0.15
0.10
0.05
0.00
PBS Immunized
Enteric Washes from Orally Immunized Hamsters
B
Specific IgG Binding to MIP-133 (OD 405)
0.35
0.30
0.25
0.20
0.15
0.10
0.05
0.00
PBS Immunized
Serum Samples from Intramuscularly Immunized Hamsters

Figure. 30. Inhibition of CPE by enteric washes from Chinese hamsters immunized orally with MIP-133. MIP-133 protein samples were adjusted to 1.5, 7.8, and 15.6 μg of protein in 25 μl of PBS before addition to HCE cells in 96-well microtiter plates for 18 hours at 35° C. Protein samples were either tested alone, co-incubated with 1:50 pooled enteric washes from Chinese hamsters orally immunized with MIP-133 (ImEW), or enteric wash from PBS immunized animals (CEW). All final volumes were 200 μl. CPE was assessed spectrophotometrically. Each bar shows the mean ± SE of triplicate counts. * and **, significantly different from untreated controls ($P < 0.05$ and $P < 0.01$, respectively).

Figure 30

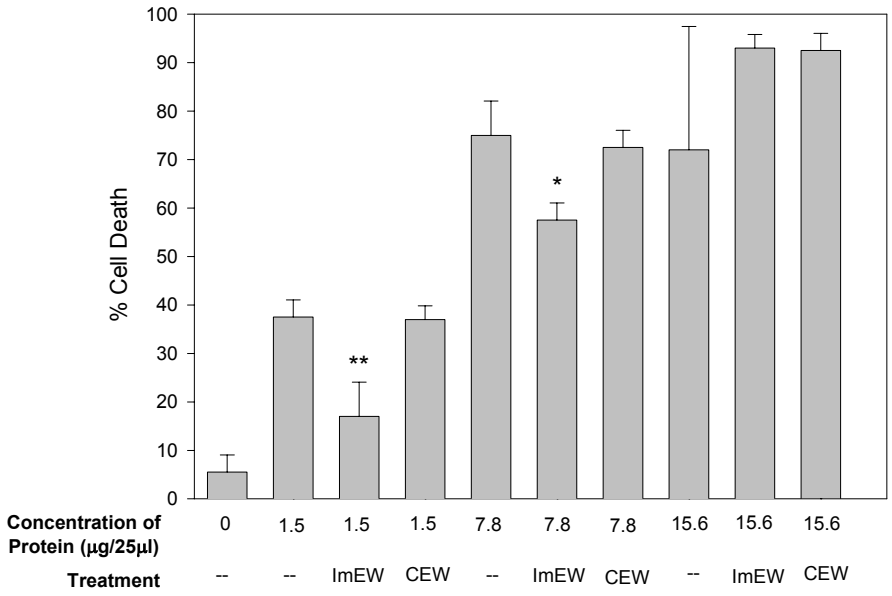
100
90
80
70
60
50
40
30
20
10
0
% Cell Death
**
*
Concentration of Protein (µg/25µl)
0 1.5 1.5 1.5 7.8 7.8 7.8 15.6 15.6 15.6
Treatment
-- -- ImEW CEW -- ImEW CEW -- ImEW CEW

intramuscularly immunized Chinese hamsters (Fig. 31) did not inhibit cytopathic activity of MIP-133 at any of the doses tested.

Acanthamoeba keratitis is a self-limiting acute infection in Chinese hamsters due to the rapid and effective response of the innate immune system, especially the conjunctival macrophages (64, 199). However, subconjunctival injection of liposomes containing the macrophagicidal drug, clodronate, removes periocular macrophages and results in a chronic infection that resembles the clinical course of *Acanthamoeba* keratitis in humans. Accordingly, we wished to determine if mucosal immunization with MIP-133 would affect a form of *Acanthamoeba* keratitis that mimicked the human counterpart in terms of its severity, persistence, and chronicity. This was tested by injecting either clodronate-containing liposomes, or PBS-containing liposomes, into the conjunctivae of Chinese hamsters. Animals were infected with parasite-laden contact lenses immediately after clodronate treatment. Oral immunizations were started 5 days after infecting with *Acanthamoebae* laden lenses. Oral immunization with MIP-133 produced a remarkable mitigation in corneal disease (Fig. 32). By contrast, infected animals treated with clodronate-containing liposomes and orally immunized with cholera toxin alone displayed clinical disease that was not significantly different from animals treated with clodronate-containing liposomes (data not shown).

Figure. 31. Inhibition of CPE by serum samples from Chinese hamsters immunized intramuscularly with MIP-133. MIP-133 protein samples were adjusted to 1.5, 7.8, and 15.6 μg of protein in 25 μl of PBS before addition to HCE cells in 96-well microtiter plates for 18 hours at 35° C. Protein samples were either tested alone or co-incubated with 1:50 or 1:100 serum sample from Chinese hamsters intramuscularly immunized with MIP-133 (SS). All final volumes were 200 μl. CPE was assessed spectrophotometrically. Each bar shows the mean ± SE of triplicate counts. * and **, significantly different from untreated controls ($P < 0.05$ and $P < 0.01$, respectively).

Figure 31

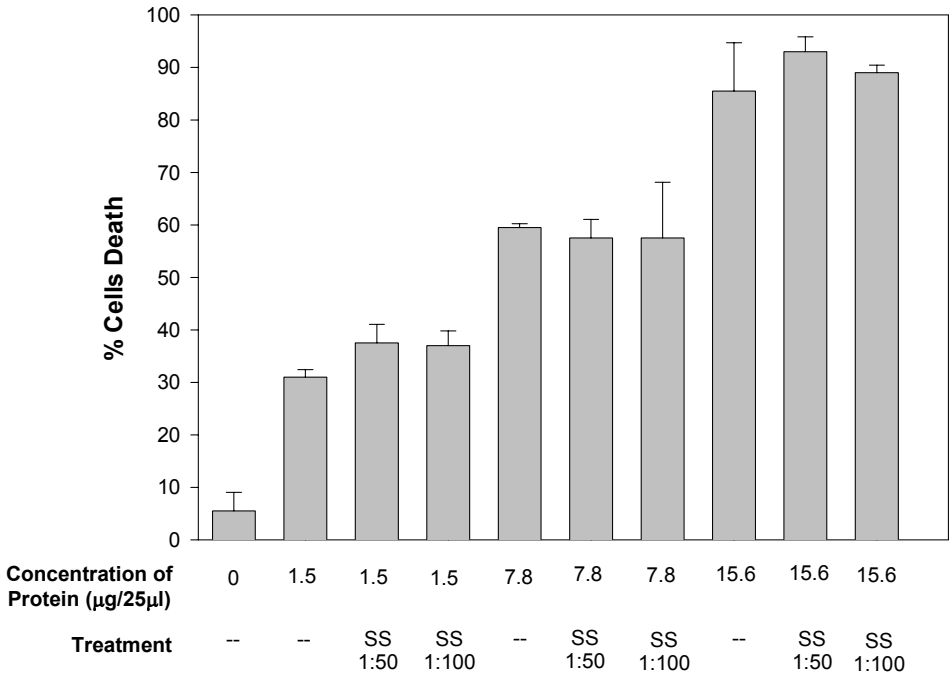
100
90
80
70
60
50
40
30
20
10
0
% Cells Death
Concentration of Protein (µg/25µl)
0 1.5 1.5 1.5 7.8 7.8 7.8 15.6 15.6 15.6
Treatment
-- -- SS 1:50 SS 1:100 -- SS 1:50 SS 1:100 -- SS 1:50 SS 1:100

Figure. 32. Effects of oral immunization with MIP-133 on chronic, progressive *Acanthamoeba* keratitis. Chinese hamsters were treated with clodronate encapsulated liposomes administered via subconjunctival injection on days -8, -6, -4, and -2 prior to infection with *A. castellanii* infected lenses on day 0. Chinese hamsters were then either untreated or orally immunized with 400 μg of MIP-133 on days 5, 12, 19, and 26 post infection. Lenses were removed five days post infection and corneas were evaluated for clinical severity of *Acanthamoeba* keratitis at the times indicated. The clinical severity for the orally immunized animals was significantly less than the control animals at all time points tested ($P<0.001$). The results shown are representative of two separate experiments for each treatment (N=8 in each group).

Figure 32

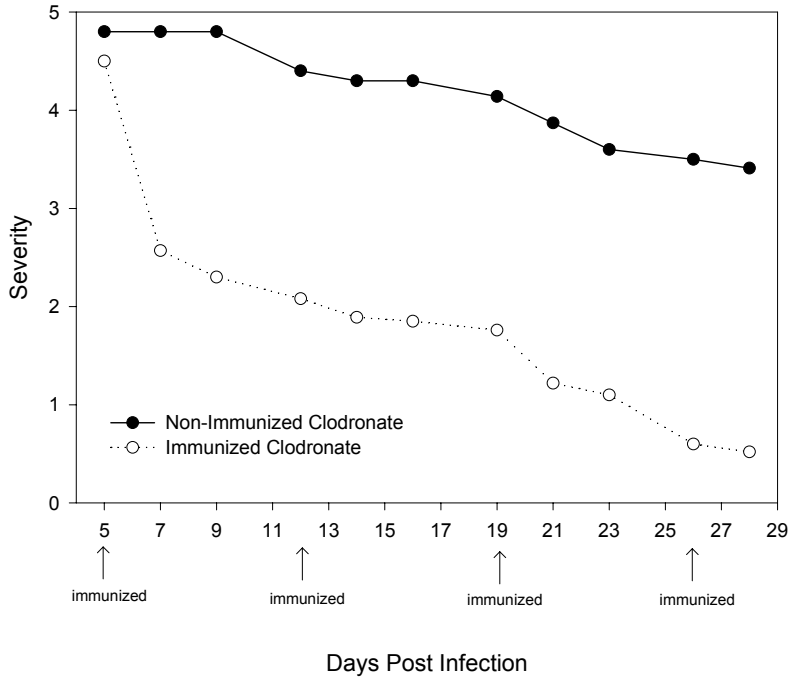
Severity
5
4
3
2
1
0
Non-Immunized Clodronate
Immunized Clodronate
5
7
9
11
13
15
17
19
21
23
25
27
29
immunized
immunized
immunized
immunized
Days Post Infection

CHAPTER FOUR
Discussion

THE EFFECTS OF MANNOSE ON *ACANTHAMOEBA* TROPHOZOITES

It has been reported that *A. castellanii* is induced to secrete cytolytic factor(s) when grown in the presence of free mannose (108). Although free mannose prevented the binding of *Acanthamoeba* trophozoites to hamster epithelial cells *in vitro*, it did not inhibit the organism's ability to lyse the cells. Under these conditions, free mannose inhibited contact-dependent cytolysis of corneal epithelial cells. However, Leher et al.'s results suggested that prolonged exposure to free mannose induced the release of cytolytic molecules that produced contact-independent cytolysis (108). It is now known that *Acanthamoeba* trophozoites bind preferentially to mannosylated glycoproteins, and that corneal epithelial cells upregulate mannose glycoproteins as part of the wound healing process (78, 143, 217). Moreover, induction of *Acanthamoeba* keratitis in experimental animals requires corneal abrasion prior to exposure to infectious trophozoites (74, 153, 196). Therefore, it is believed that pre-existing trauma to the cornea is a prerequisite for acquiring *Acanthamoeba* keratitis. These reports suggest that *Acanthamoeba* trophozoites not only utilize the mannosylated ligands for binding, but also use these ligands to induce the *Acanthamoebae* trophozoites to undergo changes that induce a more pathogenic state. Our laboratory has shown that mannose inhibits the binding of trophozoites to corneal epithelial cells, but it is unclear how the mannose affects the amoebae (108).

The purpose of this work was to examine how mannose affects *Acanthamoeba* trophozoites.

The first specific aim examined the response generated by *Acanthamoeba* trophozoites after binding to the mannosylated glycoproteins on a traumatized cornea. As mannose can represent a food source for the amoeba, it was unclear if the glycoproteins were inducing the amoebae to proliferate after binding to the traumatized eye. However, our data show that *Acanthamoeba* trophozoites incubated with mannose were not induced to proliferate. In fact, the presence of mannose reduced amoeba proliferation in culture by nearly 50%. These data suggest that the increased cytopathogenicity of mannose-treated trophozoites can not be attributed to greater numbers of amoebae being generated after binding to the mannose ligands. To examine the effects of mannose on both encystment and excystment, trophozoites and cysts were individually incubated in medium containing mannose. After six days of incubation, the *Acanthamoeba* cultures displayed three times more cysts when incubated with mannose. Additionally, whole cysts incubated with mannose also displayed a two-fold reduction in the conversion of cysts to trophozoites. These results suggest that binding to mannose causes a shift in *Acanthamoeba* biology that increases cytopathogenicity, while simultaneously slowing down proliferation. A major concern for patients requiring corneal transplants after *Acanthamoeba* keratitis is the reinfection of the transplant by excysting *Acanthamoebae*. Why the mannose induces greater numbers of cysts is unclear, yet this phenomenon may help explain how the cysts come to be located in the stroma and limbus.

The increased cytopathogenicic effects elicited by mannose were not due to mannose inducing trophozoite proliferation, and thus, increased numbers of trophozoites available to attack the corneal epithelial cells. Rather, it appears that mannose stimulates the release of one or more cytolytic molecules (75, 108). Supernatants isolated from *A. castellanii* trophozoites that were incubated with mannose displayed a 40% greater cytolytic ability against corneal cells *in vitro*. Molecular weight separation showed that the cytolytic activity was almost entirely limited to the fraction above 100 kDa. Subsequent SDS/PAGE analysis of the supernatants revealed a new 133 kDa protein that was not present in the supernatants that were grown without mannose. Precedence for pathogenicity as a result of amoeba-glycoprotein binding has been clearly defined for *Entamoeba hisolytica*. *E. histolytica* also expresses glycoprotein receptor ligands that facilitate adherence to the gastrointestinal epithelium (28, 132, 164). After binding to galactose residues found on the intestinal epithelium, *E. histolytica* secrete pore-forming molecules (amoebapores) that contribute to disease (109, 132, 201). However, soluble galactose inhibits the secretion of these molecules (28). Our data indicate that binding of *A. castellanii* trophozoites to corneal epithelial cell was inhibited by free mannose, but this inhibition did not mitigate the trophozoite's capacity to kill corneal epithelial cells.

Using FPLC and DEAE ion exchange chromatography, we were able to isolate the mannose-induced protein (MIP-133) and examine it's effects on corneal epithelial cells. It is reasonable to assume that after the amoebae bind to the mannosylated glycoproteins, secreted factors induced by this interaction would first

come in contact with the corneal epithelium. Human corneal epithelial cells were killed in a dose-dependent manner by MIP-133. All three doses (1.5, 7.8, and 15.6 μg total protein/200μl) of MIP-133 killed 100% of the Chinese hamster corneal epithelial cells *in vitro*. Further examination revealed that the Chinese hamster epithelial cells remained susceptible to MIP-133 at doses as low as 300 ng (300 ng/200μl).

Interestingly, human intestinal epithelial cells were not killed by any of the preparations of MIP-133 tested. It is unknown why MIP-133 was unable to kill the human intestinal cells. *Acanthamoeba* spp. are ubiquitously distributed in virtually every environmental habitat and have been isolated from foodstuffs including fresh vegetables and mushrooms (169). Environmental exposure to *Acanthamoeba* spp. is commonplace, as 50 – 100% of the normal adult population possess serum antibodies specific for *Acanthamoeba* antigens (5, 27, 39). It seems reasonable to assume that *Acanthamoeba* spp. are routinely ingested, yet they are not known to cause intestinal infections. The apparent resistance of human intestinal epithelium to the cytotoxic actions of *Acanthamoeba* trophozoites and MIP-133 may explain the absence of intestinal acanthamoebiasis in the human population.

Incubation of MIP-133 with serine protease inhibitors reduced cytotoxicity against the highly susceptible hamster corneal epithelial cells by 60 – 80%. No reduction of the cytopathic effect was seen when MIP-133 was incubated with a cysteine protease inhibitor. These data suggest that mannose-binding induces the secretion of a new 133 kDa serine protease that is responsible for killing corneal epithelial cells. As binding of the trophozoites to the mannosylated glycoproteins is the essential first step in generating the disease, it is likely that this interaction is also

responsible for the secretion of molecules that are needed for the amoebae to penetrate the epithelial cell layer.

MIP-133 AS A VIRULENCE FACTOR

Acanthamoeba keratitis is a very destructive disease that can lead to the loss of the infected eye if untreated. Destruction of the corneal surface can be both quick and complete. The next specific aims examined the mechanism behind how MIP-133 kills corneal cells, the correlation between production of the protein and ability to generate disease, and the role of the protein in the subsequent pathogenic cascade.

Smaller ligand-induced molecules from *E. histolytica* have been shown to adhere to the epithelial surface of the human intestine and form pore-forming complexes that lyse intestinal cells (109, 110). These 5 and 14-kDa protein complexes, called amoebapores, form ion channels that promote the osmotic lysis of eukaryotic cells (43). MIP-133 did not display pore-forming capabilities on carboxyfluorescein encapsulated liposomes. This is not surprising, as the 133 kDa protein would likely be too large to form pore-forming complexes. However, MIP-133 treatment of corneal cells produced an almost three-fold increase in apoptosis. Pretreatment with a caspase-3 inhibitor abrogated nearly 100% of the MIP-133-mediated cell death. As most pathways in the caspase cascades are routed through caspase-3, our data suggest that MIP-133 kills corneal cells through a caspase-mediated pathway (149). Inhibition of caspase-3 effectively blocks most caspase-mediated apoptosis as caspase-3 is responsible for the cleavage of the key cellular

proteins that leads to the typical morphological changes observed in cells undergoing apoptosis (149, 190, 215). However, inhibition of caspase-3 does not affect the initial start site of the cascade. Pretreatment with caspase-9 and caspase-10 inhibitors reduced MIP-133 mediated apoptosis by 50% and 90% respectively. Combined use of the inhibitors did not further increase this reduction beyond the 90% inhibition seen with the caspase-10 inhibitor alone. The caspase-9 pathway is a mitochondrial-dependent pathway that is initiated after the mitochondria experience significant damage (69). Mitochondrial damage can be produced from a number of internal and external sources, and may have a synergistic effect on other apoptotic cascades. More important were the data suggesting that caspase-10 may be responsible for the initial generation of the caspase-mediated apoptotic cascade. Caspase-10 is triggered by the "death receptors" such as Fas, tumor necrosis factor-related apoptosis-inducing ligand-receptor (TRAIL), and tumor necrosis factor (TNF)-mediated apoptosis in a Fas-Associated Death Domain protein (FADD) dependent manner (148, 207). In this model, engagement of TNF, Fas, or TRAIL at the cell surface recruits FADD to the plasma membrane (33). FADD binds directly to Fas, while binding to TNF and TRIAL is mediated via the TNF Associated Death Domain (TRADD) docking protein (33, 73). After binding to either Fas or TRADD, FADD recruits caspase-10, effectively activating the caspase-mediated apoptosis pathway. The inhibition of MIP-133-mediated apoptosis by caspase-10 inhibitor strongly suggested that MIP-133 might be interacting with one of the three surface ligands known to recruit FADD.

The data above suggest that MIP-133 may bind to one of the three surface receptors known to recruit caspase-10. Therefore, cytotoxicity experiments were performed to determine which surface receptor MIP-133 may interact with, and thus, induce apoptosis. Cell lines were chosen based on their different expression of their cell-surface death-receptors. Melanoma cells with either high (MEL270) or low (OCM1 and OCM8) surface expression of TRAIL receptors were both effectively killed by MIP-133 *in vitro*. Moreover, OM431, a melanoma cell line resistant to TRAIL-mediated apoptosis, was not protected against MIP-133 killing. Spleen cells from TNFR2 knockout mice were also killed by MIP-133, indicating that the lack of TNF-receptor did not offer protection. Finally, Fas-positive Jurkat cells actually displayed partial protection from MIP-133 mediated killing. In summary, no evidence of a pattern was generated that would establish either Fas, TRAIL, or TNF as the receptor for MIP-133-mediated apoptosis. One possible explanation for this would be that MIP-133 binds to a surface receptor that has not been described.

The genus *Acanthamoeba* includes at least 24 species, which are ubiquitously distributed in nature. To date, only 8 species have been shown to cause corneal disease (172). Although the official classification of the strains is still unresolved, it is important to identify molecules that differentiate pathogenic from non-pathogenic strains. None of the three soil isolates examined produced MIP-133. Moreover, when tested *in vivo*, all three of the soil isolates produced either no disease, or significantly less disease as compared to the standard ocular isolate of *A. castellanii*. The soil isolate *A. hatchetti* did produce mild keratitis, even though it did not secrete detectable quantities of MIP-133. It is possible that *A. hatchetti* produces one or more

proteases that can substitute for MIP-133 in the development of *Acanthamoeba* keratitis. By contrast, all of the clinical isolates of *Acanthamoeba* spp. elaborated MIP-133 and produced disease *in vivo*. Thus, there is a strong correlation between the production of MIP-133 and the severity of *Acanthamoeba* keratitis.

The pathogenic cascade of *Acanthamoeba* keratitis begins with trophozoites binding to and killing corneal epithelial cells. This step is followed by trophozoite invasion of the basement membrane and the underlying collagenous stroma. The role of MIP-133 in these steps of the pathogenic cascade was examined next. All seven of the *Acanthamoeba* spp. were examined for their ability to migrate through a collagenous matrix (i.e., Matrigel). Matrigel is considered a representative basement membrane, as it contains not only basement membrane components (collagens, laminin, and proteoglycans), but also matrix degrading enzymes, their inhibitors, and growth factors. Invasion of tumor cells into Matrigel has been used to characterize involvement of extracellular matrix receptors and matrix degrading enzymes, which play roles in tumor progression (93). As expected from the *in vivo* data, none of the soil isolates was effective in migrating through the Matrigel matrix. By contrast, all of the clinical isolates migrated through the Matrigel matrix at approximately equal levels. The correlation between migration through Matrigel and the ability to produce disease *in vivo* was not surprising. After the amoebae destroy the outer corneal epithelial cells, they must penetrate Bowman's membrane, and gain entry into the stroma. Both of these layers are primarily comprised of collagen.

To confirm the detection of MIP-133, and aid in future studies, a chicken anti-MIP-133 antiserum was produced. Chickens produce a robust IgY

response to small amounts of antigen (53, 58, 103). IgY has the same general structure as an IgG, with 2 heavy chains ("nu" chains, ~67-70 kDa) and 2 light chains (22-30 kDa), and is the lower vertebrate equivalent to IgG (209). The chicken antiserum bound to MIP-133 with high affinity, as detected by western blot and ELISA analysis. By contrast, the chicken preimmune serum did not bind to MIP-133. The antiserum did not detect MIP-133 after incubation of the protein with either pepsin or proteinase K. This confirmed that the proteases effectively degraded MIP-133. Furthermore, the antiserum was useful in confirming that the *Acanthamoeba* spp. soil isolates did not produce MIP-133, either constitutively or after incubation with mannose.

After penetrating Bowman's membrane, trophozoites enter and degrade the collagenous stroma. The role of MIP-133 in this step of the pathogenic cascade of *Acanthamoeba* keratitis was examined next. Gel lysis assays were used to determine if MIP-133 was capable of degrading collagen. MIP-133 produced extensive lysis of gelatin matrixes in a dose dependent fashion. Gelatin lysis was completely abrogated when MIP-133 was pretreated with a serine protease inhibitor PMSF, and not the cysteine protease inhibitor, cystatin. These results are consistent with the findings of He et al. (64), who showed that supernatants from *A. castellanii* trophozoite cultures contain collagenolytic factors that dissolve collagen shields *in vitro* and produce corneal lesions that mimic *Acanthamoeba* keratitis when injected into the corneas of rodents. The corneal lesions produced by the *Acanthamoeba* culture supernatants resembled *Acanthamoeba* keratitis lesions in several important ways including: edema, corneal opacity, neutrophilic infiltration, ring-like infiltrate, stromal

disintegration, and keratocyte necrosis (64). Thus, *Acanthamoeba* trophozoites elaborate one or more soluble factors that are capable of degrading the collagenous matrix of the cornea and producing the pathological sequelae that are characteristic of *Acanthamoeba* keratitis.

The data reported above strongly suggest that MIP-133 may play an important role in the degradation of the collagen that comprises the bulk of the corneal stroma. After eliminating the corneal epithelial cells, the amoebae must perforate Bowman's membrane, and enter the stroma. Both Bowman's membrane and the stroma are comprised almost entirely of collagen (Types IV and I respectively). A battery of tests demonstrated that MIP-133 was efficient at degrading both human types I and IV collagen. At 24 hours, type IV collagen was more efficiently degraded when compared to type I. However, by 72 hours, both forms of collagen were nearly completely degraded by MIP-133. These data suggest that MIP-133 may play an important role in facilitating trophozoite invasion and degradation of the stroma. Thus, the production of MIP-133 is instrumental in yet one more phase of the pathogenic cascade of *Acanthamoeba* keratitis.

After entering the corneal stroma, trophozoites are believed to kill the keratocytes that secrete the collagenous matrix. Therefore, experiments were performed to determine if MIP-133 was toxic to keratocytes. The results of several *in vitro* assays demonstrated that MIP-133 kills cells from all three layers of the human cornea: corneal epithelial cells, stromal keratocytes, and corneal endothelial cells. The capacity of MIP-133 to kill corneal endothelial cells is intriguing as there is no

compelling evidence that trophozoites ever penetrate Descemet's membrane and encounter the underlying corneal epithelium.

With the exception of three isolated cases, *Acanthamoeba* trophozoites have not been shown to produce intraocular infections or inflammation within the eye (80, 144). It is not believed that *Acanthamoeba* trophozoites go beyond the corneal endothelium, however, our data above showed that MIP-133 is effective at killing this single cell layer. It is reasonable to assume that killing of the corneal endothelial cells would facilitate invasion of the eye. Therefore, experiments were performed to determine if MIP-133 was toxic to iris ciliary body cells and retinal pigmented epithelial cells. The results of several in vitro assays demonstrated that MIP-133 was effective at killing both intraocular cell lines. However, the ability to kill intraocular cells *in vitro* does not necessarily translate to ability to produce disease *in vivo*. In fact, intraocular injection of as many as one million *A. castellanii* trophozoites failed to produce disease in Chinese hamsters (Daniel Clarke; unpublished). Although MIP-133 is toxic to intraocular cells *in vitro*, intraocular disease produced by *Acanthamoeba* trophozoites almost never occurs.

In summary, MIP-133 plays a crucial role in many steps of the pathogenic cascade of *Acanthamoeba* keratitis (Fig. 33). MIP-133 is induced by the interaction of the trophozoites with mannosylated glycoproteins on the corneal epithelium. The strong correlation between the ability to produce MIP-133 and generate disease suggests that MIP-133 is critical for initiating the pathogenic cascade of *Acanthamoeba* keratitis. Soil isolates of *Acanthamoebae* were unable to produce the protein, and thus, were not able to elicit substantial disease. After binding to the

mannosylated glycoproteins on the corneal epithelial cells, the secreted MIP-133 kills the corneal epithelial cells and exposes Bowman's membrane. Subsequently, MIP-133 degrades Bowman's membrane (via degradation of type IV collagen) and facilitates invasion of the trophozoites into the stroma. Once in the stroma, MIP-133 helps facilitate the destruction of the stroma by degrading type I collagen and by killing the resident keratocytes that maintain the collagen matrix. Furthermore, *A. castellanii* has also been shown to elaborate other enzymes and low molecular weight metabolites that can degrade the collagen of the stroma and kill epithelial cells respectively (64, 126). In summary, pathogenic *Acanthamoebae* are induced by mannose to secrete a novel serine protease, MIP-133, that is critical for many steps of the pathogenic cascade of *Acanthamoeba* keratitis.

Figure. 33. Schematic showing the role of MIP-133 in the pathogenic cascade of *Acanthamoeba* keratitis.

Figure 33

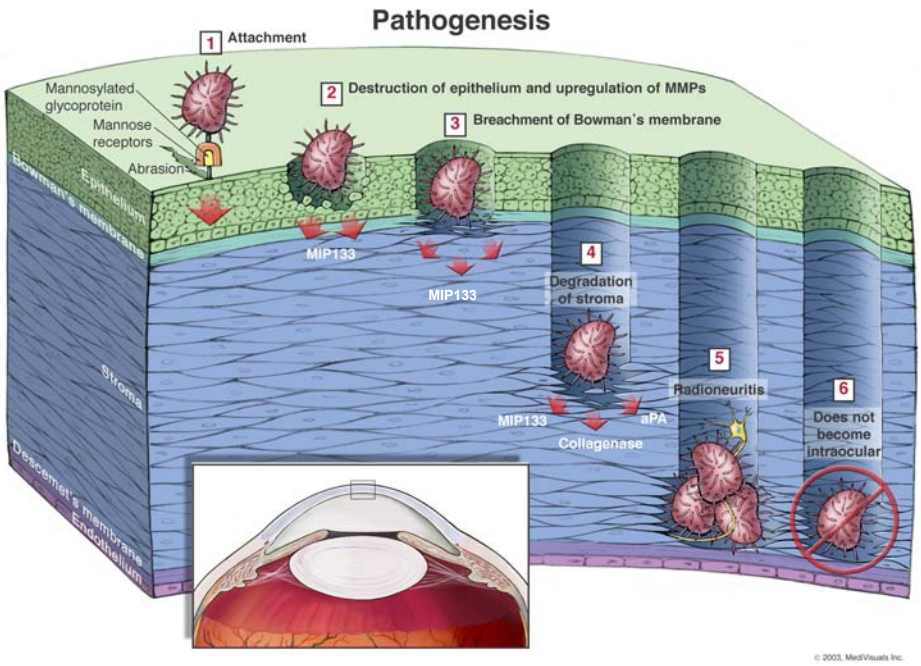
Pathogenesis
1 Attachment
Mannosylated glycoprotein
Mannose receptors
Abrasion
2 Destruction of epithelium and upregulation of MMPs
3 Breachment of Bowman's membrane
Epithelium
Bowman's membrane
Stroma
Descemet's membrane
Endothelium
MIP133
MIP133
4
Degradation of stroma
MIP133
aPA
Collagenase
5
Radioneuritis
6
Does not become intraocular
© 2003, MediVisuals Inc.

ANTIBODY NEUTRALIZATION OF MIP-133 *IN VITRO* AND USE AS AN IMMUNOGEN AGAINST DISEASE *IN VIVO*

The role of MIP-133 in multiple phases of the pathogenic cascade of *Acanthamoeba* keratitis suggests that neutralizing this molecule might prove beneficial. This hypothesis was tested by incubating MIP-133 with chicken anti-MIP-133 antiserum. The antiserum against MIP-133 blocked the ability of the protein to degrade both types I and IV collagen. Inhibition was 100% after 24 hours, and inhibition remained greater then 75% after 72 hours. Furthermore, the antiserum blocked the ability of MIP-133 to kill human corneal epithelial cells. These data suggest that the antiserum is effective at blocking the cytolytic activity of MIP-133. The anti-MIP-133 antiserum also effectively inhibited trophozoite migration through Matrigel matrixes. Inhibition of migration was greater with the antiserum than with the serine protease inhibitor. These results indicate that neutralizing antibodies can block crucial functions of this protein that contribute to the pathogenesis of *Acanthamoeba* keratitis

Based on these *in vitro* findings, we surmised that the MIP-133 protein might be used as an effective immunogen *in vivo*. This hypothesis was tested by immunizing Chinese hamsters both orally and intramuscularly with MIP-133 prior to infection with *A. castellanii* trophozoites. Chinese hamsters, immunized orally with 400 μg of MIP-133, displayed a significant reduction in both disease severity and duration. However, protection was not significant when lower doses of the protein were used in the oral immunizations, or if MIP-133 was administered

intramuscularly. Oral immunization is an effective method for inducing the production of secretory IgA antibody in a variety of mucosal secretions, including tears (107). In fact, tears have been shown to contain high quantities of secretory IgA, which is produced locally by plasma cells in the lacrimal glands (55, 89, 159). Induction of mucosal protection through oral immunizations has been shown to be effective against a variety of pathogens, including amoebae, bacteria and viruses, as well as toxic molecules (17, 32, 83, 95, 113, 174). Furthermore, our lab has shown that protection against *Acanthamoeba* keratitis can be generated in both Chinese hamsters and pigs by oral immunization with *Acanthamoeba* surface antigens (6, 107, 198). This protection was generated through the production of secretory IgA that bound to the surface of *Acanthamoeba* trophozoites and prevented their binding to the corneal surface (107). It is not surprising that intramuscular immunizations, and thus the generation of antigen-specific IgG, did not protect against disease. High titers of circulating *Acanthamoeba*-specific IgG have been shown have no effect on the severity or duration of *Acanthamoeba* keratitis (6, 198).

To confirm that both anti-MIP-133 IgG and IgA were generated, serum samples and mucosal secretions were collected for analysis. Both the serum samples and mucosal secretions produced detectable anti-MIP–133 IgG and IgA respectively. The intramuscularly immunized animals produced a robust IgG response, far surpassing the IgA response seen from the orally immunized animals. Naïve animals did not possess antibodies to MIP-133. Furthermore, enteric wash preparations from orally immunized animals protected human corneal cells from MIP-133-mediated killing *in vitro*. Serum samples from MIP-133 immunized Chinese hamsters did not

protect under similar conditions. The data strongly suggest that oral immunization with MIP-133 before challenge with *Acanthamoebae* stimulates a mucosal immune response that protects against corneal disease.

The importance of secretory IgA antibodies in resistance to *Acanthamoeba* keratitis is supported by recent findings indicating that patients with *Acanthamoeba* keratitis possess lower levels of anti-*Acanthamoeba*-specific IgA antibodies in their tears compared to non-infected, normal individuals (5). It is unclear whether the lower titer of IgA was due to ocular infection, or an inherent deficiency in overall IgA production. However, 100% of the adult individuals tested (n=48) possessed anti-*Acanthamoeba*-specific IgA in their tears. This high prevalence of anti-*Acanthamoeba*-specific IgA is believed to arise from routine environmental exposure to *Acanthamoeba* spp. In fact, *Acanthamoeba* spp. have been isolated from nasopharyngeal regions of healthy individuals that displayed no symptoms of *Acanthamoeba* keratitis (27, 208). Of interest, the levels of circulating serum IgG were actually higher in patients with *Acanthamoeba* keratitis than in non-infected, normal controls (5). These data further support the notion that mucosally-derived antigen-specific IgA can protect against *Acanthamoeba* keratitis, yet high titers of circulating *Acanthamoeba*-specific IgG antibodies fail to protect against ocular challenge with *Acanthamoeba* trophozoites.

Although oral immunization prior to corneal exposure to *Acanthamoeba* trophozoites is effective in reducing disease, it is not a realistic paradigm for managing patients. Therefore, we employed a more relevant model in which we tested the efficacy of oral immunization with MIP-133 administered after the corneal

infections had been established. The primary difference between *Acanthamoeba* keratitis in Chinese hamsters and humans is that Chinese hamsters develop an acute, self-limiting disease. Humans typically generate a more severe, chronic infection that can result in the loss of the eye if left untreated. In order to produce a severe chronic form of *Acanthamoeba* keratitis in Chinese hamsters, it is necessary to deplete the conjunctival macrophage population with a macrophagicidal drug, clodronate (199). Clodronate belongs to the family of bisphosphonates (BPs), bone-seeking agents that are potent inhibitors of osteoclasts. Like other BPs, clodronate has poor cell membrane permeability (168). Liposomes are readily taken up by cells of the reticuloendothelial system, in particular macrophages. Liposome-mediated delivery of clodronate inactivates and kills macrophages after effective phagocytosis but is not toxic to non-phagocytic cells (173, 200). The clodronate-treated animals developed a chronic form of *Acanthamoeba* keratitis. However, repeated oral immunizations with MIP-133 after infection produced a dramatic mitigation in corneal lesions and an eventual resolution of the disease. A dramatic reduction in disease severity was evident two days after the initial immunization. Immunized animals cleared the disease at approximately day 33, while non-immunized clodronate treated animals continued to display severe keratitis beyond the 55 day observation period.

These results offer glimmers of hope for immunotherapy for persistent, drug resistant *Acanthamoeba* keratitis. It will be important to enhance the immunogenicity of MIP-133 and to optimize the oral immunization protocol to obtain higher mucosal antibody titers. It may also be possible to directly apply anti-MIP-133 monoclonal

antibodies to the corneas of *Acanthamoeba* keratitis patients as a means of neutralizing the pathogenic protein and thereby mitigate corneal disease.

FUTURE RESEARCH

These studies have demonstrated that mannose stimulates pathogenic species of *Acanthamoeba* trophozoites to produce a novel 133 kDa protein that plays an important role in most of the steps of the pathogenic cascade of *Acanthamoeba* keratitis. MIP-133 is produced shortly after binding to mannose, and aids the amoebae in gaining entry into the stroma. However, as *Acanthamoeba* spp. are ubiquitously distributed in the environment, it is unknown what role MIP-133 might have in nature. The present results describe well-defined functions of MIP-133 in the development of *Acanthamoeba* keratitis. However, *Acanthamoeba* spp. are free-living amoebae that normally do not produce disease. The preservation of the MIP-133 gene suggests that this protein serves an important function in the day-to-day existence of free-living *Acanthamoeba* spp. Identifying the function of this ligand-induced protein secretion would help to further understand the biology of the organism. *Acanthamoebea* are voracious predators of bacteria, and it is plausible to assume that mannose recognition may play a role in identification and capture of bacteria. An alternative hypothesis is that *Acanthamoeba* trophozoites use a mannose receptor/MIP-133 system to recognize and kill other organisms in their environmental niche that compete with them for predation of limited bacterial foodstuffs. Protection of the amoeba may be another other role of MIP-133.

The differentiation of MIP-133 production among non-pathogenic and pathogenic strains of *Acanthamoeba* strains could be examined at the genomic level. We are currently attempting to sequence MIP-133 in an effort to clone the gene. Such information would give more detailed insights as to why the non-pathogenic strains do not secrete this protein. One possibility is that non-pathogenic strains of *Acanthamoeba* lack the gene to produce MIP-133. Another hypothesis suggests that non-pathogenic strains of *Acanthamoeba* exercise more stringent regulation on MIP-133 production. Further understanding of the differences between the non-pathogenic and pathogenic strains may aid in finding ways to neutralize the protein, and thereby mitigate *Acanthamoeba* keratitis.

Acanthamoeba keratitis is a relatively rare disease. It is possible that this pathogenic mechanism, and similar inducible pathogenic proteases, are utilized by other pathogens that infect the cornea. The mechanism of MIP-133 secretion may give insights into more fundamental pathogenic mechanisms, and may provide information on how pathogens can undermine mucosal immunity. It is plausible that other amoebae may use a similar glycoprotein-ligand mechanism to generate disease. It has been well characterized that *E. histolytica* uses such an approach to secrete small molecular weight proteins, called amoebapores, that facilitate the destruction of intestinal epithelial cells (110, 132, 201). However, other life-threatening amoebae, such as *Balamuthia mandrillaris*, have been poorly studied. *B. mandrillaris* causes a fatal meningitis, yet it is not known how it enters the body, or the pathogenic mechanisms that it invokes (119, 121, 165). As more evidence of glycoprotein-ligand interactions is described for pathogenic amoebae, it is likely that this pathogenic

mechanism may be a common theme for medically relevant amoebae. Furthermore, it is possible that other eye pathogens may secrete similar proteins that contribute to ocular disease. For example, other ocular pathogens such as *Pseudomonas aeruginosa*, *Chlamydia trachomatis*, or *Onchocerca volvulus* may also secrete a serine protease that shares epitopes with MIP-133. Anti-MIP-133 antiserum/antibodies may cross-react with secreted proteins from these pathogens. As serine proteases are commonly produced by pathogens, it is possible that MIP-133-like proteins may be secreted by other ocular pathogens as well.

These results indicate MIP-133 is very effective at killing ocular derived melanoma cells. An interesting extension of this research would be to further characterize the ability of MIP-133 to eliminate melanoma cells *in vivo*. We initiated such a study and found that intratumoral injections of MIP-133 in mice possessing aggressive subcutaneous B16 melanomas gave very promising results. Tumors displayed significant reduction in size after only 24 hours. Tumor growth was suppressed in all (n=20) of the MIP-133 treated animals. Cursory examination of the tissues adjacent to the tumors did not reveal significant damage that could be attributed to MIP-133. However, since MIP-133 kills a wide variety of cells, closer histopathological examination of the surrounding tissues would have to be performed. Although the tumors were visually smaller, accurate means to measure the mass of the existing tumors proved to be problematic. Careful reexamination of this work with more sophisticated tumor measuring techniques may provide a possible role of MIP-133 as an anti-tumor agent.

Another avenue of investigation may consider the question of why *Acanthamoeba* trophozoites have not been reported to enter the eye and produce endophthalmitis. Results reported here indicate that MIP-133 effectively kills the corneal endothelial cells. However, the absence of *Acanthamoeba* trophozoites within the anterior chamber, or in the retina, implies that some form of protection prevents fulminant intraocular infections by *Acanthamoeba* trophozoites. One hypothesis proposes that aqueous humor may be toxic to the trophozoites. This would explain the paucity of reports of intraocular infections in the literature (80, 144).

A final avenue of investigation is the topical use of anti-MIP-133-specific IgA antibodies, both prior to and after development of *Acanthamoeba* keratitis. The immunization data indicate that significant protection against disease can be produced even after the disease is manifested. This hypothesis proposes that topical application of anti-MIP-133-specific IgA might mitigate disease severity and duration. Secretory IgA protects against the disease and topical applications of IgA might offer immediate relief. As *Acanthamoeba* keratitis is a rare disease, it is not cost effective to preimmunize individuals against MIP-133. However, topical applications of MIP-133-specific IgA may offer a potential therapy for *Acanthamoeba* patients immediately after displaying symptoms.

In the final analysis, it is not uncommon for specific glycoprotein-binding to induce the secretion of biologically important molecules. The cornea provides a very formidable barrier for foreign invaders, and pathogenic organisms would have to produce specific molecules/strategies against these defenses to be successful. The

mannose receptor/MIP-133 system is an elegant strategy for circumventing the corneal barrier and may be a paradigm for understanding the pathogenesis of infections that begin at the epithelial/environmental interface.

BIBLIOGRAPHY

1. **Abraham, N. J., and E. H. Beachy.** 1985. Host defenses against adhesion of bacteria to mucosal surfaces., p. 63-88. *In* J. I. Gallin and A. S. Fauci (ed.), Advances in host defense mechanisms., vol. 4. Raven press, New York.
2. **Adams, A. D.** 1979. The morphology of human conjunctival mucus. Arch Ophthalmol **97:**730-4.
3. **Aksozek, A., K. McClellan, K. Howard, J. Y. Niederkorn, and H. Alizadeh.** 2002. Resistance of *Acanthamoeba castellanii* cysts to physical, chemical, and radiological conditions. J Parasitol **88:**621-3.
4. **Alfieri, S. C., C. E. Correia, S. A. Motegi, and E. M. Pral.** 2000. Proteinase activities in total extracts and in medium conditioned by *Acanthamoeba polyphaga* trophozoites. J Parasitol **86:**220-7.
5. **Alizadeh, H., S. Apte, M. S. El-Agha, L. Li, M. Hurt, K. Howard, H. D. Cavanagh, J. P. McCulley, and J. Y. Niederkorn.** 2001. Tear IgA and serum IgG antibodies against *Acanthamoeba* in patients with *Acanthamoeba* keratitis. Cornea **20:**622-7.
6. **Alizadeh, H., Y. He, J. P. McCulley, D. Ma, G. L. Stewart, M. Via, E. Haehling, and J. Y. Niederkorn.** 1995. Successful immunization against *Acanthamoeba* keratitis in a pig model. Cornea **14:**180-6.
7. **Alizadeh, H., J. Y. Niederkorn, and J. P. McCulley.** 1996. *Acanthamoeba* keratitis, p. 1062-1071. *In* J. S. Pepose, G. N. Holland, and K. R. Wilhelmus (ed.), Ocular Infection and Immunity. Mosby, St. Louis.
8. **Alizadeh, H., M. S. Pidherney, J. P. McCulley, and J. Y. Niederkorn.** 1994. Apoptosis as a mechanism of cytolysis of tumor cells by a pathogenic free-living amoeba. Infect Immun **62:**1298-303.
9. **Allansmith, M. R., and T. E. Gillette.** 1980. Secretory component in human ocular tissues. Am J Ophthalmol **89:**353-61.
10. **Arbuzova, A., and G. Schwarz.** 1999. Pore-forming action of mastoparan peptides on liposomes: a quantitative analysis. Biochim Biophys Acta **1420:**139-52.
11. **Auran, J. D., M. B. Starr, and F. A. Jacobiec.** 1987. *Acanthamoeba* keratitis. Cornea **6:**2-26.
12. **Badenoch, P. R., M. Adams, and D. J. Coster.** 1995. Corneal virulence, cytopathic effect on human keratocytes and genetic characterization of *Acanthamoeba*. Int J Parasitol **25:**229-39.
13. **Badenoch, P. R., A. M. Johnson, P. E. Christy, and D. J. Coster.** 1991. A model of *Acanthamoeba* keratitis in the rat. Rev Infect Dis **13 Suppl 5:**S445.
14. **Badenoch, P. R., A. M. Johnson, P. E. Christy, and D. J. Coster.** 1990. Pathogenicity of *Acanthamoeba* and a *Corynebacterium* in the rat cornea. Arch Ophthalmol **108:**107-12.
15. **Baggiolini, M., B. Dewald, and B. Moser.** 1994. Interleukin-8 and related chemotactic cytokines--CXC and CC chemokines. Adv Immunol **55:**97-179.
16. **Barker, J. N., M. L. Jones, C. L. Swenson, V. Sarma, R. S. Mitra, P. A. Ward, K. J. Johnson, J. C. Fantone, V. M. Dixit, and B. J. Nickoloff.**

1991. Monocyte chemotaxis and activating factor production by keratinocytes in response to IFN-gamma. J Immunol **146:**1192-7.

17. **Beving, D. E., C. J. Soong, and J. I. Ravdin.** 1996. Oral immunization with a recombinant cysteine-rich section of the *Entamoeba histolytica* galactose-inhibitable lectin elicits an intestinal secretory immunoglobulin A response that has in vitro adherence inhibition activity. Infect Immun **64:**1473-6.
18. **Bhan, A. K., M. C. Mihm, Jr., and H. F. Dvorak.** 1982. T cell subsets in allograft rejection. *In situ* characterization of T cell subsets in human skin allografts by the use of monoclonal antibodies. J Immunol **129:**1578-83.
19. **Bienenstock, J.** 1985. Bronchus-associated lymphoid tissue. Int Arch Allergy Appl Immunol **76 Suppl 1:**62-9.
20. **Brandtzaeg, P.** 1996. History of oral tolerance and mucosal immunity. Ann NY Acad Sci **778:**1-27.
21. **Bronson, R. A., G. W. Cooper, D. L. Rosenfeld, J. V. Gilbert, and A. G. Plaut.** 1987. The effect of an IgA1 protease on immunoglobulins bound to the sperm surface and sperm cervical mucus penetrating ability. Fertil Steril **47:**985-91.
22. **Brown, T.** 1979. Observations by immunofluorescence microscopy and electron microscopy on the cytopathogenicity of *Naegleria fowleri* in mouse embryo-cell cultures. J Med Microbiol **12:**363-71.
23. **Brown, T. J., R. T. M. Cursons, and E. A. Keys.** 1982. Amoeba from antarctic soil and water. Appl. Environ. Microbiol. **44:**491-493.
24. **Cao, Z., D. M. Jefferson, and N. Panjwani.** 1998. Role of carbohydrate-mediated adherence in cytopathogenic mechanisms of *Acanthamoeba*. J Biol Chem **273:**15838-45.
25. **Casper, T., D. Basset, C. Leclercq, J. Fabre, N. Peyron-Raison, and J. Reynes.** 1999. Disseminated *Acanthamoeba* infection in a patient with AIDS: response to 5-fluorocytosine therapy. Clin Infect Dis **29:**944-5.
26. **Castellani, A.** 1930. An amoeba found in cultures of yeast: preliminary note. J. Trop. Med. Hyg. **33:**160.
27. **Cerva, L., C. Serbus, and V. Skocil.** 1973. Isolation of limax amoeba from the nasal mucosa of man. Folia Parasitol. **20:**97-103.
28. **Chadee, K., W. A. Petri, Jr., D. J. Innes, and J. I. Ravdin.** 1987. Rat and human colonic mucins bind to and inhibit adherence lectin of *Entamoeba histolytica*. J Clin Invest **80:**1245-54.
29. **Chambers, J. A., and J. E. Thompson.** 1972. A scanning electron microscopic study of the excystment process of *Acanthamoeba castellanii*. Exp Cell Res **73:**415-21.
30. **Chamorro, L., M. J. Madrigal Sesma, and L. M. Zapatero Ramos.** 1988. [The pathogenicity of free-living amoebae isolated from the intestinal tract of reptiles]. Exp Parasitol **65:**154-5.
31. **Chandrasekar, P. H., P. S. Nandi, M. R. Fairfax, and L. R. Crane.** 1997. Cutaneous infections due to *Acanthamoeba* in patients with acquired immunodeficiency syndrome. Arch Intern Med **157:**569-72.

32. **Chen, S. C., D. H. Jones, E. F. Fynan, G. H. Farrar, J. C. Clegg, H. B. Greenberg, and J. E. Herrmann.** 1998. Protective immunity induced by oral immunization with a rotavirus DNA vaccine encapsulated in microparticles. J Virol **72:**5757-61.
33. **Chinnaiyan, A. M., C. G. Tepper, M. F. Seldin, K. O'Rourke, F. C. Kischkel, S. Hellbardt, P. H. Krammer, M. E. Peter, and V. M. Dixit.** 1996. FADD/MORT1 is a common mediator of CD95 (Fas/APO-1) and tumor necrosis factor receptor-induced apoptosis. J Biol Chem **271:**4961-5.
34. **Cho, J. H., B. K. Na, T. S. Kim, and C. Y. Song.** 2000. Purification and characterization of an extracellular serine proteinase from *Acanthamoeba castellanii*. IUBMB Life **50:**209-14.
35. **Connell, C., A. Rutter, B. Hill, M. Suller, and D. Lloyd.** 2001. Encystation of *Acanthamoeba castellanii*: dye uptake for assessment by flow cytometry and confocal laser scanning microscopy. J Appl Microbiol **90:**706-12.
36. **Center for Control,** 1987. *Acanthamoeba* keratitis in soft-contact-lens wearers--United States. MMWR **36:**397-398, 403-404.
37. **Cordingley, J. S., R. A. Wills, and C. L. Villemez.** 1996. Osmolarity is an independent trigger of *Acanthamoeba castellanii* differentiation. J Cell Biochem **61:**167-71.
38. **Cote, M. A., J. A. Irvine, N. A. Rao, and M. D. Trousdale.** 1991. Evaluation of the rabbit as a model of *Acanthamoeba* keratitis. Rev Infect Dis **13 Suppl 5:**S443-4.
39. **Cursons, R. T., T. J. Brown, and E. A. Keys.** 1978. Virulence of pathogenic free-living amebae. J Parasitol **64:**744-5.
40. **Czerkinsky, C., S. J. Prince, S. M. Michalek, S. Jackson, M. W. Russell, Z. Moldoveanu, J. R. McGhee, and J. Mestecky.** 1987. IgA antibody-producing cells in peripheral blood after antigen ingestion: evidence for a common mucosal immune system in humans. Proc Natl Acad Sci U S A **84:**2449-53.
41. **Daggett, P. M., D. Lipscomb, T. K. Sawyer, and T. A. Nerad.** 1985. A molecular approach to the phylogeny of *Acanthamoeba*. Biosystems **18:**399-405.
42. **Daheshia, M., S. Deshpande, S. Chun, N. A. Kuklin, and B. T. Rouse.** 1999. Resistance to herpetic stromal keratitis in immunized B-cell-deficient mice. Virology **257:**168-76.
43. **Dandekar, T., and M. Leippe.** 1997. Molecular modeling of amoebapore and NK-lysin: a four-alpha-helix bundle motif of cytolytic peptides from distantly related organisms. Fold Des **2:**47-52.
44. **Deluol, A. M., M. F. Teilhac, J. L. Poirot, C. Maslo, J. Luboinski, W. Rozenbaum, and F. P. Chatelet.** 1996. Cutaneous lesions due to *Acanthamoeba* spp in a patient with AIDS. J Eukaryot Microbiol **43:**130S-131S.
45. **Denisova, E., W. Dowling, R. LaMonica, R. Shaw, S. Scarlata, F. Ruggeri, and E. R. Mackow.** 1999. Rotavirus capsid protein VP5* permeabilizes membranes. J Virol **73:**3147-53.

46. **Dubois, B., B. Vanbervliet, J. Fayette, C. Massacrier, C. Van Kooten, F. Briere, J. Banchereau, and C. Caux.** 1997. Dendritic cells enhance growth and differentiation of CD40-activated B lymphocytes. J Exp Med **185:**941-51.
47. **Duma, R. J., W. B. Helwig, and A. J. Martinez.** 1978. Meningoencephalitis and brain abscess due to a free-living amoeba. Ann Intern Med **88:**468-73.
48. **Dykova, I., J. Lom, J. M. Schroeder-Diedrich, G. C. Booton, and T. J. Byers.** 1999. *Acanthamoeba* strains isolated from organs of freshwater fishes. J Parasitol **85:**1106-13.
49. **Fayette, J., B. Dubois, S. Vandenabeele, J. M. Bridon, B. Vanbervliet, I. Durand, J. Banchereau, C. Caux, and F. Briere.** 1997. Human dendritic cells skew isotype switching of CD40-activated naive B cells towards IgA1 and IgA2. J Exp Med **185:**1909-18.
50. **Ferrante, A., and T. J. Abell.** 1986. Conditioned medium from stimulated mononuclear leukocytes augments human neutrophil-mediated killing of a virulent *Acanthamoeba* spp. Infect Immun **51:**607-17.
51. **Ferrante, A., and E. J. Bates.** 1988. Elastase in the pathogenic free-living amoebae *Naegleria* and *Acanthamoeba* spp. Infect Immun **56:**3320-1.
52. **Fluckiger, U., K. F. Jones, and V. A. Fischetti.** 1998. Immunoglobulins to group A streptococcal surface molecules decrease adherence to and invasion of human pharyngeal cells. Infect Immun **66:**974-9.
53. **Fortgens, P. H., C. Dennison, and E. Elliott.** 1997. Anti-cathepsin D chicken IgY antibodies: characterisation, cross-species reactivity and application in immunogold labelling of human splenic neutrophils and fibroblasts. Immunopharmacology **36:**305-11.
54. **Franklin, R. M., and L. E. Remus.** 1984. Conjunctival-associated lymphoid tissue: evidence for a role in the secretory immune system. Invest Ophthalmol Vis Sci **25:**181-7.
55. **Fullard, R. J., and C. Snyder.** 1990. Protein levels in nonstimulated and stimulated tears of normal human subjects. Invest Ophthalmol Vis Sci **31:**1119-26.
56. **Funakoshi, S., T. Doi, T. Nakajima, T. Suyama, and M. Tokuda.** 1982. Antimicrobial effect of human serum IgA. Microbiol Immunol **26:**227-39.
57. **Garner, A.** 1988. Pathology of *Acanthamoeba* infection, p. 535-539. *In* H. D. Cavanagh (ed.), The cornea: Transactions of the world congress on the cornea III. Raven Press, New York.
58. **Gassmann, M., T. Weiser, P. Thommes, and U. Hubscher.** 1990. [The chicken egg as a supply of polyclonal antibodies]. Schweiz Arch Tierheilkd **132:**289-94.
59. **Gast, R. J.** 2001. Development of an *Acanthamoeba*-specific reverse dot-blot and the discovery of a new ribotype. J Eukaryot Microbiol **48:**609-15.
60. **Griffiths, A. J., and D. E. Hughes.** 1968. Starvation and encystment of a soil amoeba *Hartmannella castellanii*. J Protozool **15:**673-7.
61. **Hall, J. M., and J. F. Pribnow.** 1989. IgG and IgA antibody in tears of rabbits immunized by topical application of ovalbumin. Invest Ophthalmol Vis Sci **30:**138-44.

62. **Hazlett, L. D., and R. S. Berk.** 1989. Kinetics of immunoglobulin appearance at the ocular surface. Reg Immunol **2:**294-9.
63. **He, Y. G., J. P. McCulley, H. Alizadeh, M. Pidherney, J. Mellon, J. E. Ubelaker, G. L. Stewart, R. E. Silvany, and J. Y. Niederkorn.** 1992. A pig model of *Acanthamoeba* keratitis: Transmission via contaminated contact lenses. Invest Ophthalmol Vis Sci **33:**126-33.
64. **He, Y. G., J. Y. Niederkorn, J. P. McCulley, G. L. Stewart, D. R. Meyer, R. Silvany, and J. Dougherty.** 1990. *In vivo* and *in vitro* collagenolytic activity of *Acanthamoeba castellanii*. Invest Ophthalmol Vis Sci **31:**2235-40.
65. **Hearing, V. J., L. W. Law, A. Corti, E. Appella, and F. Blasi.** 1988. Modulation of metastatic potential by cell surface urokinase of murine melanoma cells. Cancer Res **48:**1270-8.
66. **Hegde, S., and J. Y. Niederkorn.** 2000. The role of cytotoxic T lymphocytes in corneal allograft rejection. Invest Ophthalmol Vis Sci **41:**3341-7.
67. **Heiligenhaus, A., and C. S. Foster.** 1994. Histological and immunopathological analysis of T-cells mediating murine HSV-1 keratitis. Graefes Arch Clin Exp Ophthalmol **232:**628-34.
68. **Helton, J., M. Loveless, and C. R. White, Jr.** 1993. Cutaneous *Acanthamoeba* infection associated with leukocytoclastic vasculitis in an AIDS patient. Am J Dermatopathol **15:**146-9.
69. **Herold, M. J., A. W. Kuss, C. Kraus, and I. Berberich.** 2002. Mitochondria-dependent caspase-9 activation is necessary for antigen receptor-mediated effector caspase activation and apoptosis in WEHI 231 lymphoma cells. J Immunol **168:**3902-9.
70. **Hingorani, M., D. Metz, and S. L. Lightman.** 1997. Characterisation of the normal conjunctival leukocyte population. Exp Eye Res **64:**905-12.
71. **Hocini, H., L. Belec, S. Iscaki, B. Garin, J. Pillot, P. Becquart, and M. Bomsel.** 1997. High-level ability of secretory IgA to block HIV type 1 transcytosis: contrasting secretory IgA and IgG responses to glycoprotein 160. AIDS Res Hum Retroviruses **13:**1179-85.
72. **Holmgren, J., N. Lycke, and C. Czerkinsky.** 1993. Cholera toxin and cholera B subunit as oral-mucosal adjuvant and antigen vector systems. Vaccine **11:**1179-84.
73. **Hsu, H., J. Xiong, and D. V. Goeddel.** 1995. The TNF receptor 1-associated protein TRADD signals cell death and NF-kappa B activation. Cell **81:**495-504.
74. **Hurt, M., S. Apte, H. Leher, K. Howard, J. Niederkorn, and H. Alizadeh.** 2001. Exacerbation of *Acanthamoeba* keratitis in animals treated with anti-macrophage inflammatory protein 2 or antineutrophil antibodies. Infect Immun **69:**2988-95.
75. **Hurt, M., J. Niederkorn, and H. Alizadeh.** 2003. Effects of mannose on *Acanthamoeba castellanii* proliferation and cytolytic ability to corneal epithelial cells. Invest Ophthalmol Vis Sci **44:**3424-3431.

76. **Hurt, M., V. Proy, J. Y. Niederkorn, and H. Alizadeh.** 2003. The interaction of *Acanthamoeba castellanii* cysts with macrophages and neutrophils. J. Parasitol. **89:**565-572.
77. **Jacobson, L. M., and R. n. Band.** 1987. Genetic heterogenicity in a natural population of *Acanthamoeba polyphaga* from soil, an isoenzyme analysis. J. Protozool. **34:**83-86.
78. **Jaison, P. L., Z. Cao, and N. Panjwani.** 1998. Binding of *Acanthamoeba* to [corrected] mannose-glycoproteins of corneal epithelium: effect of injury. Curr Eye Res **17:**770-6.
79. **Janssen, P. T., and O. P. van Bijsterveld.** 1983. Origin and biosynthesis of human tear fluid proteins. Invest Ophthalmol Vis Sci **24:**623-30.
80. **Johns, K. J., D. M. O'Day, and S. S. Feman.** 1988. Chorioretinitis in the contralateral eye of a patient with *Acanthamoeba* keratitis. Ophthalmology **95:**635-9.
81. **Jones, B. R.** 1973. Presented at the Ocular Microbiology and Immunology Meeting, Dallas, Texas.
82. **Jones, D. B., G. S. Visvesvara, and N. M. Robinson.** 1975. *Acanthamoeba polyphaga* keratitis and *Acenthamoeba* uveitis associated with fatal meningoencephalitis. Trans Ophthalmol Soc U K **95:**221-32.
83. **Kende, M., C. Yan, J. Hewetson, M. A. Frick, W. L. Rill, and R. Tammariello.** 2002. Oral immunization of mice with ricin toxoid vaccine encapsulated in polymeric microspheres against aerosol challenge. Vaccine **20:**1681-91.
84. **Kernacki, K. A., R. P. Barrett, J. A. Hobden, and L. D. Hazlett.** 2000. Macrophage inflammatory protein-2 is a mediator of polymorphonuclear neutrophil influx in ocular bacterial infection. J Immunol **164:**1037-45.
85. **Kernacki, K. A., R. P. Barrett, S. McClellan, and L. D. Hazlett.** 2001. MIP-1alpha regulates CD4+ T cell chemotaxis and indirectly enhances PMN persistence in *Pseudomonas aeruginosa* corneal infection. J Leukoc Biol **70:**911-9.
86. **Kernacki, K. A., R. P. Barrett, S. A. McClellan, and L. D. Hazlett.** 2000. Aging and PMN response to *P. aeruginosa* infection. Invest. Ophthalmol. Vis. Sci. **41:**3019-3025.
87. **Khan, N. A., E. L. Jarroll, N. Panjwani, Z. Cao, and T. A. Paget.** 2000. Proteases as markers for differentiation of pathogenic and nonpathogenic species of *Acanthamoeba*. J Clin Microbiol **38:**2858-61.
88. **Kijlstra, A., S. H. Jeurissen, and K. M. Koning.** 1983. Lactoferrin levels in normal human tears. Br J Ophthalmol **67:**199-202.
89. **Kilian, M., J. Mestecky, and M. W. Russell.** 1988. Defense mechanisms involving Fc-dependent functions of immunoglobulin A and their subversion by bacterial immunoglobulin A proteases. Microbiol Rev **52:**296-303.
90. **Kingston, D., and D. C. Warhurst.** 1969. Isolation of amoebae from the air. J. Med. Microbiol. **2:**27-36.

91. **Klyce, S. D., and R. W. Beuerman.** 1998. Structure and function of the cornea., p. 3-50. *In* H. E. Kaufman and M. B. McDonald (ed.), The Cornea, Second ed. Butterworth-Heineman, Boston.
92. **Knop, N., and E. Knop.** 2000. Conjunctiva-associated lymphoid tissue in the human eye. Invest Ophthalmol Vis Sci **41:**1270-9.
93. **Knutson, J. R., J. Iida, G. B. Fields, and J. B. McCarthy.** 1996. CD44/chondroitin sulfate proteoglycan and alpha 2 beta 1 integrin mediate human melanoma cell migration on type IV collagen and invasion of basement membranes. Mol Biol Cell **7:**383-96.
94. **Kong, H. H., T. H. Kim, and D. I. Chung.** 2000. Purification and characterization of a secretory serine proteinase of *Acanthamoeba healyi* isolated from GAE. J Parasitol **86:**12-7.
95. **Kong, Q., L. Richter, Y. F. Yang, C. J. Arntzen, H. S. Mason, and Y. Thanavala.** 2001. Oral immunization with hepatitis B surface antigen expressed in transgenic plants. Proc Natl Acad Sci U S A **98:**11539-44.
96. **Kraehenbuhl, J. P., and M. R. Neutra.** 1992. Molecular and cellular basis of immune protection of mucosal surfaces. Physiol Rev **72:**853-79.
97. **Kwaan, H. C.** 1992. The plasminogen-plasmin system in malignancy. Cancer Metastasis Rev **11:**291-311.
98. **Kwon, B., and L. D. Hazlett.** 1997. Association of CD4+ T cell-dependent keratitis with genetic susceptibility to *Pseudomonas aeruginosa* keratitis. J. Immunol. **159:**6283-6290.
99. **Lagmay, J. P., R. R. Matias, F. F. Natividad, and G. L. Enriquez.** 1999. Cytopathogenicity of *Acanthamoeba* isolates on rat glial C6 cell line. Southeast Asian J Trop Med Public Health **30:**670-7.
100. **Lamm, M. E., J. G. Nedrud, C. S. Kaetzel, and M. B. Mazanec.** 1995. IgA and mucosal defense. Apmis **103:**241-6.
101. **Larkin, D. F., M. Berry, and D. L. Easty.** 1991. *In vitro* corneal pathogenicity of Acanthamoeba. Eye **5 (Pt 5):**560-8.
102. **Larkin, D. F. P., and D. L. Easty.** 1991. Experimental *Acanthamoeba* keratitis:II:Immunological evaluation. Br. J. Ophthalmol. **75:**421-424.
103. **Larsson, A., R. M. Balow, T. L. Lindahl, and P. O. Forsberg.** 1993. Chicken antibodies: taking advantage of evolution--a review. Poult Sci **72:**1807-12.
104. **Lawton, A. W.** 1998. Structure and function of the eyelids and conjunctiva., p. 51-60. *In* H. kaufman, B. B. Barron, and M. B. McDonald (ed.), The Cornea, Second ed. Butterworth-Heinemann, Boston.
105. **Leher, H., K. Kinoshita, H. Alizadeh, F. L. Zaragoza, Y. G. He, and J. Y. Niederkorn.** 1998. Impact of oral immunization with *Acanthamoeba* antigens on parasite adhesion and corneal infection. Invest. Ophthalmol. Vis. Sci. **39:**2337-2343.
106. **Leher, H., F. Zaragoza, S. Taherzadeh, H. Alizadeh, and J. Y. Niederkorn.** 1999. Monoclonal IgA antibodies protect against *Acanthamoeba* keratitis. Exp Eye Res **69:**75-84.

107. **Leher, H. F., H. Alizadeh, W. M. Taylor, A. S. Shea, R. S. Silvany, F. Van Klink, M. J. Jager, and J. Y. Niederkorn.** 1998. Role of mucosal IgA in the resistance to *Acanthamoeba* keratitis. Invest Ophthalmol Vis Sci **39:**2666-73.
108. **Leher, H. F., R. E. Silvany, H. Alizadeh, J. Huang, and J. Y. Niederkorn.** 1998. Mannose induces the release of cytopathic factors from *Acanthamoeba castellanii*. Infect. Immun. **66:**5-10.
109. **Leippe, M.** 1997. Amoebapores. Parasitol. Today **13:**178-183.
110. **Leippe, M., S. Ebel, O. L. Schoenberger, R. D. Horstmann, and H. J. Muller-Eberhard.** 1991. Pore-forming peptide of pathogenic *Entamoeba histolytica*. Proc Natl Acad Sci U S A **88:**7659-63.
111. **Levine, S., A. E. Goldstein, M. Dahdouh, P. Blank, C. Hoffman, and C. A. Gropper.** 2001. Cutaneous *Acanthamoeba* in a patient with AIDS: a case study with a review of new therapy; quiz 386. Cutis **67:**377-80.
112. **Liang, X. P., M. E. Lamm, and J. G. Nedrud.** 1988. Oral administration of cholera toxin-Sendai virus conjugate potentiates gut and respiratory immunity against Sendai virus. J Immunol **141:**1495-501.
113. **Lundin, B. S., C. Johansson, and A. M. Svennerholm.** 2002. Oral immunization with a Salmonella enterica serovar typhi vaccine induces specific circulating mucosa-homing CD4(+) and CD8(+) T cells in humans. Infect Immun **70:**5622-7.
114. **Lyons, T. B., and R. Kapur.** 1977. Limax amoeba in public swimming pools of Albany, Schenectady, and Ransselear Counties, New York: their concentrations, correlations, and significance. Appl. Environ. Microbiol. **33:**551-555.
115. **Marciano-Cabral, F., and D. M. Toney.** 1998. The interaction of *Acanthamoeba* spp. with activated macrophages and with macrophage cell lines. J Eukaryot Microbiol **45:**452-8.
116. **Martinez, A. J.** 1982. Acanthamoebiasis and immunosuppression. Case report. J Neuropathol Exp Neurol **41:**548-57.
117. **Martinez, A. J., C. A. Garcia, M. Halks-Miller, and R. Arce-Vela.** 1980. Granulomatous amebic encephalitis presenting as a cerebral mass lesion. Acta Neuropathol (Berl) **51:**85-91.
118. **Martinez, A. J., and K. Janitschke.** 1985. *Acanthamoeba*, an opportunistic microorganism: a review. Infection **13:**251-6.
119. **Martinez, A. J., F. L. Schuster, and G. S. Visvesvara.** 2001. *Balamuthia mandrillaris*: its pathogenic potential. J Eukaryot Microbiol **Suppl:**6S-9S.
120. **Martinez, A. J., C. Sotelo-Avila, J. Garcia-Tamayo, J. T. Moron, E. Willaert, and W. P. Stamm.** 1977. Meningoencephalitis due to *Acanthamoeba* SP. Pathogenesis and clinico-pathological study. Acta Neuropathol (Berl) **37:**183-91.
121. **Martinez, A. J., and G. S. Visvesvara.** 2001. *Balamuthia mandrillaris* infection. J Med Microbiol **50:**205-7.
122. **Martinez, A. J., and G. S. Visvesvara.** 1997. Free-living, amphizoic and opportunistic amebas. Brain Pathol **7:**583-98.

123. **Masinick, S. A., C. P. Montgomery, P. C. Montgomery, and L. D. Hazlett.** 1997. Secretory IgA inhibits *Pseudomonas aeruginosa* binding to cornea and protects against keratitis. Invest Ophthalmol Vis Sci **38:**910-8.
124. **Mathers, W. D., G. Stevens, M. Rodrigues, C. C. Chan, J. Gold, G. S. Visvesvara, M. A. Lemp, and L. Z. Zimmerman.** 1987. Immunopathology and electron microscopy of *Acanthamoeba* keratitis. Am. J. Ophthalmol. **103:**626-635.
125. **Mathers, W. D., J. E. Sutphin, R. Folberg, P. A. Meier, R. P. Wenzel, and R. G. Elgin.** 1996. Outbreak of keratitis presumed to be caused by *Acanthamoeba*. Am. J. Ophthalmol. **121:**207-208.
126. **Mattana, A., F. Bennardini, S. Usai, P. L. Fiori, F. Franconi, and P. Cappuccinelli.** 1997. *Acanthamoeba castellanii* metabolites increase the intracellular calcium level and cause cytotoxicity in wish cells. Microb Pathog **23:**85-93.
127. **May, L. P., G. S. Sidhu, and M. R. Buchness.** 1992. Diagnosis of *Acanthamoeba* infection by cutaneous manifestations in a man seropositive to HIV. J Am Acad Dermatol **26:**352-5.
128. **Mazanec, M. B., J. G. Nedrud, C. S. Kaetzel, and M. E. Lamm.** 1993. A three-tiered view of the role of IgA in mucosal defense. Immunol Today **14:**430-5.
129. **Mazur, T., E. Hadas, and I. Iwanicka.** 1995. The duration of the cyst stage and the viability and virulence of *Acanthamoeba* isolates. Trop Med Parasitol **46:**106-8.
130. **McClellan, K., K. Howard, E. Mayhew, J. Niederkorn, and H. Alizadeh.** 2002. Adaptive immune responses to *Acanthamoeba* cysts. Exp Eye Res **75:**285-93.
131. **McClellan, K., K. Howard, J. Y. Niederkorn, and H. Alizadeh.** 2001. Effect of steroids on *Acanthamoeba* cysts and trophozoites. Invest Ophthalmol Vis Sci **42:**2885-93.
132. **McCoy, J. J., B. J. Mann, and W. A. Petri, Jr.** 1994. Adherence and cytotoxicity of *Entamoeba histolytica* or how lectins let parasites stick around. Infect Immun **62:**3045-50.
133. **McCulley, J. P., H. Alizadeh, and J. Y. Niederkorn.** 1995. *Acanthamoeba* keratitis. CLAO J. **21:**73-76.
134. **McDermott, M. R., and J. Bienenstock.** 1979. Evidence for a common mucosal immunologic system. I. Migration of B immunoblasts into intestinal, respiratory, and genital tissues. J Immunol **122:**1892-8.
135. **McGee, D. W., and R. M. Franklin.** 1984. Lymphocyte migration into the lacrimal gland is random. Cell Immunol **86:**75-82.
136. **Mehrad, B., M. Wiekowski, B. E. Morrison, S. C. Chen, E. C. Coronel, D. J. Manfra, and S. A. Lira.** 2002. Transient lung-specific expression of the chemokine KC improves outcome in invasive aspergillosis. Am J Respir Crit Care Med **166:**1263-8.

137. **Mestecky, J.** 1987. The common mucosal immune system and current strategies for induction of immune responses in external secretions. J Clin Immunol **7:**265-76.
138. **Mestecky, J., I. Moro, and B. Underdown.** 1999. Mucosal immunoglobulins., p. 133. *In* M. J., B. J., M. J., L. M., S. W., and O. P. (ed.), Mucosal Immunology. Academic Press, San Diego.
139. **Mitra, M. M., H. Alizadeh, R. D. Gerard, and J. Y. Niederkorn.** 1995. Characterization of a plasminogen activator produced by *Acanthamoeba castellanii*. Mol Biochem Parasitol **73:**157-64.
140. **Montgomery, P. C., J. H. Rockey, A. S. Majumdar, I. M. Lemaitre-Coelho, J. P. Vaerman, and A. Ayyildiz.** 1984. Parameters influencing the expression of IgA antibodies in tears. Invest Ophthalmol Vis Sci **25:**369-73.
141. **Moore, M. B., J. E. Ubelaker, J. H. Martin, R. Silvany, J. M. Dougherty, D. R. Meyer, and J. P. McCulley.** 1991. *In vitro* penetration of human corneal epithelium by *Acanthamoeba castellanii*: a scanning and transmission electron microscopy study. Cornea **10:**291-8.
142. **Morlet, N., G. Duguid, C. Radford, M. Matheson, and J. Dart.** 1997. Incidence of *Acanthamoeba* keratitis associated with contact lens wear. Lancet **350:**414.
143. **Morton, L. D., G. L. McLaughlin, and H. E. Whiteley.** 1991. Effects of temperature, amebic strain, and carbohydrates on *Acanthamoeba* adherence to corneal epithelium in vitro. Infect. Immun. **59:**3819-3822.
144. **Moshari, A., I. W. McLean, M. T. Dodds, R. E. Damiano, and P. L. McEvoy.** 2001. Chorioretinitis after keratitis caused by *Acanthamoeba*: case report and review of the literature. Ophthalmology **108:**2232-6.
145. **Naginton, J., P. G. Watson, T. J. Playfair, J. McGill, B. R. Jones, and A. D. Steele.** 1974. Amoebic infection of the eye. Lancet **2:**1537-40.
146. **Neutra, M. R., A. Frey, and J. P. Kraehenbuhl.** 1996. Epithelial M cells: gateways for mucosal infection and immunization. Cell **86:**345-8.
147. **Neutra, M. R., E. Pringault, and J. P. Kraehenbuhl.** 1996. Antigen sampling across epithelial barriers and induction of mucosal immune responses. Annu Rev Immunol **14:**275-300.
148. **Ng, P. W., A. G. Porter, and R. U. Janicke.** 1999. Molecular cloning and characterization of two novel pro-apoptotic isoforms of caspase-10. J Biol Chem **274:**10301-8.
149. **Nicholson, D. W., A. Ali, N. A. Thornberry, J. P. Vaillancourt, C. K. Ding, M. Gallant, Y. Gareau, P. R. Griffin, M. Labelle, Y. A. Lazebnik, and et al.** 1995. Identification and inhibition of the ICE/CED-3 protease necessary for mammalian apoptosis. Nature **376:**37-43.
150. **Niederkorn, J. Y.** 1994. Immunological barriers in the eye., p. 241-254. *In* R. Goldie (ed.), The handbook of immunopharmacology. Immunopharmacology of epithelial barriers. Academic Press, London.
151. **Niederkorn, J. Y., H. Alizadeh, H. Leher, S. Apte, S. E. Agha, L. Ling, M. Hurt, K. Howard, H. D. Cavanagh, and J. P. McCulley.** 2002. Role of tear

anti-acanthamoeba IgA in *Acanthamoeba* keratitis. Adv Exp Med Biol **506:**845-50.

152. **Niederkorn, J. Y., H. Alizadeh, H. Leher, and J. P. McCulley.** 1999. The pathogenesis of *Acanthamoeba* keratitis. Microbes Infect **1:**437-43.
153. **Niederkorn, J. Y., H. Alizadeh, H. F. Leher, and J. P. McCulley.** 1999. The immunobiology of Acanthamoeba keratitis. Springer Semin. Immunopathol. **21:**147-160.
154. **Niederkorn, J. Y., J. E. Ubelaker, J. P. McCulley, G. L. Stewart, D. R. Meyer, J. A. Mellon, R. E. Silvany, Y. G. He, M. Pidherney, J. H. Martin, and et al.** 1992. Susceptibility of corneas from various animal species to in vitro binding and invasion by *Acanthamoeba castellanii* [corrected]. Invest Ophthalmol Vis Sci **33:**104-12.
155. **Ossowski, L.** 1988. Plasminogen activator dependent pathways in the dissemination of human tumor cells in the chick embryo. Cell **52:**321-8.
156. **Page, F. C.** 1967. Re-definition of the genus *Acanthamoeba* with descriptions of three species. J Protozool **14:**709-24.
157. **Paszko-Kolva, C., H. Yamamoto, M. Shahamat, T. K. Sawyer, G. Morris, and R. R. Colwell.** 1991. Isolation of amoebae and *Pseudomonas* and *Legionella* spp. from eyewash stations. Appl. Environ. Microbiol. **57:**163-167.
158. **Pearlman, E.** 1997. Immunopathology of onchocerciasis: a role for eosinophils in onchocercal dermatitis and keratitis. Chem. Immunol. **66:**26-40.
159. **Peppard, J. V., R. V. Mann, and P. C. Montgomery.** 1988. Antibody production in rats following ocular-topical or gastrointestinal immunization: kinetics of local and systemic antibody production. Curr Eye Res **7:**471-81.
160. **Pettit, D. A., J. Williamson, G. A. Cabral, and F. Marciano-Cabral.** 1996. In vitro destruction of nerve cell cultures by *Acanthamoeba* spp.: a transmission and scanning electron microscopy study. J. Parasitol. **82:**769-777.
161. **Peyer, J. C.** 1677. Exerciato anatemico-medica de glanis intestinorium. Schaff-hausen, Switzerland.
162. **Pierce, N. F., and J. L. Gowans.** 1975. Cellular kinetics of the intestinal immune response to cholera toxoid in rats. J Exp Med **142:**1550-63.
163. **Pussard, M., and R. Pons.** 1977. Morphologies de la paroi kystique et taxonomie du genre *Acanthamoeba* (Protozoa, Amoebida). Protistologica **13:**557-610.
164. **Ravdin, J. I., P. Stanley, C. F. Murphy, and W. A. Petri, Jr.** 1989. Characterization of cell surface carbohydrate receptors for *Entamoeba histolytica* adherence lectin. Infect Immun **57:**2179-86.
165. **Reed, R. P., C. M. Cooke-Yarborough, A. L. Jaquiery, K. Grimwood, A. S. Kemp, J. C. Su, and J. R. Forsyth.** 1997. Fatal granulomatous amoebic encephalitis caused by *Balamuthia mandrillaris*. Med J Aust **167:**82-4.
166. **Ridley Lathers, D. M., R. F. Gill, and P. C. Montgomery.** 1998. Inductive pathways leading to rat tear IgA antibody responses. Invest Ophthalmol Vis Sci **39:**1005-11.

167. **Rivera, F., F. Medina, P. Ramirez, J. Alcocer, G. Vilaclara, and E. Robles.** 1984. Pathogenic and free-living protozoa cultured from the nasopharyngeal and oral regions of dental patients. Environ. Res. **33:**428-440.
168. **Rodan, G. A.** 1998. Mechanisms of action of bisphosphonates. Annu Rev Pharmacol Toxicol **38:**375-88.
169. **Rude, R. A., G. J. Jackson, J. W. Bier, T. K. Sawyer, and N. G. Risty.** 1984. Survey of fresh vegetables for nematodes, amoebae, and *Salmonella*. J Assoc Off Anal Chem **67:**613-5.
170. **Rudner, X. L., K. A. Kernacki, R. P. Barrett, and L. D. Hazlett.** 2000. Prolonged elevation of IL-1 in *Pseudomonas aeruginosa* ocular infection regulates macrophage-inflammatory protein-2 production, polymorphonuclear neutrophil persistence, and corneal perforation. J. Immunol. **164:**6576-6582.
171. **Russell, M. W., D. A. Sibley, E. B. Nikolova, M. Tomana, and J. Mestecky.** 1997. IgA antibody as a non-inflammatory regulator of immunity. Biochem Soc Trans **25:**466-70.
172. **Schaumberg, D. A., K. K. Snow, and M. R. Dana.** 1998. The epidemic of *Acanthamoeba* keratitis: where do we stand? Cornea **17:**3-10.
173. **Selander, K. S., J. Monkkonen, E. K. Karhukorpi, P. Harkonen, R. Hannuniemi, and H. K. Vaananen.** 1996. Characteristics of clodronate-induced apoptosis in osteoclasts and macrophages. Mol Pharmacol **50:**1127-38.
174. **Sharma, A., K. Honma, R. T. Evans, D. E. Hruby, and R. J. Genco.** 2001. Oral immunization with recombinant *Streptococcus gordonii* expressing porphyromonas gingivalis FimA domains. Infect Immun **69:**2928-34.
175. **Shin, H. J., M. S. Cho, S. Y. Jung, H. I. Kim, and K. I. Im.** 2000. In vitro cytotoxicity of *Acanthamoeba* spp. isolated from contact lens containers in Korea by crystal violet staining and LDH release assay. Korean J Parasitol **38:**99-102.
176. **Skelsey, M. E., E. Mayhew, and J. Y. Niederkorn.** 2003. CD25+, interleukin-10-producing CD4+ T cells are required for suppressor cell production and immune privilege in the anterior chamber of the eye. Immunology **110:**18-29.
177. **Skelsey, M. E., J. Mellon, and J. Y. Niederkorn.** 2001. Gamma delta T cells are needed for ocular immune privilege and corneal graft survival. J Immunol **166:**4327-33.
178. **Slater, C. A., J. Z. Sickel, G. S. Visvesvara, R. C. Pabico, and A. A. Gaspari.** 1994. Brief report: successful treatment of disseminated acanthamoeba infection in an immunocompromised patient. N Engl J Med **331:**85-7.
179. **Smith, P. K., R. I. Krohn, G. T. Hermanson, A. K. Mallia, F. H. Gartner, M. D. Provenzano, E. K. Fujimoto, N. M. Goeke, B. J. Olson, and D. C. Klenk.** 1985. Measurement of protein using bicinchoninic acid. Analytical Biochemistry **150:**76-85.
180. **Smolin, G., M. Okumoto, and R. A. Nozik.** 1979. The microbial flora in extended-wear soft contact-lens wearers. Am J Ophthalmol **88:**543-7.

181. **Stehr-Green, J. K., T. M. Baily, and G. S. Visvesvara.** 1989. The epidemiology of *Acanthamoeba* keratitis in the United States. Am. J. Ophthalmol. **107:**331-336.
182. **Stewart, G. L., I. Kim, K. Shupe, H. Alizadeh, R. Silvany, J. P. McCulley, and J. Y. Niederkorn.** 1992. Chemotactic response of macrophages to *Acanthamoeba castellanii* antigen and antibody-dependent macrophage-mediated killing of the parasite. J Parasitol **78:**849-55.
183. **Stewart, G. L., K. Shupe, I. Kim, R. E. Silvany, H. Alizadeh, J. P. McCulley, and J. Y. Niederkorn.** 1994. Antibody-dependent neutrophil-mediated killing of *Acanthamoeba castellanii*. Int. J. Parasitol. **24:**739-742.
184. **Stothard, D. R., J. M. Schroeder-Diedrich, M. H. Awwad, R. J. Gast, D. R. Ledee, S. Rodriguez-Zaragoza, C. L. Dean, P. A. Fuerst, and T. J. Byers.** 1998. The evolutionary history of the genus *Acanthamoeba* and the identification of eight new 18S rRNA gene sequence types. J Eukaryot Microbiol **45:**45-54.
185. **Stratford, M. P., and A. J. Griffiths.** 1978. Variations in the protperties and morphology of cysts of *Acanthamoeba castellanii*. J. Gen. Microbiol. **108:**33.
186. **Streilein, J. W., M. R. Dana, and B. R. Ksander.** 1997. Immunity causing blindness: five different paths to herpes stromal keratitis. Immunol. Today **18:**443-449.
187. **Tan, B., C. M. Weldon-Linne, D. P. Rhone, C. L. Penning, and G. S. Visvesvara.** 1993. *Acanthamoeba* infection presenting as skin lesions in patients with the acquired immunodeficiency syndrome. Arch Pathol Lab Med **117:**1043-6.
188. **Tenovuo, J., Z. Moldoveanu, J. Mestecky, K. M. Pruitt, and B. M. Rahemtulla.** 1982. Interaction of specific and innate factors of immunity: IgA enhances the antimicrobial effect of the lactoperoxidase system against *Streptococcus mutans*. J Immunol **128:**726-31.
189. **Thomas, J., S. Gangappa, S. Kanangat, and B. T. Rouse.** 1997. On essential involvement of neutrophils in the immunopathological disease: herpetic stromal keratitis. J. Immunol. **158:**1383-1391.
190. **Thornberry, N. A., and Y. Lazebnik.** 1998. Caspases: enemies within. Science **281:**1312-6.
191. **Tian, P., J. M. Ball, C. Q. Zeng, and M. K. Estes.** 1996. The rotavirus nonstructural glycoprotein NSP4 possesses membrane destabilization activity. J Virol **70:**6973-81.
192. **Tomasi, T. B.** 1976. The immune system of secretion. Prentice Hall, Englewood Cliffs.
193. **Torno, M. S., Jr., R. Babapour, A. Gurevitch, and M. D. Witt.** 2000. Cutaneous acanthamoebiasis in AIDS. J Am Acad Dermatol **42:**351-4.
194. **Van Haeringen, N. J.** 1981. Clinical biochemistry of tears. Surv Ophthalmol **26:**84-96.
195. **Van Hamme, C., M. Dumont, M. Delos, and J. M. Lachapelle.** 2001. [Cutaneous acanthamoebiasis in a lung transplant patient]. Ann Dermatol Venereol **128:**1237-40.

196. **Van Klink, F., H. Alizadeh, Y. G. He, J. A. Mellon, R. E. Silvany, J. P. McCulley, and J. Y. Niederkorn.** 1993. The role of contact lenses, trauma, and Langerhans cells in a Chinese hamster model of *Acanthamoeba* keratitis. Invest. Ophthalmol. Vis. Sci. **34:**1937-1944.
197. V**an Klink, F., H. Alizadeh, G. L. Stewart, M. S. Pidherney, R. E. Silvany, Y. He, J. P. McCulley, and J. Y. Niederkorn.** 1992. Characterization and pathogenic potential of a soil isolate and an ocular isolate of *Acanthamoeba castellanii* in relation to Acanthamoeba keratitis. Curr Eye Res **11:**1207-20.
198. **Van Klink, F., H. F. Leher, M. J. Jager, H. Alizadeh, W. Taylor, and J. Y. Niederkorn.** 1997. Systemic immune response to *Acanthamoeba* keratitis in the Chinese hamster. Ocular Immunol. Inflamm. **5:**234-244.
199. **Van Klink, F., W. M. Taylor, H. Alizadeh, M. J. Jager, N. Van Rooijen, and J. Y. Niederkorn.** 1996. The role of macrophages in *Acanthamoeba* keratitis. Invest. Ophthalmol. Vis. Sci. **37:**1271-1281.
200. **Van Rooijen, N.** 1989. The liposome-mediated macrophage 'suicide' technique. J Immunol Methods **124:**1-6.
201. **Vines, R. R., G. Ramakrishnan, J. B. Rogers, L. A. Lockhart, B. J. Mann, and W. A. Petri, Jr.** 1998. Regulation of adherence and virulence by the *Entamoeba histolytica* lectin cytoplasmic domain, which contains a beta2 integrin motif. Mol Biol Cell **9:**2069-79.
202. **Visvesvara, G. S.** 1991. Classification of *Acanthamoeba*. Rev Infect Dis **13 Suppl 5:**S369-72.
203. **Visvesvara, G. S., S. S. Mirra, F. H. Brandt, D. M. Moss, H. M. Mathews, and A. J. Martinez.** 1983. Isolation of 2 strains of *Acanthamoeba castellanii* from human tissue and their pathogenicity and isoenzyme profiles. J. Clin. Microbiol. **6:**1405-1412.
204. **Visvesvara, G. S., and J. K. Stehr-Green.** 1990. Epidemiology of free-living amoeba infections. J. Protozool. **37:**25s-33s.
205. **Volkonsky, M.** 1931. *Hartmanella castellanii Douglas*, et classification des hartmannelles. Arch. Zool. Exp. Gen. **72:**378-385.
206. **Walochnik, J., A. Hassl, K. Simon, G. Benyr, and H. Aspock.** 1999. Isolation and identification by partial sequencing of the 18S ribosomal gene of free-living amoebae from necrotic tissue of *Basilliscus plumifrons* (Sauria: Iguanidae). Parasitol Res **85:**601-3.
207. **Wang, J., H. J. Chun, W. Wong, D. M. Spencer, and M. J. Lenardo.** 2001. Caspase-10 is an initiator caspase in death receptor signaling. Proc Natl Acad Sci U S A **98:**13884-8.
208. **Wang, S. S., and H. A. Feldman.** 1967. Isolation of *Hartmannella* species from human throats. N. Engl. J. Med. **277:**1174-1179.
209. **Warr, G. W., K. E. Magor, and D. A. Higgins.** 1995. IgY: clues to the origins of modern antibodies. Immunol Today **16:**392-8.
210. **Weekers, P. H., and J. F. De Jonckheere.** 1997. Differences in isoenzyme patterns of axenically and monoxenically grown *Acanthamoeba* and *Hartmannella*. Antonie Van Leeuwenhoek **71:**231-7.

211. **Weisman, R. A.** 1976. Differentiation in *Acanthamoeba castellanii*. Annu Rev Microbiol **30:**189-219.
212. **Wells, P. A., and L. D. Hazlett.** 1985. Immunocytochemical localization of immunoglobulins at the corneal surface of the mouse. Exp Eye Res **40:**779-96.
213. **Wilhelmus, K. R.** 1991. Introduction: the increasing importance of *Acanthamoeba*. Rev Infect Dis **13 Suppl 5:**S367-8.
214. **Wilson, S. E., J. Weng, S. Blair, Y. G. He, and S. Lloyd.** 1995. Expression of E6/E7 or SV40 large T antigen-coding oncogenes in human corneal endothelial cells indicates regulated high-proliferative capacity. Invest Ophthalmol Vis Sci **36:**32-40.
215. **Woo, M., R. Hakem, M. S. Soengas, G. S. Duncan, A. Shahinian, D. Kagi, A. Hakem, M. McCurrach, W. Khoo, S. A. Kaufman, G. Senaldi, T. Howard, S. W. Lowe, and T. W. Mak.** 1998. Essential contribution of caspase 3/CPP32 to apoptosis and its associated nuclear changes. Genes Dev **12:**806-19.
216. **Yan, X. T., T. M. Tumpey, S. L. Kunkel, J. E. Oakes, and R. N. Lausch.** 1998. Role of MIP-2 in neutrophil migration and tissue injury in Herpes Simplex Virus-1-Infected Cornea. Invest. Ophthalmol. Vis. Sci. **39:**1854-1862.
217. **Yang, Z. T., Z. Y. Cao, and N. Panjwani.** 1997. Pathogenesis of *Acanthamoeba* keratitis: carbohydrate-mediated host-parasite interactions. Infect. Immun. **65:**439-445.
218. **Zachariae, C. O., A. O. Anderson, H. L. Thompson, E. Appella, A. Mantovani, J. J. Oppenheim, and K. Matsushima.** 1990. Properties of monocyte chemotactic and activating factor (MCAF) purified from a human fibrosarcoma cell line. J Exp Med **171:**2177-82.
219. **Zachariae, C. O., K. Thestrup-Pedersen, and K. Matsushima.** 1991. Expression and secretion of leukocyte chemotactic cytokines by normal human melanocytes and melanoma cells. J Invest Dermatol **97:**593-9.

VITA

Michael Allen Hurt was born in Houston, Texas on May 26, 1969. He lived in Houston until age 12, moved to Aurora, Colorado until 15, moved back to Irving, Texas for one year, and ended up in Fort Worth, Texas, where he graduated from Eastern Hills High School in 1989. That same year, he enlisted into the US Navy. In 1993, he entered the University of Texas Arlington and received Bachelor of Science in Microbiology, Magna Cum Laude, and a minor in chemistry. He entered the Graduate Program in Biomedical Sciences at the University of Texas Southwestern Medical School at Dallas in 1998, and the Molecular Microbiology Program in 1999.